Politechnika Wrocławska

FIELD OF SCIENCE: NATURAL SCIENCE

DISCIPLINE OF SCIENCE: MATHEMATICS

DOCTORAL DISSERTATION

Mathematical methods in modeling the diffusion of renewable energy sources

Mr. Tomasz Weron, MSc., Eng.

Supervisor:
dr hab. Janusz Szwabiński, prof. uczelni

Assistant supervisor:
dr hab. Katarzyna Maciejowska, prof. uczelni

Keywords: Agent-based modeling, Complex networks, Computational statistics, Diffusion of innovation, Dynamical systems, Opinion dynamics, Mathematical modeling, Renewable Energy

WROCŁAW DECEMBER 2024

Contents

Chapter 1

Introduction

1.1 Background[1]

Today, we are experiencing the effects of climate change and environmental pollution more and more often. What might have once seemed insignificant, such as glaciers melting thousands of kilometers away, now begins to affect us directly. While the gigantic fires that devastated countries like Australia, Canada, or Greece have spared Poland, we experience another environmental disaster – air pollution. In Poland, low-quality heating installations in single-family homes or multi-family housing are among the main causes of its formation [72]. Generally speaking, the problem is the generation of energy from non-renewable and often polluting sources. High emissions of pollutants directly threaten our lives and, in the future that is coming, lead to dangerous climate change [19], of which global warming is probably the most widely discussed. Not only does it affect entire ecosystems and the comfort of life, but according to some studies it may also lead to the aggravation and spread of many dangerous diseases [43].

That is why the development of renewable energy sources (renewables, RES) is so important. In the European Union in 2023, about 45% of the electricity generation came from RES [18]. Poland, although it saw a rapid expansion of renewables, still falls behind with around 26% [51]. In Europe, wind is the main source of renewable energy [17]. Unfortunately, wind farms require huge investments and vast free space, far from residential buildings. An alternative devoid of these limitations, and rapidly gaining popularity in Poland over the past few years, are photovoltaic panels (PVs), see Fig. 1.1 for exact numbers. Those can be installed on the roof of a single-family home without adversely affecting quality of life, while the cost of such a project is already achievable for a middle-income family [15]. However, it is important not only to provide this opportunity and encourage it through subsidy programs or public campaigns, but also to ensure sustainability. Excessive support of RES diffusion can lead to a significant increase in the variability of demand for conventional generation on a 24-hour basis and in extreme cases can even cause loss of stability of the power system. Examples are countries/regions with a large operation of the sun during a year, such as Australia [39] or California [38], but also Poland's neighbor – Germany [22]. Apart from that, there is another threat, more closely related to the common people. The current transmission system grids in Poland and other countries are not prepared for such a rapid expansion of PVs. If not restricted, it can lead to grid overload and blackouts. In fact, this is an already emerging risk [54].

[1] This Section is largely based on Section *Introduction* from **Paper 4**.

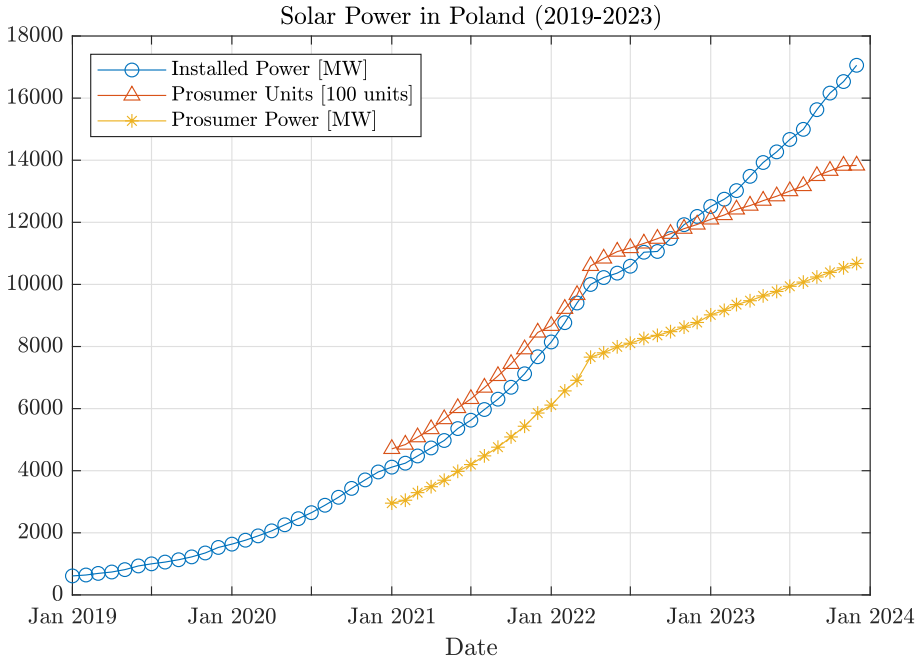

Figure 1.1: Data on solar installations in Poland in years 2019–2023, according to ARE (Polish energy market agency). More detailed data is being collected from 2021 onward, most likely due to the growing interest in the prosumer market. Data freely available at www.are.waw.pl. Source: **Paper 4**.

The diffusion of photovoltaics is an example of the so-called diffusion of innovation, understood here as a process of spreading the information of an innovation through a population and adopting it [55]. This is an interesting and very important topic, studied across many fields of science, economy, medicine, sociology, to name a few. Although innovation may refer to a variety of issues, not only products and technologies, but ideas or behaviors as well, there exist many universal features [55]. Visually, if we draw a number of adopted people (or fraction of adopted population) as a function of time, the S-shape of the curve would be noticeable. In addition, there is a critical mass (fraction) of adopters for which innovation is bound to succeed. Lastly, the diffusion of innovation process is multistage. First, we have knowledge of an innovation and an opinion on it, then a decision, adoption, and finally a confirmation of the decision. Studying and understanding this phenomenon is vitally important. It may and should support decision-making by our legislators toward a desired outcome. An example of how legislators can affect the diffusion of innovation is contained in the data in Fig. 1.1. Initially, until early 2022, the spread of PVs was supported by subsidy programs, and hence, rapid. Then, in April 2022, new regulations came in, making PVs much less profitable, and the diffusion significantly slowed down. Whether we consider them wise decisions or reckless actions depends primarily on our political sympathies.

The diffusion of innovations has been modeled for years. It started in a very simplified manner. A classic example is the Bass diffusion model – a fully deterministic one, consisting of a single differential equation [6]. However, for a problem as complex as the diffusion of PV installations, aggregated models are just not enough [52]. They are unable to describe the clustering of individuals, a phenomenon observed in real life [71]. The aforementioned Bass diffusion of innovation model can dramatically change its behavior, when rewritten to an agent-based model (ABM) and tested on a network structure [53]. In social sciences, an agent-based model is usually understood as a simulation

of certain interactions between so-called agents (representing individuals, households, companies, etc.) and taking place within a certain structure, symbolizing a network of acquaintances, contacts, or cooperation [37]. Mathematically, we would call such a structure a graph, with the vertices being the agents, and the edges the connections between them [46]. ABMs allow for a much more accurate representation of reality, including the heterogeneity of individuals and the interactions between them [46]. As such, ABMs are currently one of the most powerful tools in studying opinion dynamics and innovation diffusion [32]. Although they have been used for years to model the diffusion of new energy solutions [10, 27, 30, 66, 70], their applications in modeling the diffusion of PVs remain few [11, 40, 49, 74].

Although much more advanced than simple deterministic models, ABMs are still merely a hypothetical approximation of reality. With that in mind, one should adjust them to a problem at hand as accurately as possible, instead of constructing a one-size-fits-all model. The underlying structure plays an huge role here. For example, when modeling a spread of gossip in a high school class, a simple network of class acquaintances would be sufficient. However, to properly represent the flow of information and the exchange of opinions in the modern world, a much more complex structure is needed. This is where multi-layer networks come in. They are used in many fields of science [3], as they can provide multilevel representations of real world dependencies [8]. For instance, an individual (agent) may learn about recent sport results either from friends at work (one layer) or through social media (another layer). Sociologists have long pointed out that social interaction structures should not be reduced to single-layer networks [8]. However, multi-layer structures have only been studied intensively in the last decade [29]. Recently, they have been used in modeling the diffusion of innovation [35, 73]. Nevertheless, this is still a relatively fresh concept. One issue that arises with multi-layer networks is generalization of models' rules that where originally implemented on single-layer structures. For instance, one may assume that social influence is only effective if it comes from all the layers (the AND rule). However, it can also be assumed that the influence is effective even if it comes from only one layer (the OR rule) [34]. In this research, we follow the approach from [14] and study both variants.

1.2 Aim and objectives

The aim of my thesis is to develop mathematical models of binary opinion dynamics that can be used to model the diffusion of PV panels (or other renewable energy sources) in order to understand how various factors impact this complex process. The far-reaching goal is realized through the 3 objectives:

- **Objective 1:** Evaluate the role of the new parameter in the generalized, the one-dimensional Sznajd model.
- **Objective 2:** Evaluate the impact of the underlying network structure and the method of selecting the group of influence on the time evolution and stationary states in the q-voter model.
- **Objective 3:** Design a new model of eco-innovation diffusion. Analyze the model on a multi-layer network structure.

Objective 1 is to study generalization of an already well-established agent-based model of opinion dynamics. This is essential for a better understanding of model mechanics and the impact of, so far hidden under different variants, parameters. The research focuses on the Sznajd model (SM) [61], one of the most popular models of binary opinion dynamics. Since its birth in 2000, it has seen numerous modifications and adaptations. In [62], we provided a comprehensive review of the literature that arose around the model over two decades, and furthermore, proposed a new generalization that combines three different variants of the model, so far treated separately, into a single parameter. **Paper 1** contains a more detailed analysis of the impact of the new parameter on the probability and time of reaching a certain stationary state. In addition, the article proposes an even further extension of the model onto diluted systems that allow agents to move.

Objective 2 is to extend these models toward the final goal, i.e. modeling the diffusion of innovation, for which opinion dynamics is the key building block. This allows to examine a more basic model first, before covering it with additional parts. Building on untested foundations is a risky business and, scientifically speaking, of mediocre value. Hence, the focus lies on the q-voter model [12], another extensively studied model of binary opinions. **Paper 2** touches on the phenomenon of social polarization, present in the discussion on renewable energy sources and pro-environmental practices. It does so by combining the q-voter model with a double-clique topology, a structure containing negative links, and provides a valuable insight into the q-voter model and formation of opinions. **Paper 3** addresses one of the major issues that arose over the years and with the growing number of articles on this model – the method of selecting a group of influence (with or without repetitions). For years, the two variants of the model have been used interchangeably, with little or no concern from researchers.

Objective 3 is to construct a new model of the diffusion of PVs (or other renewables) and understand how various factors impact the process. For this part, previously studied agent-based models are utilized, coupled with multi-layer network structures. This approach allows to consider various types of heterogeneity, e.g., geographical location. **Paper 4** presents such a model. Then, its analysis is provided, with respect to the method of combining social influence from different layers (e.g., AND and OR rules mentioned in Section 1.1).

1.3 Contribution to the discipline of Mathematics

My research is interdisciplinary. Not only does it contribute to mathematics, but also to statistical physics, network science, and management science. Thus, it targets a wide audience.

Recent findings suggest that social spreading, e.g., diffusion of innovation, requires influence of a group (complex contagion) rather than of a single individual (simple contagion) [36]. Studies on such models of innovation diffusion have already been conducted, but mainly on the progressive ones, i.e. asymmetrical, in which individuals cannot unadopt. However, an innovation can be rejected [55]. Thus, the right approach would be a non-progressive one, in which individuals can revert to the unadopted state. This has been addressed by non-progressive models, but of simple contagion type [36]. There have been also attempts to use non-progressive complex contagion, but – to our best knowledge – limited to simple, non multi-layer graph structures [10]. Therefore, more realistic, non-progressive complex contagion modeling of innovation diffusion remains a gap yet to be

filled. And this is the novelty of my thesis. Precisely:

- The Sznajd model is a mathematical, non-progressive model of complex contagion (a pair of individuals is required to spread the opinion). Generalizing it for better understanding is a crucial step in filling this gap.
- The q-voter model is, in a sense, an extension of the Sznajd model. As such, it is a non-progressive, complex contagion model (q individuals are required to spread the opinion) as well. It has already been analyzed on multi-layer networks, but only those consisting of twin layers, i.e. layers represented by the same structure – two complete graphs, two square lattices, etc. Coupling it with a more complex network, one consisting of two structurally different layers, is a novelty.
- Finally, my new model of innovation diffusion, developed on the basis of my earlier research, fills the aforementioned gap, being both non-progressive and complex contagion.

1.4 Thesis structure

The remainder of this thesis is structured as follows. In Chapter 2, I provide precise descriptions of the Sznajd and q-voter models, and introduce the methods of analytical approximation used in this thesis. Then, in Chapter 3, I discuss the key findings of the 4 papers that form the core part of this thesis (which I refer to as **Papers 1 – 4**). Later, in Chapter 4, I provide a brief overview of articles I have published in the course of my undergraduate and graduate studies that do not constitute the core part of the thesis. Finally, in Chapter 5, I summarize the main findings.

Chapter 2

Models and methods

2.1 On agent-based modeling

As mentioned in Section 1.1, an agent-based model is most often understood as a simulation of certain interactions between agents, placed on a structure, symbolizing a network of acquaintances, contacts or cooperation [37]. Such a structure can be stored in an adjacency matrix, see Definition 2.1.

Definition 2.1. *Let $G = [G_{i,j}]$ denote the adjacency matrix for a network, being a connected simple graph, i.e., an unweighted, undirected graph containing no graph loops or multiple edges [20]. Then, for $i, j = 1, 2, \ldots, N$:*

- $\forall_i \forall_j G_{i,j} = 1 \iff$ *edge between i and j exists,*
- $\forall_i \forall_j G_{i,j} = 0 \iff$ *edge between i and j does not exist,*
- $\forall_i \forall_j G_{i,j} = G_{j,i}$,
- $\forall_i G_{i,i} = 0$.

Agents possess a set of characteristics, i.e. a vector of variables, with some being constant, others changing upon interaction with other agents. My thesis focuses on the binary (discrete) opinions models. There, each agent $i = 1, 2, \ldots, N$ is characterized by a single binary variable (or a pair of binary variables in **Paper 4**), denoting its opinion, S_i, on a given matter, positive, $S_i = +1$, or negative, $S_i = -1$ (or adoption state – adopted/unadopted in **Paper 4**, denoted with A_i). N denotes the size of the system (network), i.e. the number of agents. To present the state of the system on the macroscopic level, two measures are often used: concentration and magnetization.

Definition 2.2. *Let N be number of agents and $S_i = \pm 1$ opinion of agent i, for $i = 1, 2, \ldots, N$. Then, the concentration (or fraction) of positive opinions is given by the following formula:*

$$c^+ = \frac{1}{2N} \sum_{i=1}^{N} (S_i + 1). \tag{2.1}$$

By definition $c^+ \in [0, 1]$. Naturally, one could use the concentration of negative opinions, c^-, as well. However, as $c^+ + c^- = 1$, a common approach is to use $c = c^+$ and call it concentration, for simplicity. Another macroscopic measure is magnetization, also known as the average opinion [48].

Definition 2.3. *Let N be number of agents and $S_i = \pm 1$ opinion of agent i, for $i = 1, 2, \ldots, N$. Then, the magnetization (or average opinion) is given by the following formula:*

$$m = \frac{1}{N} \sum_{i=1}^{N} S_i. \tag{2.2}$$

These two quantities are often used interchangeably, as they are bound linearly by a simple relationship.

Corollary 2.1. *Let c denote the concentration of positive opinions and m – the magnetization. Then:*

$$m = 2c - 1. \tag{2.3}$$

To provide statistically accurate results, often multiple Monte Carlo simulations are required. Each simulation (trial/trajectory) is independent, starts from a given set of initial conditions (initial state) and runs until a stationary state or a specified time horizon T is achieved (final state). Time in this kind of models is usually measured in the so-called Monte Carlo steps (MCS).

Definition 2.4. *Monte Carlo step (MCS) is defined as a unit of time, consisting of N elementary updates (with N being the number of agents), each corresponding to time step Δt, i.e. $N\Delta t = 1$ [9].*

To see the general properties of a model, outcomes across the simulations can be compressed, e.g., averaged, into a single value. For instance, into an empirical probability of reaching a certain stationary state or average time to reach it.

2.2 The Sznajd model[2]

In the original formulation of the Sznajd model (SM), we consider a system consisting of N agents, each of whom has at time t opinion $S_i(t) = +1$ or $S_i(t) = -1$ for $i = 1, 2, \ldots, N$ [61]. Agents are placed in a one-dimensional lattice with periodic boundary conditions. A single simulation run is described in detail in Algorithm 1. In all Algorithms in this thesis, $\mathcal{U}[0, 1]$ stands for a continuous uniform distribution, while $\mathcal{U}\{X\}$ – for a discrete one, where each element from set X is chosen with equal probability. This version of the SM is known as USDF (*united we stand, divided we fall*) [61]. For a graphical representation, check Fig. 2.1. Note that in this Section S stands for the opinion for consistency with the rest of the thesis. In [62], it was denoted by σ.

Time is measured in Monte Carlo steps (MCS), as per Definition 2.4. Note, that within such a formulation every agent has a chance to change twice as many times in the SM as usually in MCS. However, it was shown that this difference in updating can be easily

[2]This Section is largely based on Section *The model* from [62].

Algorithm 1: Original Sznajd model

for $t \coloneqq 1$ **to** T **do**
  for $k \coloneqq 1$ **to** N **do**
    $i \coloneqq i \sim \mathcal{U}\{1, \ldots, N\}$
    if $S_i = S_{i+1}$ **then**
      $S_{i-1} \coloneqq S_i$
      $S_{i+2} \coloneqq S_i$
    else
      $S_{i-1} \coloneqq -S_i$
      $S_{i+2} \coloneqq -S_{i+1}$
    end
  end
  if $\forall i \ S_i = S_{i+2}$ **then**
    break
  end
end

suppressed by picking randomly only one neighbor of a pair, $i - 1$ or $i + 2$. As shown, it would result only in the rescaling of time by 2 [58].

In [61] another rule was also proposed under the name *if you do not know what to do, just do nothing*, which simply means: skip whole **else** part in Algorithm 1. This rule was used in most of later papers, starting from the two-dimensional rule introduced in [59]. Many other people could try to act somehow even in a situation of uncertainty. Therefore, another natural rule would be *if you do not know what to do, just do whatever*. In fact, such a rule was introduced later within the original q-voter formulation [12], see section 2.3.

These two rules and the original one could be simply incorporated within one generalized model. It would rely on a small reformulation of Algorithm 1, see Algorithm 2. Thus, 3 different values of p correspond to 3 different variants: $p = 1$ (*united we stand,*

Algorithm 2: Generalized Sznajd model

for $t \coloneqq 1$ **to** T **do**
  for $k \coloneqq 1$ **to** N **do**
    $i \coloneqq i \sim \mathcal{U}\{1, \ldots, N\}$
    if $S_i = S_{i+1}$ **then**
      $S_{i-1} \coloneqq S_i$
      $S_{i+2} \coloneqq S_i$
    else if $r \sim \mathcal{U}(0, 1) < p$ **then**
      $S_{i-1} \coloneqq -S_i$
      $S_{i+2} \coloneqq -S_{i+1}$
    end
  end
  if $\forall i \ S_i = S_{i+2}$ **then**
    break
  end
end

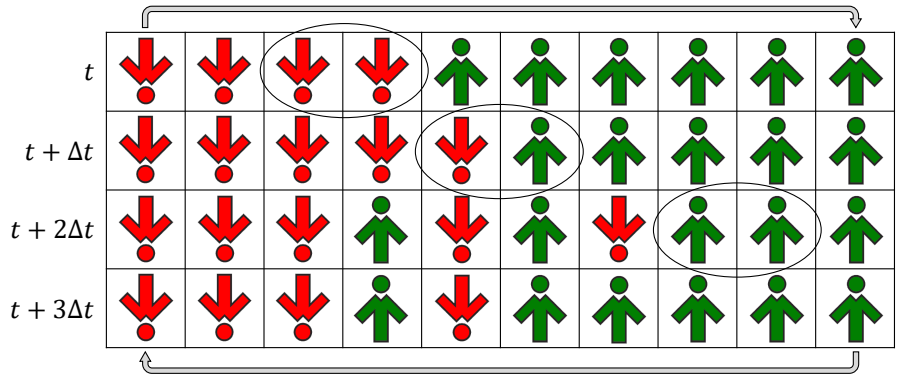

Figure 2.1: Visualization of the model. Example of several consecutive updates in the system of $N = 10$ agents with periodic boundary conditions, so the leftmost agent is a neighbor of the rightmost one. Source: **Paper 1**.

divided we fall), $p = 0.5$ (*if you do not know what to do, just do whatever*) and $p = 0$ (*if you do not know what to do, just do nothing*). It should be noted that for $p = 1$ two types of absorbing states exist: consensus, i.e. all the agents express the same opinion (positive, $c = 1$ or negative, $c = 0$) and disagreement, in which every agent has opinion opposite to its closest neighbors ($c = 0.5$). For $p \ll 1$ consensus is always reached, unless disagreement is the initial condition of the system. In other words, disagreement state is a fixed point for any p, but stable only for $p \to 1$ (more detailed study in Section 3.1).

2.3 The q-voter model

As mentioned in Section 1.2, the q-voter model is one of the most extensively studied models in the field of binary opinion dynamics. As with the SM, we consider a set of N agents, each characterized by a single variable – an opinion, either positive $(S_i = +1)$ or negative $(S_i = -1)$. However, in contrast to the SM, the dynamics is not limited to a one-dimensional lattice with periodic boundaries, i.e. a ring, but can be coupled with any graph structure without further adjustments. For the visualization of the model dynamics, see Fig. 2.2.

In the original formulation of the q-voter model [12], all agents were susceptible to social pressure at all times. However, over the years, a modification of the model became common, the so-called q-voter model with independence [47, 48]. Unsurprisingly, this extension included a possibility for an agent to act independently of its neighbors. Additionally, it neglected the probability ϵ present in the original version [12]. See Algorithm 3 for a detailed description of the q-voter model with independence. In there, G is the adjacency matrix for the underlying structure, as in Definition 2.1. This version, the q-voter model with independence, forms the basis for further modifications in **Papers 2 – 4**.

2.4 Analytical methods

In the field of agent-based modeling, Monte Carlo computer simulations are the main research method. It is the only method that can incorporate all the heterogeneities and

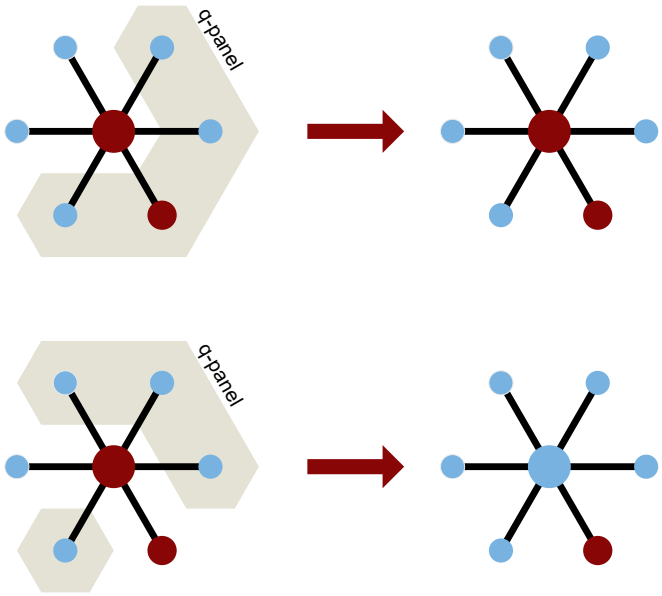

Figure 2.2: Illustration of two possible configurations. The center circle portrays the target agent, the smaller ones portray its neighbors. Light blue color represents a positive opinion ($S = +1$), dark red represents a negative one ($S = -1$). Beige color marks a chosen group of influence. Degree $k = 6$ and size of the influence group $q = 4$ in both cases. The first (top) group of influence is not unanimous and provides no change, while the second one (bottom) is unanimous and leads to change in target's opinion. Source: **Paper 3**.

Algorithm 3: q-voter model with independence

for $t := 1$ **to** T **do**
  for $k := 1$ **to** N **do**
    $i := i \sim \mathcal{U}\{1, \ldots, N\}$
    $r := r \sim \mathcal{U}[0, 1]$
    if $r < p$ **then**
      $r := r \sim \mathcal{U}[0, 1]$
      if $r < \frac{1}{2}$ **then**
        $S_i := -S_i$
    else
      for $l := 1$ **to** q **do**
        $j_l := j \sim \mathcal{U}\{j : G_{i,j} = 1\}$
      end
      $Q := \frac{1}{q} \sum_l^q S_{j_l}$
      if $Q = -S_i$ **then**
        $S_i := -S_i$
    end
  end
end

local interactions between agents, usually occurring in this kind of models. However, it possesses a number of flaws. First and foremost, it is computationally demanding. The need to examine a vast space of input parameters and the need for numerous simulations to obtain statistically accurate results leads to long run times. For this reason, analyti-

cal methods such as mean-field (MFA) [48] or pair approximation (PA) [21] have been proposed. These methods work well for random graphs with a low clustering coefficient and perfectly for complete graphs. Unfortunately, real life networks are far from these assumptions, often being characterized by a high clustering coefficient [5]. Due to this fact, MFA and PA are merely what they are called – approximations. While, they cannot simply replace Monte Carlo simulations, they do provide an insight into model dynamics over a vast space of parameters.

The mean-field approximation for the q-voter model with independence was originally presented in [48]. In this approach, we neglect the actual structure of the network and assume complete homogeneity, i.e. every agent can interact with any other, as if the network was a complete graph of size $N \to \infty$. Here, I only recall the final differential equation:

$$\frac{\mathrm{d}c}{\mathrm{d}t} = (1-c)\left(\frac{1}{2}p + (1-p)c^q\right) - c\left(\frac{1}{2}p + (1-p)(1-c)^q\right), \tag{2.4}$$

in which c is concentration of opinions, as per Definition 2.2. This basic form is not used directly in **Papers 1 – 4**. However, its extended versions, adjusted to the specifics of the models, are derived in **Papers 2 – 4** and shown in Chapter 3.

The pair approximation is a more advanced, though not always superior, method. It supplements the MFA with a second equation for the time evolution of density ρ of active links, i.e. edges connecting agent of opposite opinions [21].

Definition 2.5. *Let N be number of agents, $S_i = \pm 1$ opinion of agent i, for $i = 1, 2, \ldots, N$, and G the adjacency matrix of the underlying network. Then, the density of active links is given by the following formula:*

$$\rho = \frac{\sum_{i=1}^{N}\sum_{j=1}^{N}\left(1 - S_i S_j\right) G_{i,j}}{2\sum_{i=1}^{N}\sum_{j=1}^{N} G_{i,j}}. \tag{2.5}$$

In real world networks lots of triads (triangles of agents) are observed, i.e. the clustering coefficient is high [5]. In the PA the structure is replaced with the density of active links (active pairs) ρ. Hence, this method is still flawed, as is the MFA, although it works better for random graphs with a low clustering coefficient. For the q-voter model with independence, PA was derived first in [28]. Below, the formulas from [26] are presented (with minor notation changes for consistency):

$$\begin{aligned}
\frac{\mathrm{d}c}{\mathrm{d}t} &= \sum_{i=\oplus,\ominus} c_i \sum_k P(k) \sum_{l=0}^{k} \binom{k}{l} (1-c_i)^l c_i^{k-l} f(l,i,k)(-S_i), \\
\frac{\mathrm{d}\rho}{\mathrm{d}t} &= \sum_{i=\oplus,\ominus} c_i \sum_k P(k) \sum_{l=0}^{k} \binom{k}{l} (1-c_i)^l c_i^{k-l} f(l,i,k) \frac{2}{\langle k \rangle}(k-2l),
\end{aligned} \tag{2.6}$$

where $c_\oplus = c$, $c_\ominus = 1 - c$, $S_\oplus = 1$, $S_\ominus = -1$, $\langle k \rangle$ is the average network degree, $P(k)$ is the network degree distribution and the function $f(l,i,k)$ is model-dependent probability of changing current opinion i of an agent that is in disagreement with exactly l voters among all its k neighbors. Model-specific PA is derived in **Paper 3** and presented in Section 3.3.

Chapter 3

Summary of results

3.1 On reaching consensus (Paper 1)

As described in Section 2.2, the article [62] introduced a generalization of the model that combines all 3 variants under a single parameter. This parameter, p, could be named the probability of disagreeing with your neighbor in case of uncertainty. In there, we only studied the impact of p, initial concentration $c(0) = c_0$ and initial spacial distribution of opinions on probabilities of reaching a particular absorbing state. And we did it only by Monte Carlo simulations for the size of the system $N = 100$. Obviously, the final state depends on the initial one. However, not only does the initial concentration c_0 matter, but so does the initial spacial distribution of opinions. In [62], two types of them have been examined:

- Random: at time $t = 0$ each agent $i = 1, \ldots, N$ has a positive opinion, $S_i(0) = 1$, with probability c_0, and a negative one, $S_i(0) = -1$, with complementary probability $1 - c_0$.
- Sorted: at time $t = 0$ each agent $i = 1, \ldots, \lfloor Nc_0 \rfloor$ has a positive opinion, $S_i(0) = 1$, and each agent $i = \lfloor Nc_0 \rfloor + 1, \ldots, N$ – a negative one, $S_i(0) = -1$.

In **Paper 1**, we examined the generalized Sznajd model more thoroughly, for different sizes $N > 100$, and found out that for any $p \ll 1$ the probability of positive consensus as the final state, $c = 1$, can be approximated by:

- for random initial conditions:

$$P_+ = \frac{c_0^2}{c_0^2 + (1 - c_0)^2}, \tag{3.1}$$

- for sorted initial conditions:

$$P_+ = c_0. \tag{3.2}$$

This is consistent with previous research on the Sznajd model with $p = 0$ [33, 58]. Comparison between the above formula (only random initial conditions) and simulated results is presented in Fig. 3.1 (top).

The second novelty was the time to reach consensus, τ (measured in MCS). Previously, it was measured only for $p = 0$ [58]. Obviously, $\tau = 0$ for $c_0 = 0$ or $c_0 = 1$, since

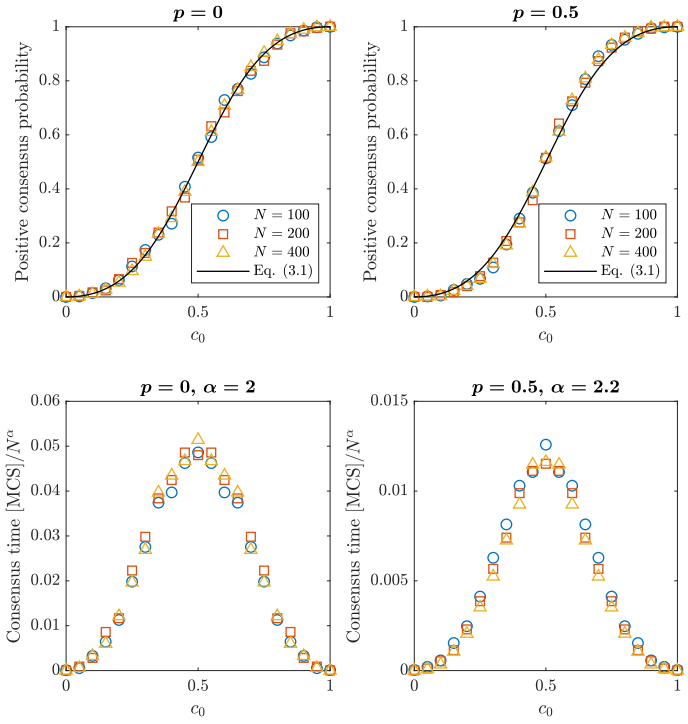

Figure 3.1: Comparison with theoretical approximations, see Eq. (3.1), and scaling with the system size N. Probability of reaching a positive consensus P_+ (top panels) and rescaled mean time to reach consensus (bottom panels) as functions of the initial concentration of positive opinion c_0. Results are presented for random initial conditions and two values of the probability of disagreeing: $p = 0$ (left panels) and $p = 0.5$ (right panels). The scaling exponent α was determined numerically. Source: **Paper 1**.

these initial states are already absorbing ones. We showed that τ has the maximum value for $c_0 = 0.5$, see Fig. 3.1 (bottom), and that times are shorter for the random initial conditions than for the ordered ones (Fig. 3.2, bottom). Moreover, we performed a size scaling and showed the impact of size N on the time to reach consensus (Fig. 3.1, bottom). This time scales with the size, as N^α, where $\alpha \geq 2$ (exact value depends on p).

As shown in Fig. 3.2 (top), consensus (positive $c = 1$ or negative $c = 0$) as the final state is always the case, unless $p > p^* \approx 0.8$. For $p > p^*$, the probability of disagreement state grows and reaches its maximum for $p = 1$. The lower the initial concentration c_0, the higher the probability of consensus (negative in this case), as the system already begins close to it. Additionally, time to reach consensus depends on p as well, but in a non-trivial way, see Fig. 3.2 (bottom). The time needed to reach consensus decreases as p increases, but only up to a certain point. Around $p^* \approx 0.8$ it reaches its minimum, and then starts to increase. This is, of course, correlated with the probability of consensus. With the second absorbing state (disagreement) emerging, the system takes longer to "decide" which path to choose. Still, $p^* \approx 0.8$ being the minimum is a surprising outcome. This means that consensus is achieved faster if we disagree with our neighbors more often.

Hence, the takeaway from **Paper 1** should be: to reach consensus, disagree with your neighbor. In a more articulate way, it is beneficial to exchange opinions more frequently, even if we disagree. This is a valid conclusion for diffusion of innovation as well. Additionally, we explored a variant of the SM model with empty spaces in the lattice and possibility of movement for agents. For more details, I encourage the reader to look into **Paper 1**.

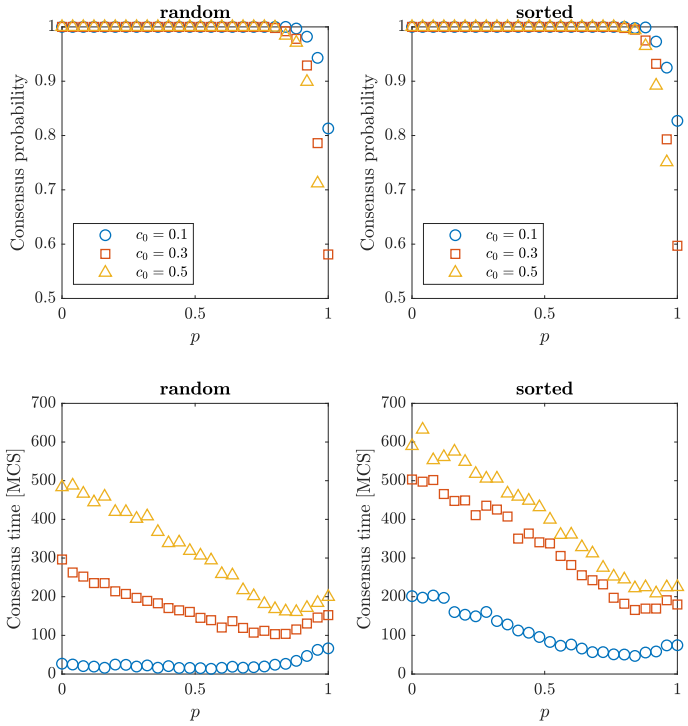

Figure 3.2: The impact of the initial concentration of positive opinion c_0. Probability of reaching consensus (top panels) and mean time to reach consensus (bottom panels) as a function of the probability of disagreeing p. Results are presented for the system size $N = 100$, under two types of initial conditions: random (left panels) and sorted (right panels). Source: **Paper 1**.

Publication details (Paper 1):

- Published as: Weron, T., & Sznajd-Weron, K. (2022). On reaching the consensus by disagreeing. Journal of Computational Science, 61, 101667.
- $\text{IF}_{2Y} = 3.1$. MNiSW: 100 pts.
- My contribution: conceptualization, implementation, simulation, visualization, review and editing.

3.2 Opinion formation in polarized society (Paper 2)

In **Paper 2**, we explore the phenomenon of social polarization. Polarization is wide concept and object of research in social and political sciences, and even economics. However, its definition differs between various fields. We use the one given in [16], i.e. that polarization is a state of a community divided into two opposing groups (cliques), characterized by opposing opinions on a given issue. This phenomenon is also known in the literature as bi-polarization, in order to distinguish it from the group polarization, the tendency for a group to take increasingly extreme decisions [24, 60]. Social polarization is alarmingly increasing in modern societies [4, 65]. Hence, the growing interest among researchers, social scientists, economists, statistical physicists and mathematicians.

In **Paper 2**, we further explore the model from our previous works [32,57]. It is based on the q-voter model and studied on the so-called double-clique network, which mimics echo chambers observed, for example, in modern social media [50]. Here, we extend this model by introducing the independence of agents, thereby putting it on par with the q-voter model with independence, while retaining our unique network structure.

In the model, we consider a set of $2N$ agents divided into two cliques, each of size N. Each clique is a complete graph with positive links within, and the two cliques are connected by $L \times N^2$ negative cross-links. The parameter L is a fraction of existing cross-links, out of N^2 possible. Agents act as conformists when affected by members of their own clique, and as anti-conformists when affected by those from the other clique. For this, we can use a slightly different version of an adjacency matrix.

Definition 3.1. *Let $G = [G_{i,j}]$ denote the adjacency matrix for the double-clique network, i.e. two complete graphs (cliques A and B) with positive links within, connected by negative cross-links, and X_i be clique to which agent i belongs ($X_i = A, B$). Then, for $i, j = 1, 2, \ldots, 2N$:*

- $\forall_i \forall_j G_{i,j} = 1 \iff$ *edge between i and j exists and $X_i = X_j$,*
- $\forall_i \forall_j G_{i,j} = -1 \iff$ *edge between i and j exists and $X_i \neq X_j$,*
- $\forall_i \forall_j G_{i,j} = 0 \iff$ *edge between i and j does not exist,*
- $\forall_i \forall_j G_{i,j} = G_{j,i}$,
- $\forall_i G_{i,i} = 0$.

The precise description of single simulation run is presented in Algorithm 4 and the visualization of conformist/anti-conformist dynamics is shown in Fig. 3.3. Here, a slightly different notation than in **Paper 2** is used to keep consistency within this thesis.

In [32], we introduced the mean-field approach, in which $L \times N^2$ cross-links are replaced by a single probability h.

Definition 3.2. *Let $L \times N^2$ be number of cross-links between the two cliques. Then:*

$$h = \frac{LN^2}{LN^2 + 2\frac{N(N-1)}{2}} \overset{N\to\infty}{\to} \frac{L}{L+1} \tag{3.3}$$

is the probability of the target agent choosing a neighbor from the other clique and $1 - h$ is the probability of choosing a neighbor from its own clique.

Algorithm 4: q-voter model with independence on double-clique network

for $t \coloneqq 1$ **to** T **do**
  for $k \coloneqq 1$ **to** $2N$ **do**
    $i \coloneqq i \sim \mathcal{U}\{1, \ldots, 2N\}$
    $r \coloneqq r \sim \mathcal{U}[0, 1]$
    if $r < p$ **then**
      $r \coloneqq r \sim \mathcal{U}[0, 1]$
      if $r < \frac{1}{2}$ **then**
        $S_i \coloneqq -S_i$
    else
      for $l \coloneqq 1$ **to** q **do**
        $j_l \coloneqq j \sim \mathcal{U}\{j : |G_{i,j}| = 1\}$
      end
      $Q \coloneqq \frac{1}{q} \sum_l^q S_{j_l} G_{i,j}$
      if $Q = -S_i$ **then**
        $S_i \coloneqq -S_i$
    end
  end
end

This approach allows for mathematical treatment. First, by defining concentration and magnetization separately for each clique (A and B), analogously to Definition 2.2.

Definition 3.3. *Let $2N$ be number of agents, $S_i = \pm 1$ opinion of agent i, for agents $i = 1, 2, \ldots, N$ belonging to the clique A and agents $i = N+1, N+2, \ldots, 2N$ to the clique B. Then, the concentrations of positive opinions for cliques A and B are given by:*

$$c_A = \frac{1}{2N} \sum_{i=1}^{N} (S_i + 1), \quad c_B = \frac{1}{2N} \sum_{i=N+1}^{2N} (S_i + 1). \tag{3.4}$$

Corollary 3.1. *Let c_A, c_B denote the concentrations of positive opinions and m_A, m_B – the magnetizations for the cliques A and B, respectively. Then:*

$$m_A = 2c_A - 1, \quad m_B = 2c_B - 1. \tag{3.5}$$

Analogously to [32], we derive the equations describing the system dynamics.

Theorem 3.1. *Let c_A, c_B denote the concentrations of positive opinions in cliques A, B, and the probabilities of choosing an agent with a positive opinion in cliques A, B, respectively, and h – the probability of choosing a neighbor from the other clique (Definition 3.2). Under the assumptions that these events are independent, and that the network is of size $2N \to \infty$, the dynamics of the system is described by the pair of equations:*

$$\begin{aligned} \frac{dc_A}{dt} &= \bar{c}_A \left(\frac{1}{2}p + \bar{p} \left(\bar{h} c_A + h \bar{c}_B \right)^q \right) - c_A \left(\frac{1}{2}p + \bar{p} \left(\bar{h} \bar{c}_A + h c_B \right)^q \right), \\ \frac{dc_B}{dt} &= \bar{c}_B \left(\frac{1}{2}p + \bar{p} \left(\bar{h} c_B + h \bar{c}_A \right)^q \right) - c_B \left(\frac{1}{2}p + \bar{p} \left(\bar{h} \bar{c}_B + h c_A \right)^q \right), \end{aligned} \tag{3.6}$$

where $\bar{c}_A = 1 - c_A$, $\bar{c}_B = 1 - c_B$, $\bar{h} = 1 - h$ and $\bar{p} = 1 - p$.

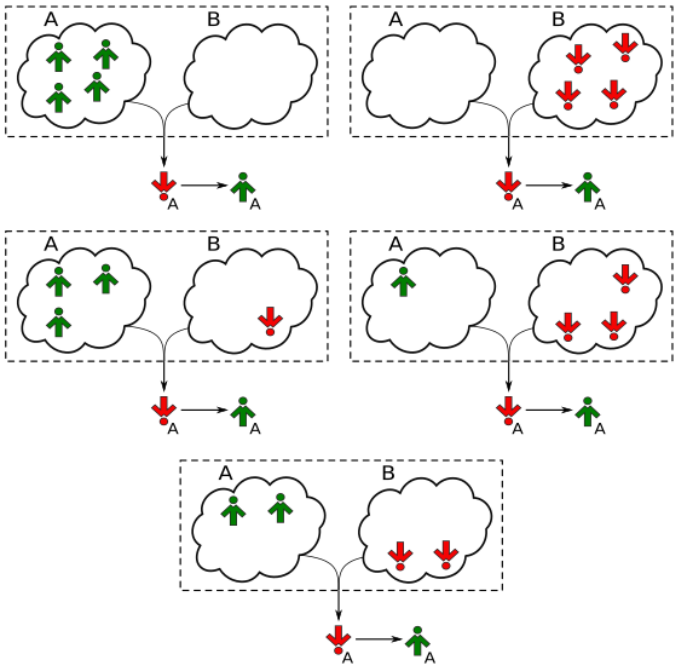

Figure 3.3: All possible choices of the influence group in the model with $q = 4$ that lead to an opinion flip by a target from clique A that was initially in state $S = -1$. The influence group may contain members from both cliques. Due to the presence of both positive and negative links, the concept of unanimity from the original q-voter model has to be extended to signals, which are then received by the target of influence. A signal is the state of a member times a sign of the link between it and the target. The target changes its opinion only if all members of the influence group emit the same signal. Source: **Paper 2**.

Proof. See Section 2.6 in **Paper 2**. □

We analyze both models: the one with fixed $L \times N^2$ cross-links by Monte Carlo simulations, the one with the probability h – numerically, based on Eqs. (3.6). Comparison between them is presented in Fig. 3.4. The system always starts in total consensus ($m_A(0)m_B(0) = 1$) initially, i.e. all the agents have the same opinion. That was our choice, to see how the presence of negative cross-links L and independence p can disrupt it. The system retains consensus ($m_A m_B \approx 1$) or transitions to one of two other final states, depending on values of L and p: polarization or disorder. Polarization means that both cliques are unanimous inside, but opposite to each other ($m_A m_B \approx -1$). Disorder is when there is no unanimity in any of the cliques ($m_A \approx 0$, $m_B \approx 0$). As shown in Fig. 3.4, $L > 0$ is necessary for polarization to occur. In both models, there are critical values L^* for which the system transitions from consensus to polarization, although the exact values depend on the model and independence p. The impact of p is twofold. For low values, $p \lesssim 0.2$, it aids polarization, by lowering L^*, as it disrupts the initial consensus. Simultaneously, it prevents both total consensus ($m_A m_B = 1$) and total polarization ($m_A m_B = -1$), since there always remains a fraction of independent agents. For large values, $p \gtrsim 0.2$, independence disables any other state but total disorder ($m_A m_B = 0$). Lastly, differences between the simulations and the MFA are only quantitative, i.e. the exact values of L and p required to transition between the states differ, but the overall picture remains. This shows, that the mean-field approximation works well in case of double-clique network.

Paper 2 provides a valuable insight to opinion dynamics. It examines the behavior

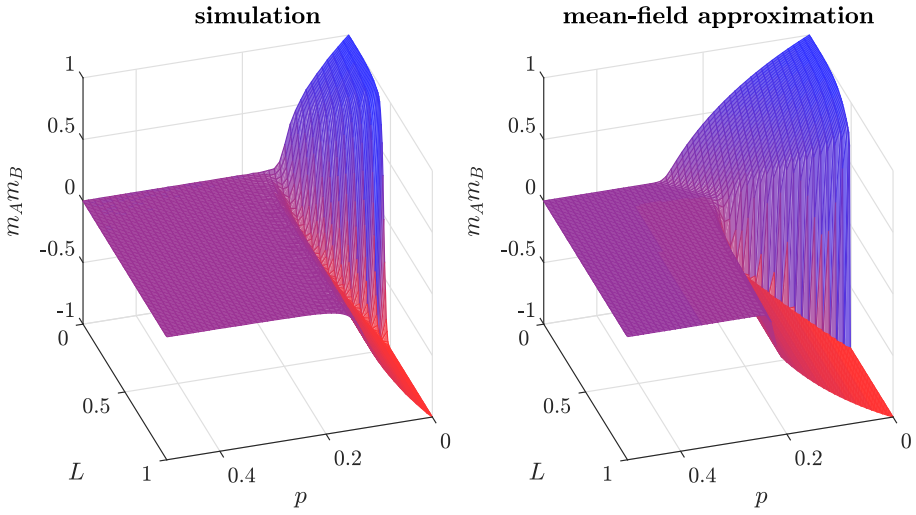

Figure 3.4: Comparison between simulations (left) and the MFA (right), given by Eqs. (3.6): final product of magnetizations $m_A m_B$. The blue, red and purple colors correspond to consensus, polarization and disorder, respectively. In both approaches, we can observe that the critical value L^* decreases with an increase of p, while L has only a marginal impact on p^*. Source: **Paper 2**.

of the q-voter model with independence on a non-trivial network structure, i.e. double-clique topology. Opinions matter when it comes to adopting a new product [70] and we incorporate the opinion part into the diffusion of innovation later, in **Paper 4**.

Publication details (Paper 2):

- Weron, T., & Szwabiński, J. (2022). Opinion evolution in divided community. Entropy, 24(2), 185.
- $\text{IF}_{2Y} = 2.1$. MNiSW: 100 pts.
- My contribution: conceptualization, implementation, simulation, analysis, visualization, review and editing.

3.3 To repeat, or not to repeat (Paper 3)

At first, **Paper 3** may seem as a side quest, not touching directly any social phenomenon. However, it focuses on an aspect of the q-voter model that remained neglected for years. Within the original formulation [12], see Section 2.3, a possibility of repetition was present when constructing the group of influence. This approach was followed by some researchers [41,44,67]. Others took the opposite path and forbade the possibility of repetition [1,2,13,23,28,47]. Some did not even specify it (with repetitions or without) at all [25,45,63,64]. To date, to the best of our knowledge, only one article addressed this issue [68]. In **Paper 3**, we further examine whether there are differences between these two variants and how significant they are (see Fig. 3.5 for visualization of differences in the dynamics). We refer to these as *repetition* and *no repetition* variants. The *repetition* variant is presented in Algorithm 3. For the *no repetition* variant, one minor modification is required, precisely: $j_l \coloneqq j \sim \mathcal{U}\{j : G_{i,j} = 1 \ \wedge \ j \neq j_1, \ldots, j_{l-1}\}$.

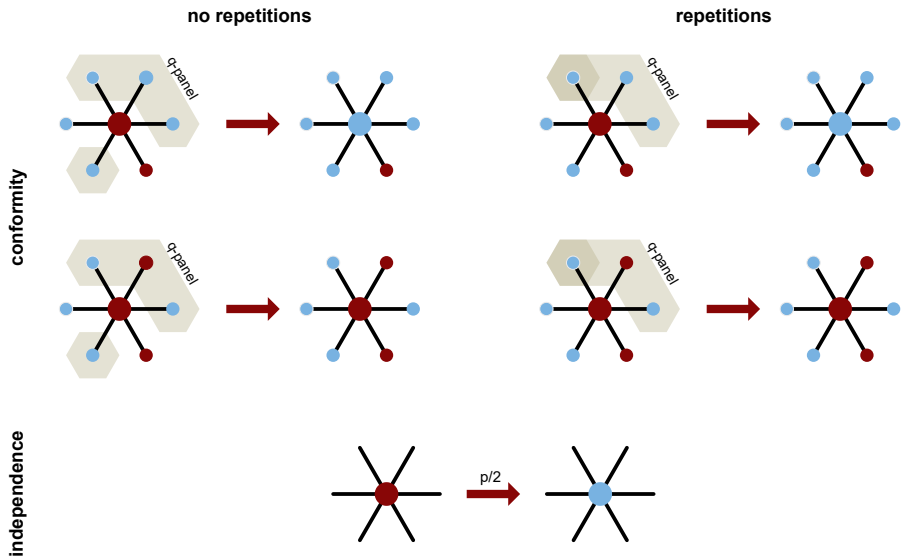

Figure 3.5: Depiction of the model dynamics in the *no repetition* (left) and the *repetition* (right) variants. The upper part corresponds to conformist behavior (probability $1-p$), while the bottom one corresponds to independence (probability p). The big circle portrays the target agent, smaller ones portray its neighbors. Light blue color represents a positive opinion ($S = +1$), dark red represents a negative one ($S = -1$), and beige marks a randomly chosen group of influence, with darker beige for repetitive choice. Degree $k = 6$ and size of the influence group $q = 4$ in all the above cases. Source: **Paper 3**.

For this task, we use not only Monte Carlo simulations, but MFA and PA as well. Simulations are treated as the "real" result. Then, we adapt approximation methods and check how they perform. All simulations are conducted on a random regular graph, i.e. a connected graph in which each node (agent) has the same degree (number of neighbors) k. We expected the differences between the *no repetition* and *repetition* variants to be most pronounced when the size of the group of influence q is close to the degree k. Hence the random regular graph, in which we can easily manipulate the degree k. However, we performed simulations on other networks (square lattice, Watt-Strogatz graph [69]) as well. The results, though not included in **Paper 3**, remain qualitatively the same.

For comparison between the variants in simulated results, see Fig. 3.6. There, we show the final concentration c as a function of probability of independence p. Indeed,

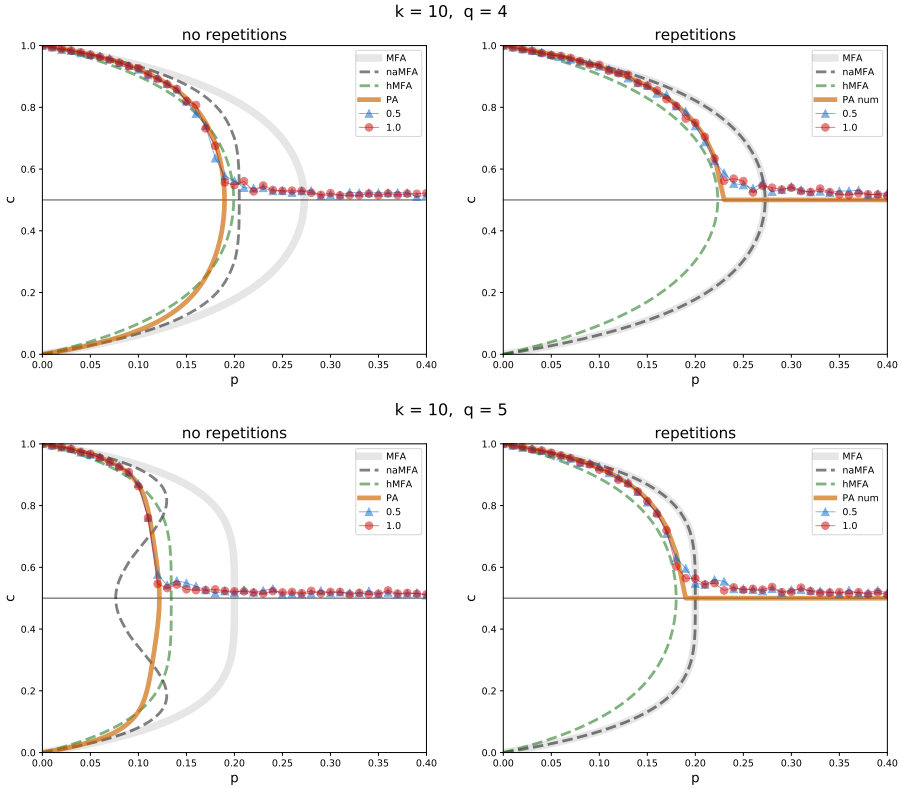

Figure 3.6: Comparison between the simulation results and the approximation methods in the *no repetition* (left) and *repetition* (right) variants, for a random regular graph of size $N = 1000$, with the degree $k = 10$ and the sizes of the group of influence $q = 4$ (top), and 5 (bottom). The solid, light gray line indicates the ordinary MFA, the dashed dark gray one indicates the network aware mean-field approximation (naMFA), the dashed green one indicates the heuristic mean-field approximation (hMFA), and the solid orange one indicates the PA. Simulation results for the initial concentration $c(0) = 0.5$ (blue triangles) and 1 (red circles) are shown. In the *repetition* variant, the PA is obtained numerically. Source: **Paper 3**.

there is a visible difference between the variants. In the *no repetition* scenario, critical value of p, p^*, required for the system to transition from consensus to disorder is significantly lower than in the *repetition* one. The closer the size of group of influence q to the degree k, the more articulated the difference. This result clearly shows that these variants of the q-voter model cannot be used interchangeably. Lastly, two sets of initial conditions ($c(0) = 0.5$ and $c(0) = 1$) are used there to check if that makes a difference – it does not.

The first approximation method that we use is the MFA. The classical MFA assumes the possibility of repetition, see Eq. (2.4). To account for the *no repetition* variant, we introduce a modified MFA, which we call the network aware mean-field approximation (naMFA).

Theorem 3.2. *Let c denote the concentration of positive opinions and the probability of choosing an agent with a positive opinion. Under the assumptions that these events are independent, and that the network is of size $N \to \infty$, the dynamics of the system in the repetition variant is described by:*

$$\frac{dc}{dt} = (1-p)\alpha + p\beta, \tag{3.7}$$

where

$$\alpha = (1-c)c^q - c(1-c)^q, \tag{3.8}$$
$$\beta = \frac{1}{2}(1-c) - \frac{1}{2}c.$$

Under the additional assumption that every agent chooses q neighbors without repetitions only from randomly determined k neighbors at any given moment, α and β in the no repetition variant are described by:

$$\alpha = (1-c)\prod_{i=0}^{q-1}\max\left[\frac{k\times c - i}{k-i}, 0\right] - c\prod_{i=0}^{q-1}\max\left[\frac{k\times(1-c)-i}{k-i}, 0\right], \tag{3.9}$$
$$\beta = \frac{1}{2}(1-c) - \frac{1}{2}c.$$

Proof. See Section 2.2 in **Paper 3**. □

In order to find the stationary states analytically, $\frac{\mathrm{d}c}{\mathrm{d}t} = 0$, we must satisfy the following relationship:

$$p = \frac{\alpha}{\alpha - \beta}. \tag{3.10}$$

And this is what is shown in Fig. 3.6 under the names MFA, α from Eq. (3.8), and naMFA, α from Eq. (3.9). In the *repetition* variant naMFA is replaced by MFA, i.e. Eq. (3.8). Unfortunately, these approximations are far from perfect, especially for $q = 5$ in the *no repetition* variant.

The second method is the PA. Concentration c is complemented here by the fraction of active links ρ (Definition 2.5), as in Eq. (2.6).

Theorem 3.3. *Let c denote the concentration of positive opinions and the probability of choosing an agent with a positive opinion, and ρ – the fraction of active links and the probability of choosing a neighbor with an opposite opinion. Under the assumptions that these events are independent, and that the network is of size $N \to \infty$, the dynamics of the system is described by:*

$$\frac{dc}{dt} = \sum_{i=\oplus,\ominus} c_i \sum_{l=0}^{k}\binom{k}{l}(1-c_i)^l c_i^{k-l} F(l,k,q,p)(-S_i),$$
$$\frac{d\rho}{dt} = \sum_{i=\oplus,\ominus} c_i \sum_{l=0}^{k}\binom{k}{l}(1-c_i)^l c_i^{k-l} F(l,k,q,p)2(k-2l). \tag{3.11}$$

where

$$F(l,k,q,p) = \frac{p}{2} + (1-p)f(l,k,q), \tag{3.12}$$

is the probability that an agent with k neighbors and l active links changes its opinion, in which

$$f(l,k,q) = \begin{cases} \binom{k-q}{l-q}/\binom{k}{l}, & \textit{no repetition}, \\ \left(\frac{l}{k}\right)^q, & \textit{repetition}. \end{cases} \tag{3.13}$$

In the no repetition variant $f(l,k,q) = 0$ if $k < q$.

Proof. See Section 2.3 in **Paper 3**. □

Note a few changes in the notification (from **Paper 3**) for consistency within this thesis. In the *no repetition* variant, one can, under condition $\frac{\mathrm{d}c}{\mathrm{d}t} = 0$, derive the following relationship:

$$p^{-1} = 1 + \frac{2^{q-1}\left(\frac{k-1}{k-2}\right)^q}{q-1}. \tag{3.14}$$

Unfortunately, in the *repetition* one, terms in Eq. (3.11) do not reduce, and a closed-form expression does not exist. Thus, one must rely on numerical solution. The PA is also shown in Fig. 3.6. It visibly outperforms MFA and naMFA.

Once more, we resort back to MFA to derive equations that can be solved entirely analytically. In this approach, referred to as the heuristic mean-field approximation (hMFA), we include the probability of constructing an unanimous group of influence, for a given local configuration of opinions.

Theorem 3.4. *Let c denote the concentration of positive opinions and the probability of choosing an agent with a positive opinion. Under the assumptions that these events are independent, that the network is of size $N \to \infty$, and that every agent first chooses k agents randomly, and then q neighbors out of these k, the dynamics of the system is described by:*

$$\frac{dc}{dt} = (1-p)\alpha + p\beta, \tag{3.15}$$

where

$$\begin{aligned}\alpha &= (1-c)\sum_{i=1}^{k}\binom{k}{i}c^i(1-c)^{k-i}\left(\frac{i}{k}\right)^q - c\sum_{i=1}^{k}\binom{k}{i}(1-c)^i c^{k-i}c\left(\frac{i}{k}\right)^q, \\ \beta &= \frac{1}{2}(1-c) - \frac{1}{2}c,\end{aligned} \tag{3.16}$$

in the repetition variant, and

$$\begin{aligned}\alpha &= (1-c)\sum_{i=q}^{k}\binom{k}{i}c^i(1-c)^{k-i}\prod_{j=0}^{q-1}\frac{i-j}{k-j} - c\sum_{i=q}^{k}\binom{k}{i}(1-c)^i c^{k-i}\prod_{j=0}^{q-1}\frac{i-j}{k-j}, \\ \beta &= \frac{1}{2}(1-c) - \frac{1}{2}c,\end{aligned} \tag{3.17}$$

in the no repetition one.

Proof. See Section 2.4 in **Paper 3**. □

Then, we can use Eq. (3.15) to compute stationary states, analogously to Eq. (3.10). Unfortunately, by itself, this approach still performs poorly when k is small in relative to q. Hence, we include a heuristic correction h to Eq. (3.15):

$$p' = \frac{\alpha}{\alpha - h\beta}, \tag{3.18}$$

where h ($h > 1$) is there to artificially magnify the impact of independence, which has greater effect in the case of low k than the classical MFA accounts for. It occurs that h should be a function of model parameters, $h = h(q,k,p)$. In **Paper 3** an example of $h(q,k,p)$ was proposed, however not derived, only guessed. For this reason, it bears no

significant value and is not included here. For details, see **Paper 3**. This approach, the hMFA, is presented in Fig. 3.6 as well. It performs slightly worse than the PA, but in return is solvable completely analytically.

They key points of **Paper 3** are the following. First, we show that the different variants of the q-voter model with independence, the *no repetition* and *repetition* one, differ in outcomes, especially when the average network degree k is low. Specifically, the critical value p^* for which the system transitions from consensus ($c \approx 1$) to disorder ($c \approx 0.5$) is lower in the *no repetition* variant. Therefore, they are not simply interchangeable. Second, we examine a number of approximation methods. The classical MFA and our slightly modified naMFA do not perform well when k is low and close to q. The PA and hMFA do much better, with the PA being the most accurate method. However, the PA provides a closed-form solution only in the *no repetition* variant, while the hMFA does so in both variants, and additionally yields much simpler formulas.

Publication details (Paper 3):

- Weron, T., Nyczka, P., & Szwabiński, J. (2024). Composition of the Influence Group in the q-Voter Model and Its Impact on the Dynamics of Opinions. Entropy, 26(2), 132.
- $\text{IF}_{2Y} = 2.1$. MNiSW: 100 pts.
- My contribution: conceptualization, implementation, analysis, visualisation, original draft preparation, review and editing.

3.4 Diffusion of photovoltaic installations (Paper 4)

In **Paper 4**, we introduce a new model of eco-innovation diffusion (PVs diffusion precisely). It utilizes q-voter-like dynamics, expanded however to a multi-layer structure. The aim is to model both opinion evolution and diffusion of the new product jointly. Therefore, we introduce a second agent's attribute, in addition to the opinion S – an adoption state A. It is a binary variable, same as opinion in the q-voter model, i.e. $S_i = \pm 1$, $A_i = \pm 1$ for $i = 1, 2, \ldots, N$. Positive value means that an agent possesses a PV installation, negative – it does not. An agent (representing a household in our model) can be tempted to install PVs in two ways. Either it sees panels on rooftops of neighbors, or discusses the matter with friends. Therefore, we utilize a two-layer network structure, to model this twofold dynamics. The first layer represents location of agents in space, similarly to [31, 56, 70]. For this reason, it is a square lattice (SL) with Moore's neighborhood [42], meaning that each agent possesses 8 neighbors surrounding it (except for agents in the corners and along the edges, which have 3 and 5 neighbors, respectively), and non-periodic boundaries. Through links of this layer, agent can only see PV panels, or lack thereof, on the roofs of its neighbors (adoption state). It cannot exchange opinions. For this, there is the second layer that depicts agents' friendships, contacts, relationships, etc. We desire a structure closely related to a SL, but with characteristics of real world social networks. Hence, we use two-dimensional Watts-Strogatz graph (WS2D) [7,46,69] to describe the second layer. In the special case (when randomness $\beta = 0$), WS2D reduces to a square lattice. In opposition to the first layer, here agents can only see others' opinions, not adoption states. Social influence, described by the q-voter dynamics, combined from the both layers (either AND or OR rule, similarly to [14]) impacts the target's opinion, not the adoption state. Finally, an agent with a positive opinion (but negative adoption state) decides to adopt with a certain probability, a_1. Analogously, a one with a negative opinion and positive adoption state unadopts with probability $a_2 = ha_1$, where $h \in (0, 1)$. We consider only $a_1 > a_2$ (i.e. $h < 1$), so that adopting is always more probable than unadopting. For visualization of the model and the two-layer network, see Fig. 3.7, for simulation details – Algorithm 5. In Algorithm 5, G_1 and G_2 denote the adjacency matrices for the first and the second layer, respectively.

We examine the model using both Monte Carlo simulations and the MFA. With the latter, we are able to examine a much wider range of input parameters. One cannot achieve it with simulations in a reasonable amount of time. First, we define concentrations of opinions and adoptions states, in analogy to Definition 2.2.

Definition 3.4. *Let N be number of agents, $A_i \pm 1$ adoption state and $S_i = \pm 1$ opinion of agent i, for $i = 1, 2, \ldots, N$. Then, the concentrations of positive adoption states c_A and opinions c_S are given by:*

$$c_A = \frac{1}{2N} \sum_{i=1}^{N} (A_i + 1), \quad c_S = \frac{1}{2N} \sum_{i=1}^{N} (S_i + 1). \tag{3.19}$$

Then, we derive a set of equations describing the dynamical system.

Theorem 3.5. *Let c_A denote the concentration of positive adoption states and the probability of choosing an agent with a positive adoption state, and c_S – the concentration of positive opinions and the probability of choosing an agent with a positive opinion. Under*

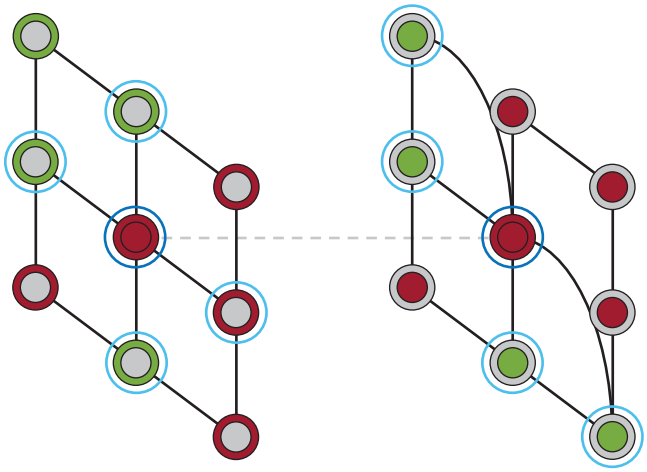

Figure 3.7: Graphical representation of the model. The network consists of 2 layers: Square Lattice (SL, left side), on which adoption states A_i are visible and two-dimensional Watts-Strogatz (WS2D, right side) with opinions S_i. Adoption states A_i are represented by outer circles (green – $A_i = +1$, red – $A_i = -1$), while opinions – by inner circles. Grey areas correspond to adoption states or opinions unknown to the target agent (marked with a dark blue circle). Groups of influence (of size $q = 4$, marked with light blue circles) are constructed independently on each layer. In the given example, such a choice would be sufficient to change target's opinion ($S_{target} \to +1$) in the OR variant, but not in the AND variant, as unanimity is only achieved in one of the two groups of influence. Source: **Paper 4**.

the assumptions that these events are independent, and that each layer of the network is of size $N \to \infty$, the dynamics of the system is described in the AND variant by:

$$\frac{dc_A}{dt} = c_S\,(1-c_A)\,a_1 - (1-c_S)\,c_A h a_1, \tag{3.20}$$

$$\begin{aligned}\frac{dc_S}{dt} =\ & (1-c_S)\left(\frac{1}{2}p + (1-p)c_S^q c_A^q\right) \\ & - c_S\left(\frac{1}{2}p + (1-p)(1-c_S)^q(1-c_A)^q\right),\end{aligned} \tag{3.21}$$

and in the OR variant by:

$$\begin{aligned}\frac{dc_A}{dt} &= c_S\,(1-c_A)\,a_1 - (1-c_S)\,c_A h a_1, \\ \frac{dc_S}{dt} &= (1-c_S)\Big\{\frac{1}{2}p + (1-p)\left(c_S^q\left(1-c_A^q-(1-c_A)^q\right)\right. \\ &\quad \left. + c_A^q\left(1-c_S^q-(1-c_S)^q\right) + c_S^q c_A^q\right)\Big\} \\ &\quad - c_S\Big\{\frac{1}{2}p + (1-p)\left((1-c_S)^q\left(1-c_A^q-(1-c_A)^q\right)\right. \\ &\quad \left. + (1-c_A)^q\left(1-c_S^q-(1-c_S)^q\right) + (1-c_S)^q(1-c_A)^q\right)\Big\}.\end{aligned} \tag{3.22}$$

Proof. See Section 2.2 in **Paper 4**. □

Due to the power of q in Eqs. (3.21)-(3.22), time trajectories of the system given by Eqs. (3.20)-(3.22) cannot be determined analytically. Hence, one must resort to numerical methods. However, stationary states can be found analytically and their existence can be proven.

Theorem 3.6. *Let c_A denote the concentration of positive adoption states and the probability of choosing an agent with a positive adoption state, and c_S – the concentration of positive opinions and the probability of choosing an agent with a positive opinion. Under the assumptions that these events are independent, and that each layer of the network is of size $N \to \infty$, for any $q \in \mathbb{N}$, $q \geq 2$, $p \in [0,1]$, $h \in (0,1)$ and $a_1 \in (0,1]$, there always exists at least one stationary state, and all stationary states must satisfy:*

$$c_A = \frac{c_S}{c_S + h - c_S h}, \tag{3.23}$$

$$p = \frac{f_2(c_S)}{f_2(c_S) + f_3(c_S)}, \tag{3.24}$$

in the AND variant, and:

$$c_A = \frac{c_S}{c_S + h - c_S h},$$

$$p = \frac{f_5(c_S)}{f_5(c_S) + f_3(c_S)}, \tag{3.25}$$

in the OR variant. Here:

$$\begin{aligned}
f_2(c_S) &= c_S(1-c_S)\left(c_S^{2q-1} - h^q(1-c_S)^{2q-1}\right), \\
f_3(c_S) &= \left(c_S - \frac{1}{2}\right)(c_S + h - c_S h)^q, \\
f_5(c_S) &= c_S(1-c_S)\Big\{\left(c_S^{q-1} - (1-c_S)^{q-1}\right)(c_S + h - c_S h)^q \\
&\quad + c_S^{q-1}(1-c_S)^{q-1}(1+h^q)(2c_S - 1) \\
&\quad + c_S^{q-1} - c_S^{2q-1} + h^q(1-c_S)^{2q-1} - h^q(1-c_S)^{q-1}\Big\}.
\end{aligned}$$

Proof. See Section 2.2 in **Paper 4**. □

For the comparison between the simulations and numerically obtained time trajectories from Eqs. (3.20)-(3.22), see Fig. 3.8. They remain consistent with each other for the most part. For a narrow range of parameters they differ significantly, however. This is due to the fact, that in the simulation the adoption is achieved more easily, i.e. for lower value of independence p. Below this range, both versions (simulation and numerical) behave the same (the system remains unadopted), above – the same as well (the system becomes adopted).

Mean-field time trajectories, and hence times to reach a stationary state, are obtained numerically from Eqs. (3.20)-(3.22). Analytically, we are only able to compute stationary states, see Eqs. (3.23)-(3.25). We compare the two in Fig. 3.9 (left side). Numerically computed stationary states perfectly match analytical ones. Segments not covered by the numerical results are due to the fact that the analytical solution shows all the possible stationary states, while the numerical one only those achievable from given initial conditions ($c_A(0) = 0$, $c_S(0) = 0$).

There exist three groups of stationary states: unadopted ($c_A(T) \approx 0$, $c_S(T) \approx 0$), adopted ($c_A(T) \approx 1$, $c_S(T) \approx 1$) and disordered ($c_A(T) \approx 0.5$, $c_S(T) \approx 0.5$). The system transitions from the first, through the second, to the third, as the probability of independence p increases, although a transition between the latter two in the OR variant is

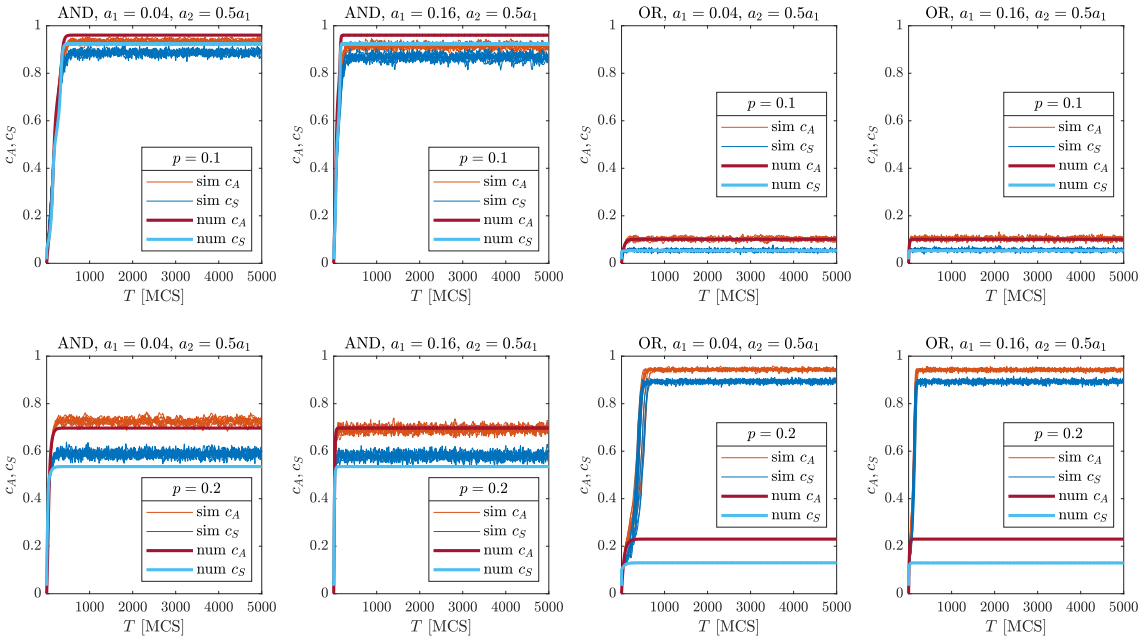

Figure 3.8: 10 simulated time trajectories of c_A and c_S versus numerically obtained time trajectory from Eqs. (3.20)-(3.22), for different values of p and a_1. The AND (left 4) and the OR variant (right 4). First layer – SL(N,1), second layer – WS2D(N,1,0.2), size $N = 2500$ and $a_2 = 0.5a_1$ in all cases. Source: **Paper 4**.

very smooth. If the system starts from the unadopted, negative state ($c_A(0) = 0$, $c_S(0) = 0$), independence is essential for the adoption process to take off. Later on, however, independence hinders innovation and ultimately prevents full adoption.

The time to reach a stationary state is presented in Fig. 3.9 (right side), with respect to a_1 ($a_2 = 0.5a_1$) and p. As shown in Eq. (3.20), the value of $a_1 \in (0, 1]$ itself has no impact on a stationary state. It dramatically affects the time to reach a stationary state however, but only in a range of low values. For high values of a_1, the changes are unnoticeable. The "ridges" for certain values of p that one can observe, correspond to transitions between the groups of stationary states. There are two such ridges in the AND variant, but only one in the OR variant, as transition between adopted and disordered states is very smooth there. These increases in times are logical, as the system needs more time to "decide" which path to take, and consistent with our knowledge on phase transitions (**Paper 1**).

Though not by a_1 itself, the system is greatly impacted by the relation between a_1 and a_2, i.e. the h coefficient. For visualization, I encourage the reader to see **Paper 4**. Basically, the greater the difference between people's willingness to install solar panels versus their willingness to get rid of them, the better for the innovation. This difference not only amplifies independence in the initial phase of adoption, but dilutes it in the final phase as well.

Publication details (Paper 4):

- Weron, T. (2024). Multi-layer diffusion model of photovoltaic installations. arXiv preprint arXiv:2408.09904v2.

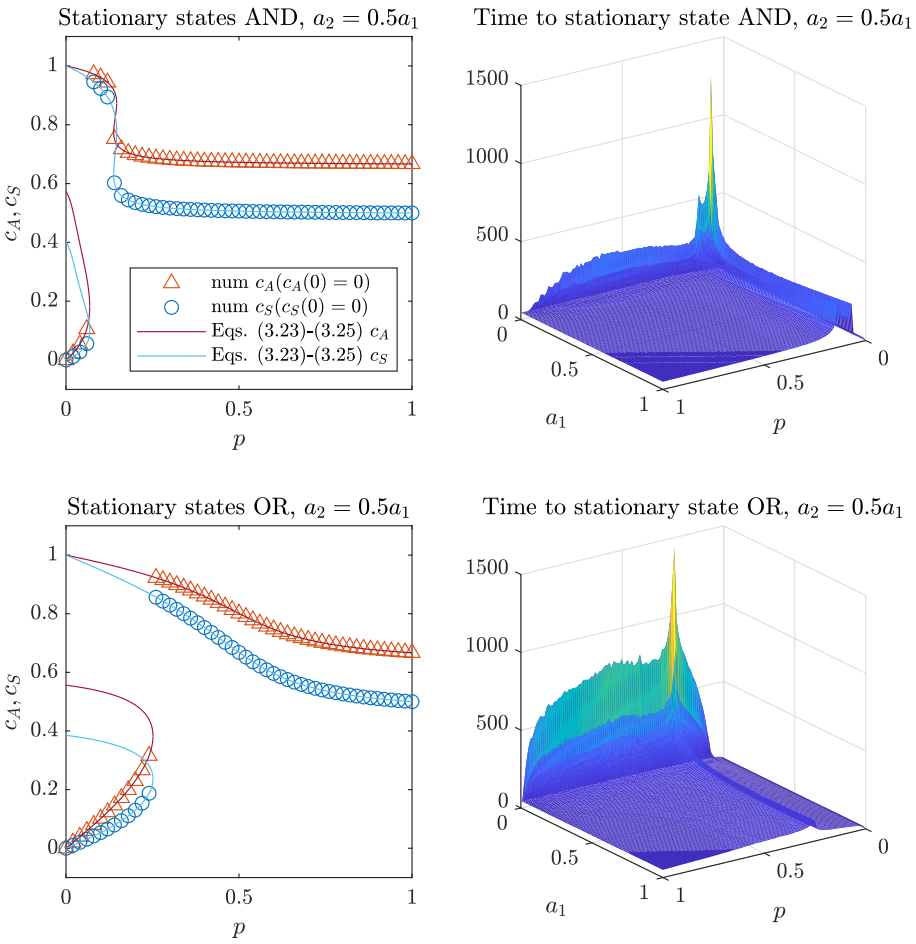

Figure 3.9: Stationary states (left) and time to reach a stationary state (right) for the AND (top) and the OR variant (bottom). Left side compares numerical results (from Eqs. (3.20)-(3.22); markers) vs analytical (from Eqs. (3.23)-(3.25); continuous lines). Numerical results cover only a portion of analytical ones, as they present stationary states from a single pair of initial conditions $(c_A(0) = 0, c_S(0) = 0)$ only, while the latter show all the possible stationary states. Right side shows time to reach a stationary state obtained with numerical methods. Adoption probabilities $a_1 = 0.5$ (left side only) and $a_2 = 0.5a_1$. Source: **Paper 4**.

Algorithm 5: Simulation dynamics

for $t \coloneqq 1$ **to** T **do**
  for $k \coloneqq 1$ **to** N **do**
    $i \coloneqq i \sim \mathcal{U}\{1, \ldots, N\}$
    $r \coloneqq r \sim \mathcal{U}[0, 1]$
    if $r < p$ **then**
      $r \coloneqq r \sim \mathcal{U}[0, 1]$
      if $r < \frac{1}{2}$ **then**
        $S_i \coloneqq -S_i$
    else
      for $l \coloneqq 1$ **to** q **do**
        $j_{1,l} \coloneqq j_1 \sim \mathcal{U}\{j_1 : G_{1,i,j_1} = 1\}$
        $j_{2,l} \coloneqq j_2 \sim \mathcal{U}\{j_2 : G_{2,i,j_2} = 1\}$
      end
      $Q_1 \coloneqq \frac{1}{q} \sum_l^q A_{j_{1,l}}$
      $Q_2 \coloneqq \frac{1}{q} \sum_l^q S_{j_{2,l}}$
      if *Variant* $=$ *AND* **then**
        if $Q_1 + Q_2 = -2S_i$ **then**
          $S_i \coloneqq -S_i$
      else if *Variant* $=$ *OR* **then**
        if $(Q_1 = -S_i$ **and** $Q_2 \neq S_i)$ **or** $(Q_1 \neq S_i$ **and** $Q_2 = -S_i)$ **then**
          $S_i \coloneqq -S_i$
      end
    end
    $r \coloneqq r \sim \mathcal{U}[0, 1]$
    if $S_i = 1$ **and** $A_i = -1$ **and** $r < a_1$ **then**
      $A_i = 1$
    else if $S_i = -1$ **and** $A_i = 1$ **and** $r < a_2$ **then**
      $A_i = -1$
    end
  end
end

Chapter 4

Auxiliary results

During my scientific career, I have published 12 articles in peer-reviewed journals on agent-based modeling and opinion dynamics or electricity market forecasting. Three of them plus one available on arXiv form this thesis. The rest either covers different topics or was published before my doctoral studies. I include and briefly summarize them here to provide a full picture of my research.

1. Sznajd-Weron, K. Szwabiński, J., Weron, R., & Weron, T. (2014). Rewiring the network. What helps an innovation to diffuse? Journal of Statistical Mechanics: Theory and Experiment, 2014(3), P03007.

2. Siedlecki, P., Szwabiński, J., & Weron, T. (2016). The Interplay Between Conformity and Anticonformity and its Polarizing Effect on Society. Journal of Artificial Societies and Social Simulation, 19(4).

3. Krueger, T., Szwabiński, J., & Weron, T. (2017). Conformity, anticonformity and polarization of opinions: insights from a mathematical model of opinion dynamics. Entropy, 19(7), 371.

4. Weron, T., Kowalska-Pyzalska, A., & Weron, R. (2018). The role of educational trainings in the diffusion of smart metering platforms: An agent-based modeling approach. Physica A: Statistical Mechanics and its Applications, 505, 591-600.

5. Maciejowska, K., Nitka, W., & Weron, T. (2019). Day-ahead vs. Intraday – Forecasting the price spread to maximize economic benefits. Energies, 12(4), 631.

6. Kath, C., Nitka, W., Serafin, T., Weron, T., Zaleski, P., & Weron, R. (2020). Balancing generation from renewable energy sources: Profitability of an energy trader. Energies, 13(1), 205.

7. Sznajd-Weron, K., Sznajd, J., & Weron, T. (2021). A review on the Sznajd model – 20 years after. Physica A: Statistical Mechanics and its Applications, 565, 125537.

8. Weron, T., Sznajd-Weron, K. (2021). How to Reach Consensus? Better Disagree with Your Neighbor. In: Paszynski, M., Kranzlmüller, D., Krzhizhanovskaya, V.V., Dongarra, J.J., Sloot, P.M. (eds) Computational Science – ICCS 2021. ICCS 2021. Lecture Notes in Computer Science(), vol 12744. Springer, Cham.

9. Maciejowska, K., Nitka, W., & Weron, T. (2021). Enhancing load, wind and solar generation for day-ahead forecasting of electricity prices. Energy Economics, 99, 105273.

10. Weron, T., & Sznajd-Weron, K. (2022). On reaching the consensus by disagreeing. Journal of Computational Science, 61, 101667 → **Paper 1**.

11. Weron, T., & Szwabiński, J. (2022). Opinion evolution in divided community. Entropy, 24(2), 185 → **Paper 2**.

12. Weron, T., Nyczka, P., & Szwabiński, J. (2024). Composition of the Influence Group in the q-Voter Model and Its Impact on the Dynamics of Opinions. Entropy, 26(2), 132 → **Paper 3**.

13. Weron, T., & Szwabinski, J. (2024). multi-layer diffusion model of photovoltaic installations. arXiv preprint arXiv:2408.09904v2 → **Paper 4**.

Sznajd-Weron et al. (2014) is my first scientific paper and, at the same time, first on the diffusion of innovation. We examined the q-voter model with independence and additional advertisement represented by a global external field. We performed simulations on a whole range of Watts-Strogatz networks, and checked how the parameters of the model or the network affect the diffusion of innovation. The key findings were that: the innovation diffuses more likely in more regular graphs and it is harder for the innovation the spread in more dense networks.

Siedlecki et al. (2016) is the first article in which we proposed the new model of social polarization, that we later extended in **Paper 2**. Back then, it was just the q-voter model without independence, studied solely with Monte Carlo simulations. However, it already introduced the double-clique topology. We found out that there is a critical number of negative cross-links $L \times N^2$ between the cliques, which polarizes an initially unanimous system.

In Krueger et al. (2017), we derived the mean-field approximation for the very same model and examined it analytically and numerically, in addition to the simulations. New results confirmed our previous findings. Although they differed quantitatively, qualitatively they presented the same outcome as the simulations. Further analysis, for the q-voter model with independence, was done in **Paper 2**.

In Weron et al. (2018), we proposed a new agent-based model of diffusion of smart metering platforms (SMPs). The model was based on the q-voter model, but with a new knowledge factor included. It depicted the knowledge necessary for an individual to use a SMP. We compared the effectiveness of different training strategies that a company, for instance, can use to spread the knowledge. It occurred that group trainings (all agents in a given area) are never worse than random ones (scattered over the whole network), and are superior for a certain range of input parameters.

Maciejowska et al. (2019) is my first article on electricity price forecasting. We utilized autoregressive models with exogenous components (ARX) and probit models to forecast the price spread between day-ahead market and continuous trading markets (intraday, balancing markets). Firstly, we showed that the sign of the price spread can be successfully predicted for economics benefits. Secondly, that the statistical measures of forecast accuracy, such as the percentage of correct sign classifications, do not necessarily coincide with economic benefits.

Kath et al. (2020) was a research conducted from a point of view of a small trading company, that acts as a broker between a wind farm and the energy market, i.e. buys the forecasted volume of generated energy and then, sells the actual volume in the market. We showed that publicly available forecasts of wind generation, published by the transmission system operator (TSO), can be corrected with simple ARX models, significantly improving trader's strategies and profits.

Sznajd-Weron et al. (2021) provides a comprehensive review on the literature that arose around the Sznajd model over 20 years since its publication in 2000 [61]. Apart from that, the article introduces a generalization of the model that combines all 3 variants under a single parameter (as described in Section 2.2).

Weron et al. (2021) was a short paper that expanded the research on the generalized Sznajd model, introduced in the previous article. In the latter, we only studied the impact of input parameters on exit probabilities (probabilities of reaching a particular absorbing state). And we did only it by Monte Carlo simulations for the size of the system $N = 100$. In this paper, we examined it more thoroughly for different sizes. Additionally, we studied exit time, i.e. time to reach an absorbing state, as it was never measured in the generalized Sznajd model.

In Maciejowska et al. (2021), we discovered that TSO forecasts of fundamental variables (load, wind and solar generation) are systematically biased, and once again confirmed that they can be significantly improved with ARX models. Then, we used these enhanced fundamentals' forecasts successfully to improve the accuracy of electricity price forecasts. These support the decision process (which market to trade in) and bring in additional revenue.

Chapter 5

Conclusions

The aim of my thesis was to develop mathematical models of binary opinion dynamics that can be used to model the diffusion of PV panels (or other renewable energy sources) to understand how various factors impact this complex process. This far-reaching goal was realized through three objectives:

- **Objective 1:** Evaluate the role of the new parameter in the generalized, the one-dimensional Sznajd model.

In [62], we introduced a new parameter that contains and describes three different variants of the Sznajd model, so far analyzed separately. In **Paper 1**, we thoroughly examined the generalized Sznajd model and the impact of the new parameter that describes three different variants of the model on stationary states and time to reach them. Additionally, we proposed even further generalization onto a diluted system that allows agents to move. The findings provided valuable insights for **Objective 3**.

- **Objective 2:** Evaluate the impact of the underlying network structure and the method of selecting the group of influence on the time evolution and stationary states in the q-voter model.

In **Paper 2**, we studied the phenomenon of social polarization. Precisely, we examined the q-voter model's behavior on a double-clique topology, consisting of two complete graphs connected by negative links. **Paper 2** showed how the independence can disrupt initial consensus, which is related to **Objective 3**. In **Paper 3**, we once more analyzed the q-voter model with independence, this time with regard to the method of selecting a group of influence (with or without repetitions). This research marked the differences between these two variants.

- **Objective 3:** Design a new model of eco-innovation diffusion. Analyze the model on a multi-layer network structure.

Finally, in **Paper 4**, we proposed a new model of diffusion of photovoltaic panels. We based it on the q-voter model with independence and examined on the multi-layer network. We provided a basis for further development, by studying the impact of input parameters and method of combining social influence across the layers (AND and OR rules).

In summary, my thesis expanded current knowledge on opinion dynamics and diffusion innovation. It generalized and extended two well-established mathematical models

of binary opinions: the Sznajd and the q-voter models. Finally, it presented a new model of diffusion of innovation, which being a non-progressive and complex contagion one, filled the gap in studies on diffusion of innovation.

Bibliography

[1] A. ABRAMIUK AND K. SZNAJD-WERON, *Generalized Independence in the q-Voter Model: How Do Parameters Influence the Phase Transition?*, Entropy, 22 (2020), p. 120.

[2] A. ABRAMIUK-SZURLEJ, A. LIPIECKI, J. PAWŁOWSKI, AND K. SZNAJD-WERON, *Discontinuous phase transitions in the q-voter model with generalized anticonformity on random graphs*, Scientific Reports, 11 (2021), p. 17719.

[3] A. ALETA AND Y. MORENO, *Multilayer networks in a nutshell*, Annual Review of Condensed Matter Physics, 10 (2019), pp. 45–62.

[4] C. A. BAIL, L. P. ARGYLE, T. W. BROWN, J. P. BUMPUS, H. CHEN, M. B. F. HUNZAKER, J. LEE, M. MANN, F. MERHOUT, AND A. VOLFOVSKY, *Exposure to opposing views on social media can increase political polarization*, Proceedings of the National Academy of Sciences, 115 (2018), pp. 9216–9221.

[5] A.-L. BARABÁSI AND M. PÓSFAI, *Network Science*, Cambridge University Press, 2016.

[6] F. M. BASS, *A new product growth for model consumer durables*, Management science, 15 (1969), pp. 215–227.

[7] A. BATOOL, Z. DANKU, G. PÁL, AND F. KUN, *Temporal evolution of failure avalanches of the fiber bundle model on complex networks*, Chaos: An Interdisciplinary Journal of Nonlinear Science, 32 (2022).

[8] G. BIANCONI, *Multilayer Networks: Structure and Function*, Oxford University Press, 2018.

[9] K. BINDER AND D. HEERMANN, *Monte Carlo Simulation in Statistical Physics: An Introduction*, Graduate Texts in Physics, Springer Berlin Heidelberg, 2010.

[10] K. BYRKA, A. JĘDRZEJEWSKI, K. SZNAJD-WERON, AND R. WERON, *Difficulty is critical: The importance of social factors in modeling diffusion of green products and practices*, Renewable & Sustainable Energy Reviews, 62 (2016), pp. 723–735.

[11] C. CAPRIOLI, M. BOTTERO, AND E. DE ANGELIS, *Supporting policy design for the diffusion of cleaner technologies: A spatial empirical agent-based model*, ISPRS International Journal of GEO-information, 9 (2020), p. 581.

[12] C. CASTELLANO, M. A. MUÑOZ, AND R. PASTOR-SATORRAS, *Nonlinear q-voter model*, Physical Review E, 80 (2009), p. 041129.

[13] A. CHMIEL, J. SIENKIEWICZ, A. FRONCZAK, AND P. FRONCZAK, *A Veritable Zoology of Successive Phase Transitions in the Asymmetric q-Voter Model on Multiplex Networks*, Entropy, 22 (2020), p. 1018.

[14] A. CHMIEL AND K. SZNAJD-WERON, *Phase transitions in the q-voter model with noise on a duplex clique*, Physical Review E, 92 (2015), p. 052812.

[15] B. DERSKI, *Ile kosztuje instalacja fotowoltaiczna dofinansowana z programu „mój prąd"?* `wysokienapiecie.pl`, 2019.

[16] P. DIMAGGIO, J. EVANS, AND B. BRYSON, *Have american's social attitudes become more polarized?*, American Journal of Sociology, 102 (1996), pp. 690–755.

[17] EUROSTAT, *Electricity from renewable sources up to 41% in 2022*. `ec.europa.eu/eurostat`, 2024.

[18] ——, *Renewables take the lead in power generation in 2023*. `ec.europa.eu/eurostat`, 2024.

[19] F. GEELS, B. SOVACOOL, T. SCHWANEN, AND S. SORRELL, *Sociotechnical transitions for deep decarbonization*, Science, 357 (2017), pp. 1242–1244.

[20] A. GIBBONS, *Algorithmic graph theory*, Cambridge university press, 1985.

[21] J. GLEESON, *Binary-state dynamics on complex networks: Pair approximation and beyond*, Physical Review X, 3 (2013), p. 021004.

[22] S. GOODARZI, H. PERERA, AND D. BUNN, *The impact of renewable energy forecast errors on imbalance volumes and electricity spot prices*, Energy Policy, 134 (2019), p. 110827.

[23] T. GRADOWSKI AND A. KRAWIECKI, *Pair approximation for the q-voter model with independence on multiplex networks*, Physical Review E, 102 (2020), p. 022314.

[24] D. J. ISENBERG, *Group polarization: A critical review and meta-analysis.*, Journal of Personality and Social Psychology, 50 (1986), pp. 1141–1151.

[25] M. A. JAVARONE AND T. SQUARTINI, *Conformism-driven phases of opinion formation on heterogeneous networks: the q-voter model case*, Journal of Statistical Mechanics: Theory and Experiment, 2015 (2015), p. P10002.

[26] A. JĘDRZEJEWSKI AND K. SZNAJD-WERON, *Statistical physics of opinion formation: Is it a spoof?*, Comptes Rendus Physique, 20 (2019), pp. 244–261.

[27] T. JENSEN, G. HOLTZ, AND E. CHAPPIN, *Agent-based assessment framework for behavior-changing feedback devices: Spreading of devices and heating behavior*, Technological Forecasting & Social Change, 98 (2015), pp. 105–119.

[28] A. JĘDRZEJEWSKI, *Pair approximation for the q -voter model with independence on complex networks*, Physical Review E, 95 (2017), p. 012307.

[29] M. KIVELÄ, A. ARENAS, M. BARTHELEMY, J. GLEESON, Y. MORENO, AND M. PORTER, *Multilayer networks*, Journal of Complex Networks, 2 (2014), pp. 203–271.

[30] A. KOWALSKA-PYZALSKA, K. MACIEJOWSKA, K. SUSZCZYŃSKI, K. SZNAJD-WERON, AND R. WERON, *Turning green: Agent-based modeling of the adoption of dynamic electricity tariffs*, Energy Policy, 72 (2014), pp. 164–174.

[31] A. KOWALSKA-STYCZEŃ, K. MALARZ, AND K. PARADOWSKI, *Model of knowledge transfer within an organisation*, JASSS, 21 (2018), p. 3.

[32] T. KRUEGER, J. SZWABIŃSKI, AND T. WERON, *Conformity, anticonformity and polarization of opinions: insights from a mathematical model of opinion dynamics*, Entropy, 19 (2017), p. 371.

[33] R. LAMBIOTTE AND S. REDNER, *Dynamics of non-conservative voters*, EPL, 82 (2008).

[34] K.-M. LEE, C. BRUMMITT, AND K.-I. GOH, *Threshold cascades with response heterogeneity in multiplex networks*, Physical Review E, 90 (2014), p. 062816.

[35] W. LI, L. TIAN, H. LIU, AND Q. SU, *Heterogeneous adoption of eco-innovation considering commuting mobility patterns*, Journal of Cleaner Production, (2019), p. 119499.

[36] A. LIPIECKI, *Strategic promotional campaigns for sustainable behaviors: Maximizing influence in competitive complex contagions*, in International Conference on Computational Science, Springer, 2024, pp. 62–70.

[37] M. W. MACY AND R. WILLER, *From factors to actors: Computational sociology and agent-based modeling.*, Annual Review of Sociology, 28 (2002), pp. 143–166.

[38] K. MAIZE, *Duck hunting at the California Independent System Operator*, Power, 161 (2017).

[39] M. MATICKA, *The SWIS DUCK – value pricing analysis of commercial scale photovoltaic generation in the South West Interconnected System*, Electricity Journal, 32 (2019), pp. 57–65.

[40] A. MITTAL, C. KREJCI, M. DORNEICH, AND D. FICKES, *An agent-based approach to modeling zero energy communities*, Solar Energy, 191 (2019), pp. 193–204.

[41] M. MOBILIA, *Nonlinear q -voter model with inflexible zealots*, Physical Review E, 92 (2015), p. 012803.

[42] E. F. MOORE, *Machine models of self-reproduction*, in Proceedings of symposia in applied mathematics, American Mathematical Society New York, 1962, pp. 17–33.

[43] C. MORA, T. MCKENZIE, I. M. GAW, J. M. DEAN, H. VON HAMMERSTEIN, T. A. KNUDSON, R. O. SETTER, C. Z. SMITH, K. M. WEBSTER, J. A. PATZ, ET AL., *Over half of known human pathogenic diseases can be aggravated by climate change*, Nature climate change, 12 (2022), pp. 869–875.

[44] P. MORETTI, S. LIU, C. CASTELLANO, AND R. PASTOR-SATORRAS, *Mean-field analysis of the q-voter model on networks*, Journal of Statistical Physics, 151 (2013), pp. 113–130.

[45] R. MUSLIM, R. A. NQZ, AND M. A. KHALIF, *Mass Media and Its Impact on Opinion Dynamics of the Nonlinear q-Voter Model*, SSRN Electronic Journal, (2023).

[46] M. NEWMAN, *Networks: An Introduction*, Oxford University Press, 2010.

[47] P. NYCZKA AND K. SZNAJD-WERON, *Anticonformity or independence?—insights from statistical physics.*, Journal of Statistical Physics, 151 (2013), pp. 174–202.

[48] P. NYCZKA, K. SZNAJD-WERON, AND J. CISLO, *Phase transitions in the q-voter model with two types of stochastic driving.*, Physical Review E, 86 (2012), p. 011105.

[49] J. PALMER, G. SORDA, AND R. MADLENER, *Modeling the diffusion of residential photovoltaic systems in Italy: An agent-based simulation*, Technological Forecasting & Social Change, 99 (2015), pp. 106–131.

[50] E. PARISER, *The Filter Bubble. What the Internet Is Hiding from You?*, Penguin Press, 2011.

[51] A. PTAK, *Poland produced record 26% of electricity from renewables in 2023*. `notesfrompoland.com`, 2024.

[52] H. RAHMANDAD AND J. STERMAN, *Heterogeneity and network structure in the dynamics of diffusion: Comparing agent-based and differential equation models*, Management Science, 54 (2008), pp. 998–1014.

[53] W. RAND AND R. RUST, *Agent-based modeling in marketing: Guidelines for rigor*, International Journal of Research in Marketing, 28 (2011), pp. 181–193.

[54] R. REIBSCH, P. BLECHINGER, AND J. KOWAL, *The importance of battery storage systems in reducing grid issues in sector-coupled and renewable low-voltage grids*, Journal of Energy Storage, 72 (2023), p. 108726.

[55] E. M. ROGERS, *Diffusion of Innovations, 5th Edition*, Simon and Schuster, 2003.

[56] T. SCHELLING, *Dynamic models of segregation*, Journal of Mathematical Sociology, 1 (1971), pp. 143–186.

[57] P. SIEDLECKI, J. SZWABIŃSKI, AND T. WERON, *The interplay between conformity and anticonformity and its polarizing effect on society*, Journal of Artificial Societies and Social Simulation, 19 (2016), p. 9.

[58] F. SLANINA, K. SZNAJD-WERON, AND P. PRZYBYŁA, *Some new results on one-dimensional outflow dynamics*, Europhysics Letters, 82 (2008), p. 18006.

[59] D. STAUFFER, A. O. SOUSA, AND S. M. DE OLIVEIRA, *Generalization to square lattice of sznajd sociophysics model*, International Journal of Modern Physics C, 11 (2000), pp. 1239–1245.

[60] C. R. SUNSTEIN, *The law of group polarization.*, Journal of Political Philosophy, 10 (2002), pp. 175–195.

[61] K. SZNAJD-WERON AND J. SZNAJD, *Opinion evolution in closed community.*, International Journal of Modern Physics C, 11 (2000), p. 1157.

[62] K. SZNAJD-WERON, J. SZNAJD, AND T. WERON, *A review on the sznajd model—20 years after*, Physica A: Statistical Mechanics and its Applications, 565 (2021), p. 125537.

[63] K. SZNAJD-WERON, J. SZWABIŃSKI, AND R. WERON, *Is the person-situation debate important for agent-based modeling and vice-versa?*, PLoS ONE, 9 (2014), p. e112203.

[64] K. SZNAJD-WERON, J. SZWABIŃSKI, R. WERON, AND T. WERON, *Rewiring the network. what helps an innovation to diffuse?*, Journal of Statistical Mechanics, 2014 (2014), p. P03007.

[65] UNKNOWN, *The Global Risk Report 2017*, World Economic Forum, Geneva, 2017.

[66] M. VAN DER KAM, A. PETERS, W. VAN SARK, AND F. ALKEMADE, *Agent-based modelling of charging behaviour of electric vehicle drivers*, JASSS, 22 (2019), p. 7.

[67] A. R. VIEIRA AND C. ANTENEODO, *Threshold q-voter model*, Physical Review E, 97 (2018), p. 052106.

[68] A. R. VIEIRA, A. F. PERALTA, R. TORAL, M. S. MIGUEL, AND C. ANTENEODO, *Pair approximation for the noisy threshold q -voter model*, Physical Review E, 101 (2020), p. 052131.

[69] S. WASSERMAN AND K. FAUST, *Social Network Analysis: Methods and Applications.*, Cambridge University Press, 1994.

[70] T. WERON, A. KOWALSKA-PYZALSKA, AND R. WERON, *The role of educational trainings in the diffusion of smart metering platforms: An agent-based modeling approach*, Physica A, 505 (2018), pp. 591–600.

[71] K. WOLSKE, K. GILLINGHAM, AND P. SCHULTZ, *Peer influence on household energy behaviours*, Nature Energy, 5 (2020).

[72] WORLD BANK, *Air Quality Management in Poland*, World Bank, 2019.

[73] H. XIONG, D. PAYNE, AND S. KINSELLA, *Identifying mechanisms underlying peer effects on multiplex networks*, JASSS, 21 (2018), p. 6.

[74] N. ZHANG, Y. LU, J. CHEN, AND B.-G. HWANG, *An agent-based diffusion model for residential photovoltaic deployment in singapore: Perspective of consumers' behaviour*, Journal of Cleaner Production, 367 (2022), p. 132793.

Paper 1

On reaching the consensus by disagreeing

Tomasz Weron, Katarzyna Sznajd-Weron

Journal of Computational Science 61 (2022) 101667

Contents lists available at ScienceDirect

Journal of Computational Science

journal homepage: www.elsevier.com/locate/jocs

On reaching the consensus by disagreeing

Tomasz Weron [a], Katarzyna Sznajd-Weron [b,*]

[a] Department of Applied Mathematics, Wrocław University of Science and Technology, Wrocław, Poland
[b] Department of Theoretical Physics, Wrocław University of Science and Technology, Wrocław, Poland

ARTICLE INFO

Keywords:
Opinion dynamics
Sznajd model
Agent-based modeling
Consensus

ABSTRACT

This paper is an extended version of the article published at the International Conference on Computational Science (ICCS-2021) Weron and Sznajd-Weron (2021). In Weron and Sznajd-Weron (2021) we studied a generalization of the original one-dimensional Sznajd model, which was based on the addition of a new parameter — the probability p of disagreeing with the neighbor in case of uncertainty. Here, we introduce a further generalization by diluting the system and allowing for the movement of agents. We investigate the model via Monte Carlo simulations and show that the intriguing results, summarized as 'Better disagree with your neighbor', are valid also for the model with movement.

1. Introduction

Belief or opinion dynamics is a highly interdisciplinary subject, studied by social psychologists, sociologists, economists, philosophers, biologists, engineers, computer scientists, statistical physicists, and mathematicians [1–7]. One of the main methods in this field is agent-based modeling (ABM), which is known as a tool that builds a bridge between micro and macro scale [8,9]. ABM is generally understood as a simulation modeling technique, in which a system is modeled as a collection of autonomous decision-making entities called agents [10]. Sometimes a more general concept is used that does not reduce ABM solely to a simulation model. Under such a concept ABM is a model, which consists of many (usually mutually interacting) individuals, analogously to a microscopic model in statistical physics [11] or the multi-agent system (MAS) in engineering and technology [12].

Within the ABM of opinion dynamics, one of the most studied issues is achieving consensus [1,2,4,6,13–16]. The approach to this, i.e., research questions, etc., varies greatly from discipline to discipline. For instance, in statistical physicists we are often interested in the phase transitions between consensus (order) and disagreement (disorder), which appear as a result of a competition between different factors (conformity vs. nonconformity, inner interactions vs. environment, etc.). [11,17–25].

The problem of competing interactions and the possibility of reaching consensus under such a competition has also been studied extensively in the context of signed networks [26–28], for a recent review see [29]. Within this approach, agents occupy nodes of a network with each link being associated with either a positive or a negative sign that can be interpreted as trust/distrust, like/dislike, etc. In the physics of complex systems, this kind of approach is called quenched (static). In contrast, within the so-called annealed approach the random rules, which apply in the system (related to structure of the system, interactions, etc.) change in time [30]. In this paper, we deal with the annealed one, which is related to the situation-based approach and seems to be particularly useful in modeling various social processes, including the diffusion of green products and practices [31].

Another topic of interest is the convergence of the process [4,14–16,32–38]. Again, depending on the discipline, various (more or less formal) approaches are used to achieve different goals [6]. As expected, mathematicians are mainly focused on the convergence of the process from the theoretical point of view; for a review see [4,6,35]. On the other hand, in systems science and control engineering, consensus is considered the basis of distributed coordinated control of MASs [38]. As such, it is significant for application to mobile robots, unmanned air vehicles, autonomous underwater vehicles, satellites, aircraft, spacecraft, automated highway systems, etc. [36]. Therefore, in this domain one of the main goals is *to develop information flow algorithms or protocols, which specify the information exchange between an agent and its neighbors, such that the group as a whole can reach an agreement regarding a certain quantity of interest* [37]. Yet another approach, which we use here, is typical for statistical physicists — we are mainly interested in how fast consensus is reached in a given microscopic model and what factors influence the probability of consensus and the time to reach it [14–16,32,33,33,34,39].

In this paper, we are interested in whether and how quickly consensus is reached, and what factors accelerate achieving consensus in the generalized one-dimensional Sznajd model (SM) [40]. SM itself is

* Corresponding author.
E-mail addresses: tomasz.weron@pwr.edu.pl (T. Weron), katarzyna.weron@pwr.edu.pl (K. Sznajd-Weron).

https://doi.org/10.1016/j.jocs.2022.101667
Received 14 October 2021; Received in revised form 25 March 2022; Accepted 8 April 2022
Available online 18 April 2022

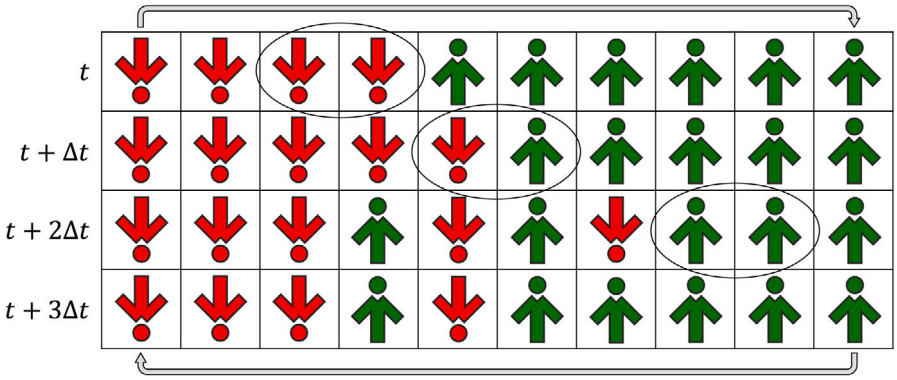

Fig. 1. Visualization of the model. Example of several consecutive updates for the model without movement in the system of $N = 10$ agents with probability of disagreeing $p = 1$. There are periodic boundary conditions, so the leftmost agent is a neighbor of the rightmost one. At time t concentration of positive opinions $c(t) = 0.6$ and the system is divided into two clusters of opposite opinions. After a single update, at time $t + \Delta t$ concentration of positive agents decreases to $c(t + \Delta t) = 0.5$ and the system still consists of two opposing groups. After another time step still $c(t + 2\Delta t) = 0.5$, but a quarrelsome group (a disagreement state) arises between two opposing groups.

one of the most popular opinion dynamics models in the field of sociophysics to date cited over 1000 times according to SCOPUS. Part of its popularity is due to the fact that, being extremely simple, it has become a good basis for further development and applications in marketing and politics, for a recent review check [40]. As a result, several versions of it have been proposed, differing mainly in the rules for agents' uncertainty condition. The main rule, that conformity appears only in the case of a unanimous influence group, was kept in all modifications of SM. Moreover, it has also been applied to the basic q-voter model, which can be regarded as a generalization of the SM [41]. However, in the case of a nonunanimous group, several rules have been proposed, including: disagreeing with the nearest neighborhood (original rule in SM based on the wisdom 'united we stand divided we fall') and keeping the old state (the most popular rule). To incorporate both rules within a single model and explore additional different scenarios, a generalized version of the model was proposed [40].

Such a generalized model leads to an intriguing result: generally, the consensus is reached more rapidly if agents disagree more often with their nearest neighbors in the case of uncertainty. Here, we introduce a further generalization to examine whether this unexpected behavior will occur in a diluted system in which agents can move. That is to answer the question, are the results obtained previously just an artifact of the very specific setup. One of the main advantages of the presented approach is that the introduced generalization allows us to reduce the model, in special cases, to already known variants, which supports its verification.

The paper is organized as follows. In the next section we describe the model, which was already studied in [42]. In the consecutive Section 3 we recall the results for this model that was already presented [42], as well as some results that were missing previously. Subsequently, in Section 4 we introduce a further generalization, which was inspired by one of the reports of the previous paper. In Section 5 we present the Monte Carlo results of the model, and finally, in Section 6 we wrap up.

2. The model without movement

We study a system of N agents placed in cells of a one-dimensional lattice with periodic boundary conditions. Each agent can be in one of two states $S_i(t) = \pm 1$, representing alternative opinions (yes/no, agree/disagree, etc.) that change over time t due to interactions between agents. In this version of the model, as in the original SM [40, 43], each cell is occupied by exactly one agent, and hence the agents cannot move.

We use the random sequential update scheme, which mimics continuous time. An elementary update consists of the following substeps:

1. A pair of adjacent cells $(i, i + 1)$, which we call the source of influence, is chosen at random, to influence two neighboring cells: one on the pair's left side, i.e. $i - 1$, and one on the right side, i.e. $i + 2$.
2. If the pair $(i, i + 1)$ is unanimous, i.e. $S_i(t) = S_{i+1}(t)$, then the two neighbors take the same state as a pair: $S_{i-1}(t + \Delta t) = S_i(t)$, $S_{i+2}(t + \Delta t) = S_i(t)$, where Δt is a period needed for a single update.
3. Otherwise, if $S_i(t) = -S_{i+1}(t)$, cells $(i - 1, i + 2)$ take the states opposite to their nearest neighbors with probability p: $S_{i-1}(t + \Delta t) = -S_i(t)$, $S_{i+2}(t + \Delta t) = -S_{i+1}(t)$. It means that in case of uncertainty, agents disagree with their nearest neighbors with the probability p: $p = 1$ corresponds to the original "United we stand, divided we fall" rule, whereas $p = 0$ to the rule, which has been mostly used in the literature within the SM [40].

As usual in this type of models, a time unit consists of N elementary updates, that is, $N\Delta t = 1$. An example of several consecutive updates in the small system of $N = 10$ agents is presented in Fig. 1. It shows that in the system of two opposing, internally unanimous groups, a quarrelsome group (a disagreement state) can emerge.

We realize that the assumptions of the one-dimensional structure and the lack of movement describe only a limited number of real-life scenarios, such as opinion formation during a round-table discussion. In the previous paper, we wrote that allowing for agents' movement would also be an interesting idea but, unfortunately, would require an additional parameter describing the density of occupied cells. In Section 4 of this paper, we introduce such a parameter and generalize the model. Furthermore, we show how this new parameter influences the process of reaching a consensus. Another interesting research would be to check how the structure of the social network impacts the formation of consensus in such a model but that we leave for the future.

We study the model within Monte Carlo simulations with different initial conditions, parameterized by the concentration $c_0 \equiv c(0)$ of agents with positive opinion at time $t = 0$:

$$c(t) = \frac{N_+(t)}{N} = \frac{1}{2N}\sum_{i=1}^{N}\left(S_i(t) + 1\right), \tag{1}$$

where $N_+(t)$ is the number of agents with opinion $+1$ at time t. To precisely define the initial conditions, in addition to the concentration of positive agents c_0, we have to decide on their spatial distribution. We consider two limiting cases, as in [40]:

- **Random**: choose randomly $N_+(0)$ out of N cells for agents with positive opinions. For large systems, it is almost identical to a much simpler rule: for $i = 1$ to N, with probability $c_0 = N_+(0)/N$, set $S_i(0) = 1$ and, with complementary probability $1 - c_0$, set $S_i(0) = -1$.

- **Sorted**: for $i = 1$ to $N_+(0)$ set $S_i(0) = 1$ and for $i = N_+(0)$ to N set $S_i(0) = -1$.

We average the results over $L = 10^3$ independent samples, i.e. for each set of parameters (p, c_0, N) we perform L independent simulations (see Algorithm 1 for a single simulation). We stop the simulation once the absorbing state is reached or the simulation time t exceeds the time limit T. The latter was introduced to avoid overly long simulations. However, in practice we used $T = 10^4$ which was large enough for the system to always achieve an absorbing state.

Algorithm 1: Algorithm for the model without movement

```
for t ← 1 to T do
    for k ← 1 to N do
        i ← i ~ U{1, ..., N}
        if S_i = S_{i+1} then
            S_{i-1} ← S_i
            S_{i+2} ← S_i
        else if r ~ U(0, 1) < p then
            S_{i-1} ← −S_i
            S_{i+2} ← −S_{i+j}
        end
    end
    if ∀i S_i = S_{i+2} then
        break
    end
end
```

After each of the L simulations, we collect the data:

- The final (absorbing) configuration, which for this model is one of the following [40]: (1) positive consensus $(+ + + + + \cdots)$, (2) negative consensus $(- - - - - \cdots)$ or (3) a state of disagreement $(+ - + - + \cdots)$. Note that each of these states is described by the same simple rule: $\forall i\ S_i = S_{i+2}$, which allows for a simple stop condition used in Algorithm 1. Collecting these data allows us to calculate the probability of reaching each absorbing state: P_+, P_-, P_{+-}, so-called **exit probability** [13,44]. For the sake of clarity, we will also refer directly to a given final state using terms **consensus probability, positive consensus probability**, etc.
- The time required to reach an absorbing state, so-called **exit time**, which allows us to calculate the average exit time τ [44]. For the sake of clarity, we will also use the terms **consensus time, positive consensus time**, etc.

3. Results for the model without movement

The model described in the previous section evolves towards one of the three absorbing states: (1) positive consensus, in which every agent has a positive opinion, (2) negative consensus, in which every agent has a negative opinion, and (3) a disagreement state in which every agent disagrees with the nearest neighbors. Once an absorbing state is reached, the system shall never leave it.

It was previously claimed that only for $p = 1$ the consensus or disagreement state can be reached, whereas for $p < 1$ only consensus is possible, so the probability of disagreement $P_{+-} = 0$ [40,42]. However, this claim has not been confirmed by any simulations so far. Therefore, we decided to check what is the probability to reach the disagreement state as a function of probability of disagreeing p, for different lattice sizes N.

Fig. 2 shows that in the smallest of the systems studied, $N = 100$, consensus is reached with probability 1 only for $p < p^* \approx 0.8$. Above this threshold $p = p^*$, the probability of consensus begins to decrease. At the same time, the complementary probability of disagreement begins to increase with p, until 0.5 for $p = 1$. For $p = 1$ both states, consensus and disagreement are equally likely for any system size N. However, as N increases, the value $p = p^*$ above which the state of disagreement is likely to occur, grows and tends towards 1. Therefore, for very large N it will only be observable for $p^* \to \infty$. Interestingly, the same final states are obtained for both random and sorted initial conditions. The only difference is the time needed to reach them, shortened for random ones. This means that, in a system of two internally unanimous groups, a state of disagreement can arise.

By showing in Fig. 2 both the probability of reaching consensus (top panels) and the time required to reach this state (bottom panels), we can observe an interesting fact, overlooked in the original short version of this article [42]. As we see here, the consensus time decreases with p only to $p = p^*$, that is, to the point at which the disagreement state starts to appear. This is due to the competition between the two forces that drives the evolution of the system. The first occurs when the source of influence is unanimous and results in the building of consensus, the second when the agents in the source of influence are in opposite states and with probability p supporting the disagreement. For $p \geq p^*$ the system is frustrated, in a sense that "it cannot decide" towards which steady state to evolve and therefore, the exit time increases.

The above result, although overlooked previously, does not contradict the claim of the previous work that the consensus time generally decreases with p. This is indeed true because, as mentioned above, p^* increases with N, and for $N \to \infty$ the threshold $p^* \to 1$. Moreover, it occurs that $p = p^*$ depends not only on the size of the system, but also on the initial concentration of positive opinions c_0, as seen in Fig. 3. The maximum value of p^* occurs at $c_0 = 0.5$ and the further away from this half–half initial condition is, the higher value of p^*. Thus, disagreement is achieved very rarely, only for a narrow range of parameters.

For this reason, in the further part of this paper, and in analogy to the previous one [42], we focus solely on reaching the consensus, namely, on the exit probability of the consensus and the exit time needed to reach such a state. In [40] the exit probability was measured within the Monte Carlo simulations for $N = 100$. In [42] we checked it more systematically for different sizes, $N \geq 100$, which is presented in the top panels of Fig. 4.

It occurs that for any $p < 1$ the exit probability of the positive consensus can be approximated by the following formulas:

- for random initial conditions (see Fig. 4):

$$P_+ = \frac{c_0^2}{c_0^2 + (1 - c_0)^2}, \tag{2}$$

- for sorted initial conditions: $P_+ = c_0$.

The same results have been obtained previously for the original SM without disagreement rule, which corresponds to $p = 0$ [45,46]. Note that the above formulas and the corresponding top panels in Fig. 4 describe the probability of reaching the positive consensus P_+, in contrast to Fig. 2, which shows the probability of any consensus, that is, P_+ and P_-. If the probability of any type of consensus would be shown in Fig. 4 then we would see just a horizontal line at value 1, because independently of c_0 the consensus is reached with probability 1 for values of p presented in this figure. However, the probability of a given type of consensus, here positive, is far less clear, and in the case of the original SM this issue caused an extended debate [46–48].

The second important characteristic is the exit time to reach consensus, which was measured for the first time in [46], but only for the original model, which corresponds to $p = 0$ [46]. In the previous paper, it was measured for the generalized model, that is, for an arbitrary value of p [42]. It is obvious that $\tau = 0$ for $c_0 = 0$ or $c_0 = 1$ because the initial state is already absorbing one. Furthermore, we expect that τ has the maximum value for $c_0 = 0.5$ [39,46]. Indeed, as shown in the bottom panels of Fig. 4, all these expectations are confirmed. Unlike exit probability, the average exit time depends on the size of the system, as shown in Fig. 4. For $p = 0$ it scales with an exponent of 2, i.e., $\tau \sim L^2$, as already shown in [46]. For other values of p the scaling exponent $\alpha \approx 2$, but it is not exactly equal to 2.

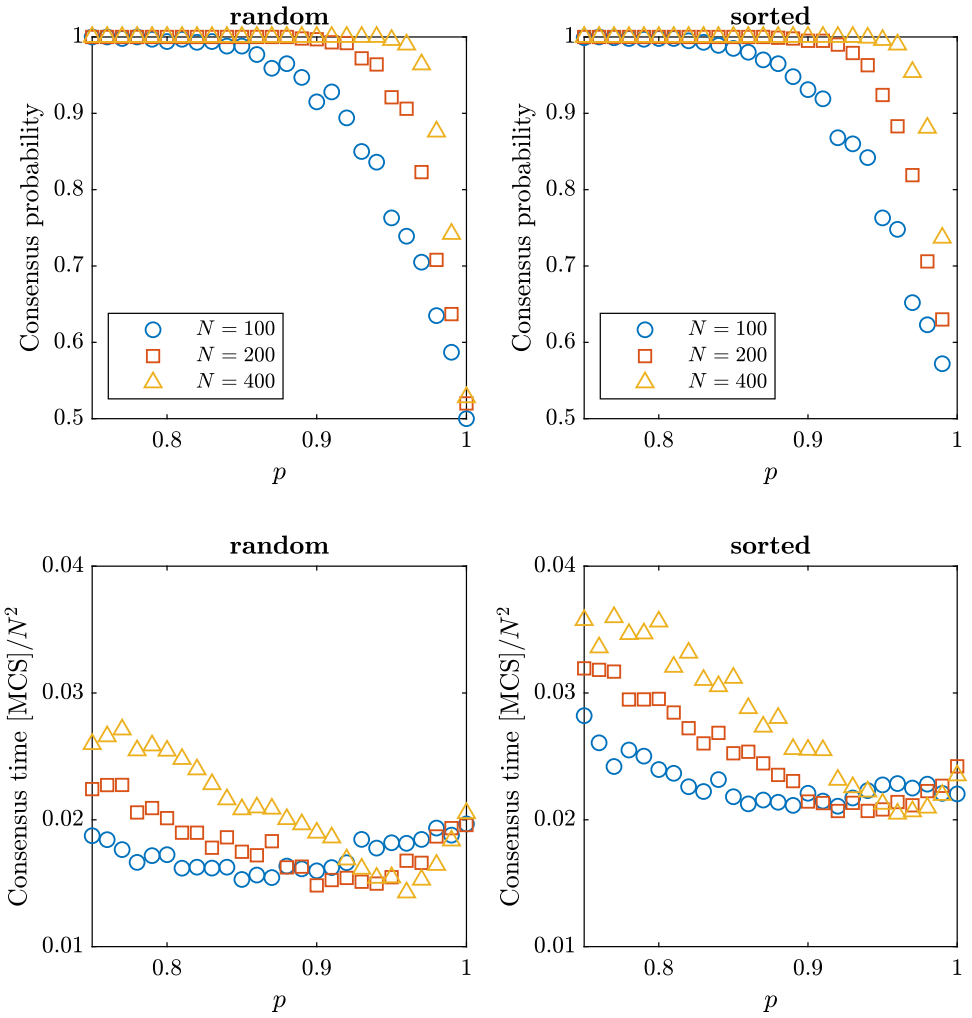

Fig. 2. The impact of the system size N (model without movement). Probability of reaching consensus (top panels) and rescaled mean time to reach consensus (bottom panels) as a function of the probability of disagreeing p. Results are presented for the initial concentration of positive opinion $c_0 = 0.5$, under two types of initial conditions: random (left panels) and sorted (right panels).

4. Model with movement

In the short version of this article, it was suggested that allowing agents to move would bring the model closer to reality. In fact, movement has been interpreted as a search for happiness [49] or information [50]. Moreover, it is interesting from the theoretical point of view, as it introduces more freedom for agents and, simultaneously, more randomness to the system. Our expectation is that this may substantially change the results obtained previously, in particular the relationship between model parameters and types of stationary states, or the times required to reach them.

Therefore, in this paper, we decided to further generalize the model. In the generalized version, we randomly distribute $N \times d$ agents over N cells of a one-dimensional lattice with periodic boundary conditions, i.e. ring, where $d \in [0, 1]$ is an additional model parameter, denoting the density of the occupied cells. As previously, each agent can be in one of the two states $S_i(t) = \pm 1$. For $d = 1$ the model boils down to the previous [42], while for $d < 1$ some cells remain empty, which is indicated by $S_i(t) = 0$, allowing agents to move.

Each elementary update consists of the following sub-steps:

1. Agent i, i.e. an occupied cell, is chosen at random from all cells for which $S_i(t) \neq 0$.
2. The direction j ($j \in \{-1, +1\}$), i.e. left/right, with which an agent interacts, is determined randomly.
3. If the neighboring cell in the chosen direction is empty, $S_{i+j}(t) = 0$, the agent moves into this direction, $S_{i+j}(t + \Delta t) = S_i(t)$, leaving the previously occupied cell empty, $S_i(t + \Delta t) = 0$.
4. Otherwise, if the neighboring cell is occupied, $S_{i+j}(t) \neq 0$, and the pair $(i, i + j)$ is unanimous, $S_i(t) = S_{i+j}(t)$, pair's neighbors $(i-j, i+2j)$ take its state, provided that they are not empty cells, $S_{i-j}(t + \Delta t) = S_i(t) \times |S_{i-j}(t)|$, $S_{i+2j}(t + \Delta t) = S_i(t) \times |S_{i+2j}(t)|$.
5. Lastly, if the pair is not unanimous, $S_i(t) \neq S_{i+j}(t)$, cells $(i - j, i + 2j)$ take states opposite to their nearest neighbors with probability p, provided that they are not empty, $S_{i-j}(t + \Delta t) = -S_i(t) \times |S_{i-j}(t)|$, $S_{i+2j}(t + \Delta t) = -S_{i+j}(t) \times |S_{i+2j}(t)|$.

A single time step consists of $N \times d$ elementary events, and the concentration of agents with positive opinion at any time t is given by:

$$c(t) = \frac{N_+(t)}{N \times d} = \frac{1}{2N \times d} \sum_{i=1}^{N} \left(S_i(t) + |S_i(t)| \right). \tag{3}$$

As previously, we consider two types of initial condition:

- **Random**: choose randomly $N_+(0) \times d$ out of N cells for agents with positive opinions, and $N_-(0) \times d$ – for agents with negative opinions. The rest remain empty.
- **Sorted**: choose randomly $N_+(0) \times d$ out of N cells for agents with positive opinions, and $N_-(0) \times d$ – for agents with negative, so that $\forall i, j \; S_i(0) = 1 \; \wedge \; S_j(0) = -1 \implies i < j$. The rest remains empty.

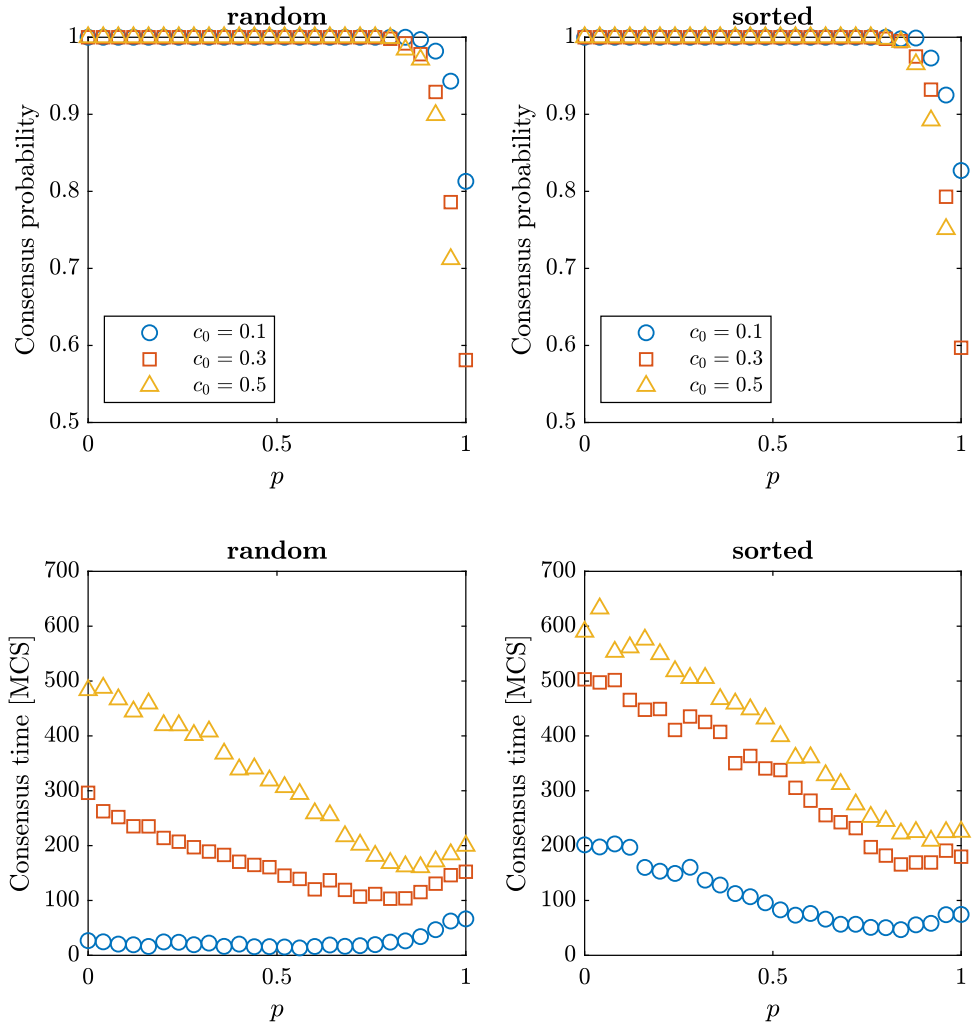

Fig. 3. The impact of the initial concentration of positive opinion c_0 (model without movement). Probability of reaching consensus (top panels) and mean time to reach consensus (bottom panels) as a function of the probability of disagreeing p. Results are presented for the system size $N = 100$, under two types of initial conditions: random (left panels) and sorted (right panels).

For the model without movement, we average the results over $L = 10^3$ independent samples: after initialization, we perform Algorithm 2. Again, we stop the simulation once the opinion-absorbing state is reached or the simulation time t exceeds T. One should notice that there is a small difference between the procedure for the model without and with movement, which is expressed by the usage of the term "opinion-absorbing", instead of "absorbing". This change is due to the fact that for $d < 1$, the system never reaches the real absorbing state, as agents can still move. However, one can imagine that the system reaches the state in which the agents' opinions would never change, agents would only move, such a state we call here an opinion-absorbing one. Again, we have only two types of such state:

1. Consensus, i.e. all agents have the same opinion but they still can move.
2. Disagreement, defined in the following way: any agent moving in any direction will always eventually meet an agent with the opposite opinion. If such a disagreement would be reached, then the agents' opinions would never change, agents would only move.

We can write a simple mathematical rule for such opinion-absorbing states, which gives us the stop condition as presented in Algorithm 2.

Algorithm 2: Algorithm for the model with movement

for $t \leftarrow 1$ **to** T **do**
  for $k \leftarrow 1$ **to** $N \times d$ **do**
    $A \leftarrow \{i \leq N : S_i \neq 0\}$
    $i \leftarrow i \sim \mathcal{U}\{A\}$
    $j \leftarrow j \sim \mathcal{U}\{-1, 1\}$
    if $S_{i+j} = 0$ **then**
      $S_{i+j} \leftarrow S_i$
      $S_i \leftarrow 0$
    else if $S_i = S_{i+j}$ **then**
      $S_{i-j} \leftarrow S_i \times |S_{i-j}|$
      $S_{i+2j} \leftarrow S_i \times |S_{i+2j}|$
    else if $r \sim \mathcal{U}(0, 1) < p$ **then**
      $S_{i-j} \leftarrow -S_i \times |S_{i-j}|$
      $S_{i+2j} \leftarrow -S_{i+j} \times |S_{i+2j}|$
    end
  end
  if $\forall i\ \forall m \in \mathbb{N}\ S_i = S_{i+2m} \vee S_i = 0$ **then**
    break
  end
end

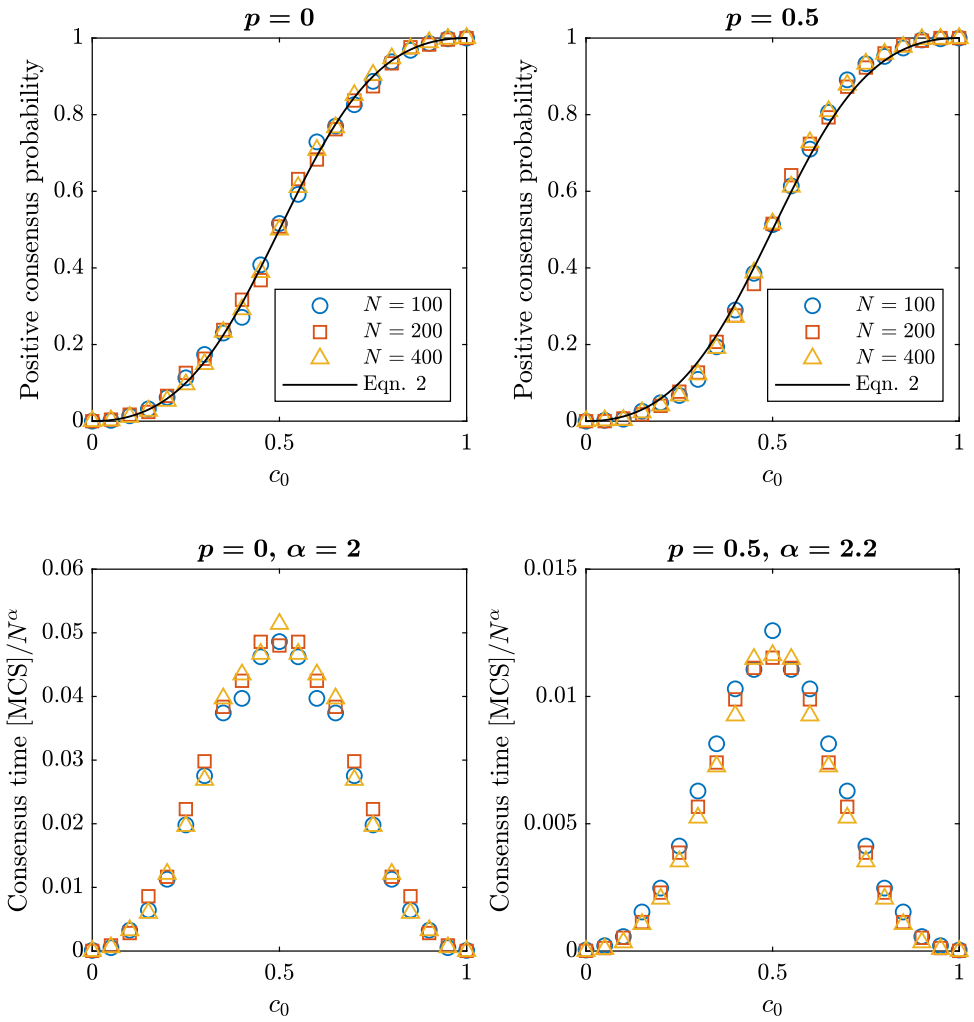

Fig. 4. Comparison with theoretical predictions and scaling with the system size N (model without movement). Probability of reaching a positive consensus P_+ (top panels) and rescaled mean time to reach consensus (bottom panels) as a function of the initial concentration of positive opinion c_0. Results are presented for random initial conditions and two values of the probability of disagreeing: $p = 0$ (left panels) and $p = 0.5$ (right panels).

5. Results for the model with movement

In the short version of this paper, in which only the model that corresponds to $d = 1$ was studied, we reported that for larger values of p the time to reach consensus is shorter. This is not very intuitive, because it means that disagreement with the nearest neighbor accelerates the consensus. The question is if this intriguing result survives in the model with movement $d < 1$.

The first novelty that we see for $d < 1$, is that the system never reaches the real absorbing state, because the agents can move, as mentioned in the previous section. However, the consensus can still be reached and it will remain for ever, as shown in the right panels of Fig. 5. Surprisingly, disagreement can also be reached, as defined in the previous section, which is visible in the left bottom panel of Fig. 5. However, since Fig. 5 presents results only for a densely occupied system ($d = 0.8$), one can ask the question if disagreement can also appear in a more diluted system. To answer this question, we performed simulations for many values of d – the corresponding results are presented in Fig. 6.

As seen in Fig. 6, the results for the model with movement are almost identical to those of the model without movement. First of all, in all the simulations conducted, the system reached one of the opinion-absorbing states, consensus or disagreement. Therefore, we plot in Fig. 6 only the consensus probability — the disagreement probability is just the complementary one. Again, we observe the threshold value p^* below which only consensus is reached, as presented in the upper panels of Fig. 6. Furthermore, the time to reach consensus is still decreasing with p for $p < p^*$. The threshold value p^* decreases with decreasing d, but still approaches 1 for the infinite system. We have checked even very diluted systems (e.g., $d = 0.2$) and in all cases the behavior remained the same.

In more diluted systems, the evolution to consensus is longer. This result is not surprising, as for small values of d interactions with others are rare. First, it is more difficult to form a pair, which is needed to convince others. Second, it is harder to find someone to convince. In summary, contrary to the first result, this one is very intuitive.

6. Discussion

It is often claimed that the key lesson from agent-based modeling can be summarized with the quote by Epstein [9,51]: “We get macro-surprises despite complete micro-level knowledge”. In this paper, we show one such surprise. We expected that for $p = 0$ the time evolution would be long because then the change of state is possible only if the source pair is unanimous. However, we did not expect that even for relatively large values of p, the exit time will decrease with increasing p.

We are aware that the noise in the system can speed up the evolution to the stationary state, but here we have an evolution towards the consensus, and the noise is not really a noise, but the probability of a

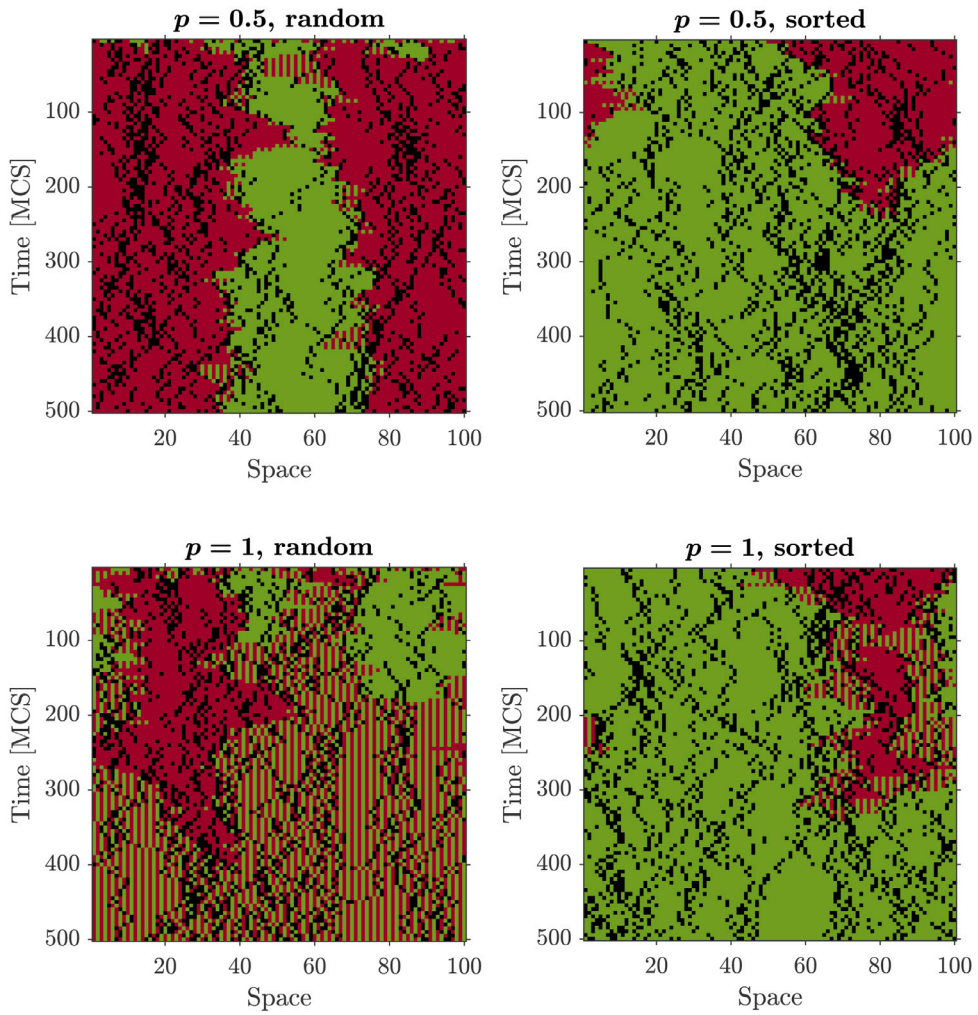

Fig. 5. Temporal–spatial evolution of the system (model with movement) for two values of p and two types of initial conditions, for $c_0 = 0.5$ and $d = 0.8$. Each row correspond to the configuration of opinions in a given time step: black corresponds to an empty site, red (dark) to an agent with a negative opinion and green (light) – with a positive one.

disagreement. It means that consensus is reached faster if we disagree with neighbors more often in case of uncertainty. This intriguing result survives even if we introduce the possibility of movement.

We do realize that the results obtained within the model with movement are related to the chosen rule of the movement, which is purely random. Alternatively, we could introduce the movement towards like-minded agents. However, here we implemented the random movement similarly to the one proposed in [50,52]. In this way, the motion plays a role as a noise. This is particularly desirable from a theoretical point of view because we are studying a one-dimensional system. The results obtained previously, for the model without movement, may have been an artifact of limited freedom of agents. Here, we checked that extending this freedom does not change the results substantially. Probably, changing the topology of the system would influence the results. However, that is a task for the future, as generalization of SM to other structures is not trivial [40].

There is one more issue related to the competition between agreement and disagreement that needs to be pointed out here. In the seminal work on consensus on signed networks, Altafini asked if it is *possible to achieve a form of agreement in presence of antagonistic interactions* [26]. A similar question was asked here in the context of the generalized SM. However, there is a crucial difference between our model and the models of opinion formation on signed networks: In our model, positive and negative interactions are not associated with links. The very same link may be in one time step positive and in another — negative, since the type of interaction solely depends on the dynamically changing state of the source of influence. Moreover, the source of influence itself is also randomly chosen in each update, which means that in one update agent i can be influenced by pair $(i-2, i-1)$ and in another by $(i+1, i+2)$. This kind of approach can be related to the so-called annealed disorder, while the signed network represents the quenched disorder, and it is well known that the type of disorder can significantly change the behavior of the system [53–56]. Nevertheless, relating our results to the ones from the signed networks is definitely interesting. For example, very recently, the threshold q-voter model, which can be treated as a certain generalization of the SM, was studied on signed networks [28]. It was shown that in such a model the noise appearing in the case of uncertainty hinders the emergence of the majority states. This finding is, in a sense, opposite to ours and, using Epstein's language, far less surprising.

We recognize that Epstein's notion of macro-surprises can be criticized by saying that the level of surprise depends on the perceptiveness and experience of the researcher, the ability to find cause–effect relationships, etc. We cannot argue with that, as we cannot state whether our intuition about what facilitates reaching consensus is the same as the intuition of the reader of this work. However, we hope that our paper will inspire at least some readers to explore the model further, for example, on a more realistic social structure.

Another direction for the future research should consist of determining the universality of our findings. The statement in the Introduction that *generally the consensus is reached more rapidly if agents disagree more often with their nearest neighbors in case of uncertainty*, was confirmed in

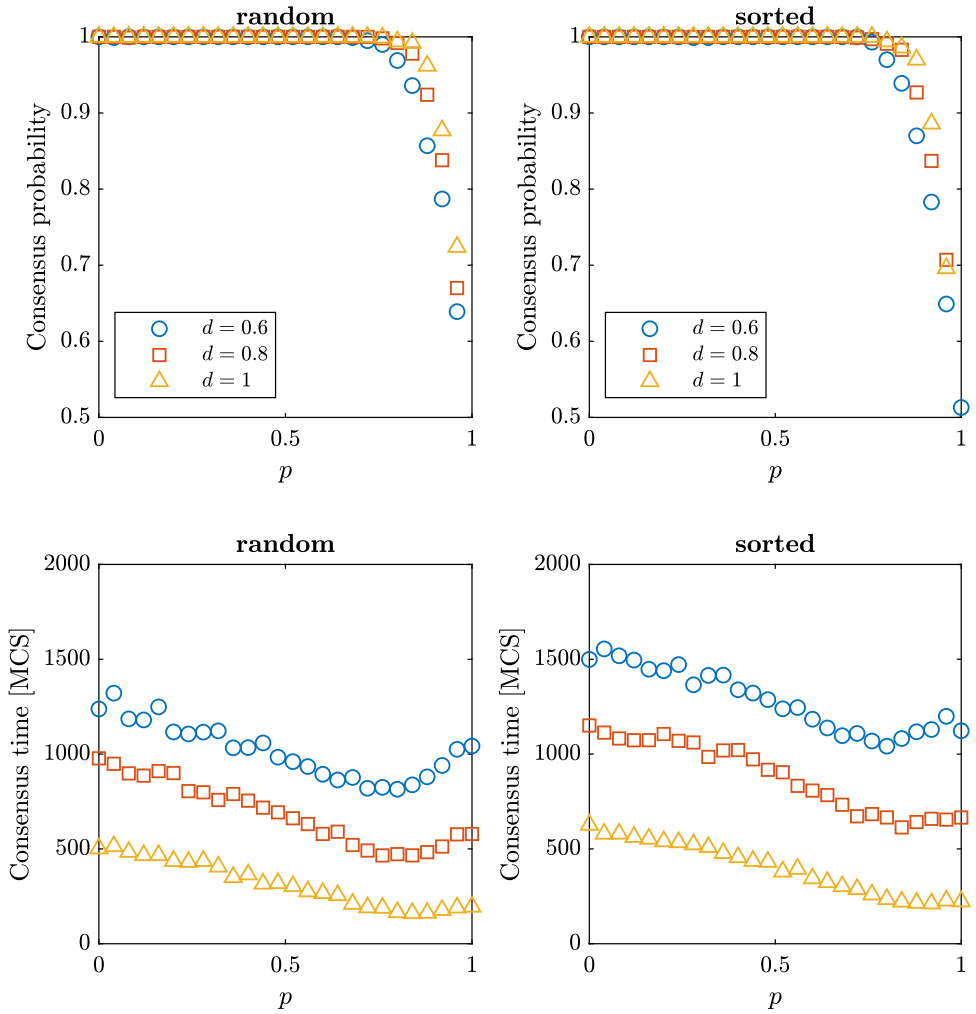

Fig. 6. The impact of the density of occupied cells d (model with movement). Probability of reaching consensus (top panels) and mean time to reach consensus (bottom panels) as a function of the probability of disagreeing p for the system size $N = 100$. Results are presented for the initial concentration of positive opinion $c_0 = 0.5$ under two types of initial conditions: random (left panels) and sorted (right panels).

this paper within a single model. To determine the universality of our finding, one has to examine the entire spectrum of models, which is a desirable task for the future.

CRediT authorship contribution statement

Tomasz Weron: Implementation, Simulation, Visualization, Conceptualization, Funding acquisition, Writing – review & editing. **Katarzyna Sznajd-Weron:** Supervision, Writing – original draft, Conceptualization, Funding acquisition, Writing – review & editing.

Declaration of competing interest

The authors declare that they have no known competing financial interests or personal relationships that could have appeared to influence the work reported in this paper.

Acknowledgments

T. W. was supported by the Ministry of Science and Higher Education, Poland, within the "Diamond Grant" Program through grant no. DI2019 0008 49 and K. S-W. by the National Science Center (NCN, Poland) through grant no. 2019/35/B/HS6/02530.

References

[1] A. Proskurnikov, R. Tempo, A tutorial on modeling and analysis of dynamic social networks, part i, Annu. Rev. Control 43 (2017) 65–79.
[2] A. Proskurnikov, R. Tempo, A tutorial on modeling and analysis of dynamic social networks, part ii, Annu. Rev. Control 45 (2018) 166–190.
[3] P. Sobkowicz, Whither now, opinion modelers? Front. Phys. 8 (2020).
[4] H. Noorazar, Recent advances in opinion propagation dynamics: a 2020 survey, Eur. Phys. J. Plus 135 (6) (2020) cited By 3.
[5] P.-A. Toupance, L. Lefèvre, B. Chopard, Influence measurement in a complex dynamical model: an information theoretic approach, J. Comput. Sci. 44 (2020).
[6] M. Grabisch, A. Rusinowska, A survey on nonstrategic models of opinion dynamics, Games 11 (4) (2020) 1–28.
[7] M. Galesic, H. Olsson, J. Dalege, T. Van Der Does, D. Stein, Integrating social and cognitive aspects of belief dynamics: Towards a unifying framework, J. R. Soc. Interface 18 (176) (2021).
[8] N. Gilbert, R. Conte, Artificial societies: The computer simulation of social life, 2006.
[9] J. Epstein, Generative Social Science: Studies in Agent-Based Computational Modeling, Princeton University Press, 2020.
[10] E. Bonabeau, Agent-based modeling: Methods and techniques for simulating human systems, Proc. Natl. Acad. Sci. USA 99 (SUPPL. 3) (2002) 7280–7287.
[11] C. Castellano, S. Fortunato, V. Loreto, Statistical physics of social dynamics, Rev. Modern Phys. 81 (2) (2009) 591–646.
[12] C.-L. Liu, F. Liu, Stationary consensus of heterogeneous multi-agent systems with bounded communication delays, Automatica 47 (9) (2011) 2130–2133.
[13] V. Sood, S. Redner, Voter model on heterogeneous graphs, Phys. Rev. Lett. 94 (17) (2005).
[14] M. Gastner, B. Oborny, M. Gulyás, Consensus time in a voter model with concealed and publicly expressed opinions, J. Stat. Mech. Theory Exp. 2018 (6) (2018).

[15] M. Gastner, K. Takács, M. Gulyás, Z. Szvetelszky, B. Oborny, The impact of hypocrisy on opinion formation: A dynamic model, PLoS One 14 (6) (2018).
[16] M. Gastner, K. Ishida, Voter model on networks partitioned into two cliques of arbitrary sizes, J. Phys. A 52 (50) (2019).
[17] N. Crokidakis, P. De Oliveira, Inflexibility and independence: Phase transitions in the majority-rule model, Phys. Rev. E 92 (6) (2015).
[18] T. Raducha, M. Wilinski, T. Gubiec, H. Stanley, Statistical mechanics of a coevolving spin system, Phys. Rev. E 98 (3) (2018).
[19] J. Encinas, P. Harunari, M. De Oliveira, C. Fiore, Fundamental ingredients for discontinuous phase transitions in the inertial majority vote model, Sci. Rep. 8 (1) (2018).
[20] A. Chmiel, J. Sienkiewicz, A. Fronczak, P. Fronczak, A veritable zoology of successive phase transitions in the asymmetric q-voter model on multiplex networks, Entropy 22 (9) (2020).
[21] J. Davis, N. Perra, Q. Zhang, Y. Moreno, A. Vespignani, Phase transitions in information spreading on structured populations, Nat. Phys. 16 (5) (2020) 590–596.
[22] T. Raducha, M. San Miguel, Emergence of complex structures from nonlinear interactions and noise in coevolving networks, Sci. Rep. 10 (1) (2020).
[23] P. Górski, K. Bochenina, J. Hołyst, R. D'Souza, Homophily based on few attributes can impede structural balance, Phys. Rev. Lett. 125 (7) (2020).
[24] S. Galam, T. Cheon, Tipping points in opinion dynamics: A universal formula in five dimensions, Front. Phys. 8 (2020).
[25] K. Malarz, K. Kułakowski, Comment on phase transition in a network model of social balance with glauber dynamics, Phys. Rev. E 103 (6) (2021).
[26] C. Altafini, Consensus problems on networks with antagonistic interactions, IEEE Trans. Automat. Control 58 (4) (2013) 935–946.
[27] A. Proskurnikov, A. Matveev, M. Cao, Opinion dynamics in social networks with hostile camps: Consensus vs. polarization, IEEE Trans. Automat. Control 61 (6) (2016) 1524–1536.
[28] Z. Lou, L. Guo, Threshold q-voter model with signed relationships, J. Stat. Mech. Theory Exp. 2021 (9) (2021).
[29] G. Shi, C. Altafini, J. Baras, Dynamics over signed networks, SIAM Rev. 61 (2) (2019) 229–257.
[30] B. Derrida, D. Stauffer, Phase transitions in two-dimensional kauffman cellular automata, Europhys. Lett. 2 (10) (1986) 739–745, http://dx.doi.org/10.1209/0295-5075/2/10/001.
[31] K. Byrka, A. Jedrzejewski, K. Sznajd-Weron, R. Weron, Difficulty is critical: The importance of social factors in modeling diffusion of green products and practices, Renew. Sustain. Energy Rev. 62 (2016) 723–735, http://dx.doi.org/10.1016/j.rser.2016.04.063.
[32] P. Krapivsky, S. Redner, Dynamics of majority rule in two-state interacting spin systems, Phys. Rev. Lett. 90 (23) (2003) 4.
[33] D. Bhat, S. Redner, Polarization and consensus by opposing external sources, J. Stat. Mech. Theory Exp. 2020 (1) (2020).
[34] D. Bhat, J. Pinero, S. Redner, Fixation in fluctuating populations, J. Stat. Mech. Theory Exp. 2019 (6) (2019).
[35] M. Grabisch, F. Li, Anti-conformism in the threshold model of collective behavior, Dynam. Games Appl. 10 (2020).
[36] W. Ren, R. Beard, E. Atkins, A survey of consensus problems in multi-agent coordination, 3 (2005) 1859–1864.
[37] J. Qin, Q. Ma, Y. Shi, L. Wang, Recent advances in consensus of multi-agent systems: A brief survey, IEEE Trans. Ind. Electron. 64 (6) (2017) 4972–4983.
[38] Y. Li, C. Tan, A survey of the consensus for multi-agent systems, Syst. Sci. Control Eng. 7 (1) (2019) 468–482.
[39] F. Slanina, H. Lavicka, Analytical results for the sznajd model of opinion formation, Eur. Phys. J. B 35 (2) (2003) 279–288.
[40] K. Sznajd-Weron, J. Sznajd, T. Weron, A review on the sznajd model — 20 years after, Physica A 565 (2021).
[41] C. Castellano, M. Muñoz, R. Pastor-Satorras, Nonlinear q -voter model, Phys. Rev. E 80 (4) (2009).
[42] T. Weron, K. Sznajd-Weron, How to reach consensus? better disagree with your neighbor, in: Lecture Notes in Computer Science (Including Subseries Lecture Notes in Artificial Intelligence and Lecture Notes in Bioinformatics), in: LNCS, vol. 12744, 2021, pp. 309–315.
[43] K. Sznajd-Weron, J. Sznajd, Opinion evolution in closed community, Internat. J. Modern Phys. C 11 (6) (2000) 1157–1165.
[44] S. Redner, A Guide to First Passage Processes, Cambridge University Press, 2001.
[45] R. Lambiotte, S. Redner, Dynamics of non-conservative voters, Europhys. Lett. 82 (1) (2008).
[46] F. Slanina, K. Sznajd-Weron, P. Przybyła, Some new results on one-dimensional outflow dynamics, Europhys. Lett. 82 (1) (2008).
[47] S. Galam, A. Martins, Pitfalls driven by the sole use of local updates in dynamical systems, Europhys. Lett. 95 (4) (2011).
[48] A. Timpanaro, S. Galam, Testing validity of the kirkwood approximation using an extended sznajd model, Phys. Rev. E 92 (6) (2015).
[49] T. Schelling, Dynamic models of segregation, J. Math. Sociol. 1 (2) (1971) 143–186.
[50] A. Kowalska-Styczeń, K. Sznajd-Weron, From consumer decision to market share - unanimity of majority? JASSS 19 (4) (2016).
[51] E. Smith, F. Conrey, Agent-based modeling: A new approach for theory building in social psychology, Personal. Soc. Psychol. Rev. 11 (1) (2007) 87–104.
[52] A. Jędrzejewski, J. Toruniewska, K. Suchecki, O. Zaikin, J. Hołyst, Spontaneous symmetry breaking of active phase in coevolving nonlinear voter model, Phys. Rev. E 102 (4) (2020).
[53] M. Aizenman, J. Wehr, Rounding of first-order phase transitions in systems with quenched disorder, Phys. Rev. Lett. 62 (21) (1989) 2503–2506, http://dx.doi.org/10.1103/PhysRevLett.62.2503.
[54] A. Jędrzejewski, K. Sznajd-Weron, Statistical physics of opinion formation: Is it a spoof? [physique statistique de la formation d'opinion: est-ce une blague ?], C. R. Phys. 20 (4) (2019) 244–261.
[55] P. Villa Martín, J. Bonachela, M. Muñoz, Quenched disorder forbids discontinuous transitions in nonequilibrium low-dimensional systems, Phys. Rev. E 89 (1) (2014) http://dx.doi.org/10.1103/PhysRevE.89.012145.
[56] G. Ódor, B. De Simoni, Heterogeneous excitable systems exhibit griffiths phases below hybrid phase transitions, Phys. Rev. Res. 3 (1) (2021) http://dx.doi.org/10.1103/PhysRevResearch.3.013106.

Tomasz Weron is currently a Ph.D. student at the Wroclaw University of Science and Technology, Poland. A mathematician by training and political scientist by heart. Possesses experience in energy forecasting, network analytics, modeling opinion dynamics and Monte Carlo simulations.

Katarzyna Sznajd-Weron is a Professor and the Head of the Department of Theoretical Physics, at the Wroclaw University of Science and Technology, Poland. She collaborates actively with social scientists and she is the principal investigator of two grants in the field of social sciences. She is one of the leading world experts on opinion dynamics and social agent-based modeling. She is the winner of the Young Scientist Award for Socio- and Econophysics 2007 and she is mainly known as a coauthor of the Sznajd model of opinion formation, which according to SCOPUS gained so far over 1000 citations, without self-citations.

Paper 2

Opinion Evolution in Divided Community

Tomasz Weron, Janusz Szwabiński

entropy

MDPI

Article

Opinion Evolution in Divided Community

Tomasz Weron * and Janusz Szwabiński

Hugo Steinhaus Center, Faculty of Pure and Applied Mathematics, Wrocław University of Science and Technology, 50-370 Wrocław, Poland; janusz.szwabinski@pwr.edu.pl
* Correspondence: tomasz.weron@pwr.edu.pl

Abstract: Our agent-based model of opinion dynamics concerns the current vast divisions in modern societies. It examines the process of social polarization, understood here as the partition of a community into two opposing groups with contradictory opinions. Our goal is to measure how mutual animosities between parties may lead to their radicalization. We apply a double-clique topology with both positive and negative ties to the model of binary opinions. Individuals are subject to social pressure; they conform to the opinions of their own clique (positive links) and oppose those from the other one (negative links). There is also a chance of acting independently, which alters the system's behavior in various ways, depending on its magnitude. The results, obtained with both Monte-Carlo simulations and the mean-field approach, lead to two main conclusions: in such a system, there exists a critical quantity of negative relations that are needed for polarization to occur, and (rather surprisingly) independent actions actually support the process, unless their frequency is too high, in which case the system falls into total disorder.

Keywords: opinion dynamics; social polarization; agent-based model; Monte-Carlo simulation

Citation: Weron, T.; Szwabiński, J. Opinion Evolution in Divided Community. *Entropy* **2022**, *24*, 185. https://doi.org/10.3390/e24020185

Academic Editors: Francis Heylighen, Tomas Veloz, Olaf Witkowski and Daniela Flores

Received: 14 November 2021
Accepted: 24 January 2022
Published: 26 January 2022

1. Introduction

Polarization is a frequently used concept in social and political science as well as economics, but its definition may differ between domains. Within this paper, we will follow the one given by DiMaggio et al. and assume that polarization refers to a situation in which a group of people is divided into two opposing cliques with contrasting positions on a given issue [1]. This type of polarization is sometimes called bi-polarization [2] to distinguish it from the group polarization phenomenon, i.e., the tendency for a group to make more extreme decisions than the initial inclination of its members [3,4].

Recent observers point to a growing polarization of modern societies [5]. This seems to be a defining feature of many public domains and was identified in the World Economic Forum's 2017 Global Risk Report as one of the top threats to the global order [6]. Consequently, it is gaining increasing attention from researchers working at the intersection of many fields, including social and political science, economics, mathematics and statistical physics.

High and increasing levels of polarization are attributed to a variety of sources, including the isolating effects of social media or news outlets focusing more on outraged rants than reasoned debates. Although significant progress has been observed in our understanding of polarization mechanisms in recent years, our knowledge remains sketchy and there is still a lot of room for improvement. Each new insight into polarization is important, because it is known to have a huge impact on societies. This leads to social tension and conflicts, and may result in the segregation of societies [1].

Interestingly, not all debates have the potential to polarize societies. From the observations, it follows that, in order to drive people to extreme and opposing opinions, the topic of a discussion has to be perceived as important and emotionally charged by all participants. That is why polarizing topics comprise controversial issues such as abortion rights, homosexuality, public funding for the arts, gun control, global warming, vaccination and, last but not least, politics [7–12].

Starting with Eli Pariser's book [13], social media sites are increasingly blamed for intensifying (political) polarization. The artificial intelligence algorithms used by sites such as Facebook, Twitter or Google to profile the users create so-called "echo chambers" (or "filter bubbles"), which separate people from the information that disagrees with their viewpoints. The idea behind these algorithms was to let the people stay in their comfort zones. An unexpected side effect of this approach is an unconscious confirmation bias, because people are mainly confronted with information that reinforces their beliefs and opinions. The bias may contribute to overconfidence in personal beliefs and can maintain or strengthen them in the face of contrary evidence, which leads to polarization [5].

Several possible mechanisms leading to a stable bi-polar distribution of opinions within a simulation have been already proposed. There is, for instance, a series of papers showing that opinion homophily may support opinion plurality, including polarization [14–17]. This type of homophily is understood as a relationship between a similarity in peoples' views and an increased likeliness of their interaction. This was usually implemented as a bounded confidence, i.e., threshold mechanisms that switch off influence in case the discrepancy in opinion is too big. Long-range ties (bridges between clusters) in a social network may also foster polarization if homophily and assimilation at the microlevel are combined with some negative influence, e.g., xenophobia [18,19]. From social balance theories, it follows that a mixture of positive and negative ties is needed for polarization to emerge and prevail [20–22]. In the argument-communication model, agents with a similar attitude mutually reinforce that attitude by the exchange of supportive arguments, which, in some circumstances, also leads to polarization [2]. Both the majority model [23] and the Ising model [24] in a segmented network only support the initial polarization in the presence of conforming relations if the density of connections between the segments remains low. Finally inflexibility, understood here as an internal opinion that encodes how many encounters with different-minded agents are needed for an agent to change its external opinion, has been shown to polarize a population in the sense that two opposing camps of increasingly inflexible supporters may emerge [25–27].

Recently, we proposed a simple polarization model based on the q-voter model with both conformity and anticonformity [21,22]. We considered the model of a double-clique social network, because it mimics the echo chambers that are observed on social media platforms as well as the interactions between their members. We found that if the number of inter-clique connections stays below a critical value, a consensus between two antagonistic cliques is possible. Thus, in light of these results, the artificial intelligence algorithms producing echo chambers on many platforms may have a positive impact in terms of polarization, because they reduce exposure to different opinions. In this paper, we are going to extend our model with independence to make the spectrum of possible responses to social influence more realistic from the social science perspective [28–30].

The paper is organized as follows. In the next section, we provide a detailed description of the models and methods used to analyze them. Then, we present the results. Finally, in Section 4, we discuss the results and draw some conclusions.

2. Models and Methods

2.1. Modelling Framework

The basic assumptions of our model have been already extensively discussed in Refs. [21,22]. Therefore, we start this section with only a short overview of its major premises:

- A binary opinion model with a single trait.
- q-voter model with conformity and anti-conformity as the general modeling framework.
- Double clique topology as the underlying social network.
- Conformity between agents within a clique and anti-conformity in the interactions between the cliques.

All of the above assumptions can be justified by recent findings in the opinion dynamics community. For instance, the analysis of many social networks revealed that

the polarization of opinions within those networks may be correlated with their segmentation [31–33]. Hence, we assumed that the network is already modular and took the double-clique topology [34] as its model. Choosing a binary model with a single trait is rooted in the observation that, in many situations, people's opinions may be interpreted as simple "yes/no" (i.e., binary) answers [35]. Moreover, social networks are often characterized by a semantic unicity, i.e., the opinions and interactions of network members are restricted to a single topic [36].

The q-voter model is one of the extensively studied models of binary opinions. Within the original formulation [37], the dynamics is given by the following update rule:

1. Pick a target agent at random.
2. Choose randomly q neighbors of the target (possibility of repetition).
3. If all the q neighbors are in the same state, the target changes its state accordingly.
4. Otherwise, the target changes its state with probability ϵ.

The unanimity rule embedded in the model is in line with a number of social experiments [38–40]. Please note that, in our studies, we only consider $\epsilon = 0$, following the setup in the previous papers [21,22].

Conformity, understood as the act of matching opinions to the group norm, is the only social force in the original q-voter model. However, it is relatively easy to extend it, with other possible responses, to social influences such as independence and/or anticonformity [30,41–48]. The first one is simply unwillingness to yield to group pressure and introduces noise to the system; the latter means a deliberate challenging of the group position. In Refs. [21,22], we used anticonformity to mimic negative ties between agents belonging to two opposite cliques, in agreement with the social balance theories [20]. It should be noted that the double-clique topology, with conformity inside a clique and anticonformity between the cliques, resembles, to some extent, the controversial echo chambers generated by social platforms [13].

2.2. Independence of Agents

In Refs. [21,22], we have shown, both theoretically and by means of Monte Carlo simulations, that a system consisting of two connected antagonistic cliques undergoes a phase transition as the number of cross-links between the cliques changes. Below the critical point (i.e., loosely connected cliques), the intra-clique conformity takes over and consensus in the entire system is possible as an asymptotic state. Above the critical point, the system ends up in a polarized state, with the cliques having opposite opinions and a local consensus between them. This was a surprising result, because it actually defies the criticism of echo chambers that was started by Pariser [13]. Since the algorithms generating the echo chambers reduce the exposure time to different-minded people, in light of our findings, they should lower the polarization level between antagonistic groups, instead of enhancing it.

However, one of the drawbacks of the model presented in Refs. [21,22] was the lack of independence in the behavior of agents. This concept has been already considered in a series of models [30,41,49–52]. It actually implies the failure of an attempted social influence, because an independent individual makes decisions independently of the group norm. From the perspective of social science, it falls (together with anticonformity) into the category of non-conformal behaviors [28,29,53]. From a physical point of view, it plays the role of social temperature that induces an order–disorder transition [41,54,55]. Thus, it would be interesting to check how the introduction of independence into our model will change the behavior of the entire system, and if our findings still hold in the extended version of the model.

We will introduce the independence to the model in a situation-oriented manner [44,46]. In a given time step, a target of influence will behave independently with probability h or will become a conformist with probability $1 - h$ (Figure 1). Thus, an additional control parameter h will be used to simulate the impact of the situational factors on the behavior of agents. Within this approach, every agent may change his behavior from step to step, and

sometimes act independently, and sometimes like a conformist (see Section 2.4 for detailed, updated rules of the model).

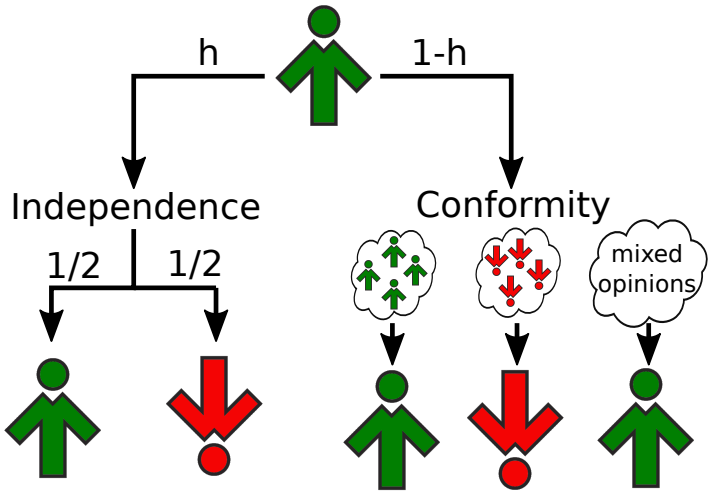

Figure 1. Schematic representation of the opinion update of a single agent that was initially in the up state. With probability h, the agent acts independently and changes opinion randomly. With complementary probability $1-p$, the agent is subject to social influence.

2.3. Quenched and Annealed Disorder Models

In Ref. [22], two versions of the model were considered. In the quenched disorder one, two cliques of size N are connected with $L \times N^2$ cross-links. The parameter L is simply the fraction of the existing cross-links; N^2 is their maximum number. Once the links between cliques are chosen randomly, they remain fixed—the resulting network does not change in time during the evolution of the system.

Instead of working with the fixed-cross links, in the annealed version of the model, we assume that every agent from one clique is connected with probability p with an agent from the other clique, and with probability $1-p$, with an agent from its own clique. Technically, this approximation is nothing but an average of the quenched disorder model over different cross-link configurations in the network.

Given the fraction of existing cross-links L, the probability p of choosing one cross-link out of all possible connections between agents in the double-clique network is given by

$$p = \frac{LN^2}{LN^2 + 2\frac{N(N-1)}{2}} \simeq \frac{L}{L+1}. \tag{1}$$

If the number of cross-links is smaller than their maximum number, the agents in the quenched disorder model differ from each other, because some of them may have no connections to the other clique, while some others have multiple ones. While it can be handled with ease within a computer simulation, this feature usually constitutes a challenge for mathematical modeling due to the necessity of performing a quenched average over the disorder [56]. The annealed model is easier, in the sense that it allows for mathematical treatment.

2.4. Updating Rules of the Models

To recap, we consider a set of $2N$ agents, each of whom may be in one of two possible states, reflecting an opinion on some given issue: $S_i = -1$ or $S_i = 1$ for $i = 1, 2, \ldots, 2N$. We put the agents into a double-clique network, which consists of two complete graphs of N nodes connected with $L \times N^2$ cross-links.

We assume that the social response of agents depends on their group identity. Thus, an agent will strive for agreement within his/her own clique (conformity) and simultaneously challenge the opinions of individuals from the other clique (anticonformity). As in

Ref. [22], we introduce the notion of signals to the q-voter model and slightly alter the concept of unanimity of the influence group in order to account for the fact that an agent may act as both a conformist and anticonformist at the same time. A signal is just the state of the neighbor when coming from the target's clique, or its inverted state otherwise. The target of influence only changes its opinion if all members of the influence group emit the same signal (Figure 2).

We will use Monte Carlo simulations with a random sequential updating scheme as the main tool to analyze the models. Each Monte Carlo step in a simulation consists of $2 \times N$ elementary events, each of which may be divided into the following substeps with $\Delta t = \frac{1}{2N}$:

1. Pick a target agent at random (uniformly from $2N$ nodes).
2. Draw a random number form a uniform distribution, $r \sim U(0,1)$.
3. If $r < h$ (i.e., with probability h), the agent is independent:
   (a) Change its state with probability $1/2$. To this end, draw a random number f from a uniform distribution, $f \sim U(0,1)$:
      i. if $f < 1/2$, change the state of the target, i.e., $S_i(t + \Delta t) = -S_i(t)$,
      ii. otherwise, do nothing.
   (b) Go to step 1.
4. If $r > h$ (i.e., with probability $1 - h$), the agent is subject to social influence:
   (a) Randomly choose a group of q distinct neighbors of the target node:
      Quenched model — simply look at the actual neighbors of the target (sampling with replacement).
      Annealed model — first decide to which clique every member of the influence group will belong (with probability $1 - p$ to the target's clique, with p to the other one), then randomly choose the member from the appropriate clique.
   (b) Convert the states of the group members to signals. Assume that the signals of the neighbors from target's clique are equal to their states. Invert the states when from the other clique.
   (c) Calculate the total signal of the influence group by summing up the individual signals of its members.
   (d) If the total signal is equal to $\pm q$ (i.e., all group members emit the same signal), the target changes its opinion accordingly (see Figure 2). Otherwise, nothing happens.
5. Go to step 1.

2.5. Quantities of Interest

The macroscopic state of an opinion dynamics model is usually described by either the concentration of agents in state $+1$ or the average opinion (i.e., magnetization in physical systems). Noting that the total number of agents in our model is $2N$, we obtain the following formula for the concentration:

$$c(t) = \frac{N^{\uparrow}(t)}{2N}. \tag{2}$$

Here, $N^{\uparrow}(t)$ stands for the number of agents in state $+1$. Similarly, the average opinion is given by

$$m(t) = \frac{1}{2N} \sum_{i=1}^{2N} S_i = \frac{N^{\uparrow}(t) - N^{\downarrow}(t)}{2N}, \tag{3}$$

where $N^{\downarrow}(t)$ denotes the number of agents in state -1. Both quantities may be used interchangeably, because

$$m(t) = 2c(t) - 1. \tag{4}$$

Knowing the concentration of the entire system may be not enough to describe it uniquely in case of the double-clique topology. For instance, the value $c(t) = 1/2$ may correspond to no ordering in the system (i.e., a perfect mixture of $+1$ and -1 states in both cliques) or to polarization (all agents in state $+1$ in one clique and in state -1 in the other). This is why it would be more insightful to calculate the above quantities for single cliques rather than for the entire system,

$$\begin{aligned} c_X(t) &= \frac{N_X^{\uparrow}(t)}{N}, \quad X = A, B, \\ m_X(t) &= \frac{1}{N}\sum_{i=1}^{N} S_{X,i} = \frac{N_X^{\uparrow}(t) - N_X^{\downarrow}(t)}{2}. \end{aligned} \tag{5}$$

The interpretation of their values is summarized in Table 1. Moreover, from the above definition, it follows that c_X may be interpreted as the probability of finding an agent in state 1 within the clique X.

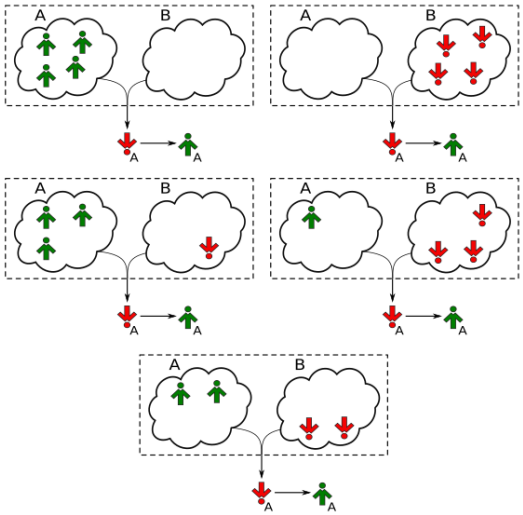

Figure 2. All possible choices of the influence group in the model with $q = 4$ that lead to an opinion flip by a target from clique A that was initially in state $S = -1$. The influence group may contain members from both cliques. Due to the presence of both positive and negative ties, the concept of unanimity from the original q-voter model has to be extended to signals, which are then received by the target of influence. A signal is the state of a member when coming from target's clique, or its inverted state otherwise. The target changes its opinion only if all members of the influence group emit the same signal.

It is also interesting to look at the product $m_A(t)m_B(t)$ of the clique magnetizations, as it immediately indicates a consensus (the value of the product equal to 1) and polarization (-1) for the entire system.

2.6. Transition Probabilities and Dynamical System

The random sequential updating scheme in our model means that, in each time step $\Delta t = 1/2N$, only one agent can change its opinion. Three scenarios are possible: (1) the total amount of agents in state $+1$ in a clique may increase by 1 within this step, (2) the total amount may decrease by 1 or (3) it may remain unchanged.

Table 1. Interpretation of different values of the concentration $c_X(t)$ and the average opinion $m_X(t)$ within a single clique X (see Equation (5) for definitions).

Meaning	$c_X(t)$	$m_X(t)$
Positive consensus (all agents in clique X in state $+1$)	$c_X = 1$	$m_X = 1$
Partial positive consensus (majority of agents in clique X in state $+1$)	$1/2 < c_X < 1$	$0 < m_X < 1$
No ordering in clique X	$c_X = 1/2$	$m_X = 0$
Partial negative consensus (majority of agents in clique X in state -1)	$0 < c_X < 1/2$	$-1 < m_X < 0$
Negative consensus (all agents in clique X in state -1)	$c_X = 0$	$m_X = -1$

Let us have a look at the first of the above scenarios. The number of agents in state $+1$ in one clique—say A—can increase by 1 only if:

1. a target from clique A is chosen (probability $1/2$),
2. the target is in state -1 (probability $1 - c_A$),
3. it flips due to independence (probability $h/2$) or follows an influence group emitting signal $+q$.

Thus, the transition probability for such an event will be given by

$$\Pr\left\{N_A^{\uparrow}(t+\Delta t) = N_A^{\uparrow}(t) + 1\right\} = \frac{1}{2}(1 - c_A(t))\left(\frac{1}{2}h + (1-h)[(1-p)c_A(t) + p(1 - c_B(t))]^q\right). \quad (6)$$

One can easily check that the term of the form $(u+v)^q$ in the above equation is the generating function for the probabilities of those compositions of q members of an influence group that can cause an opinion-switch event (see Figure 2 for more details). Similarly, the number of agents in state $+1$ in clique A decreases by 1 if:

1. A target from clique A is chosen (probability $1/2$).
2. The target is in state $+1$ (probability c_A).
3. It flips due to independence (probability $h/2$) or follows an influence group emitting signal $-q$.

These conditions lead to the following transition probability:

$$\Pr\left\{N_A^{\uparrow}(t+\Delta t) = N_A^{\uparrow}(t) - 1\right\} = \frac{1}{2}c_A(t)\left(\frac{1}{2}h + (1-h)[(1-p)(1 - c_A(t)) + pc_B(t)]^q\right). \quad (7)$$

It is also possible that the number of agents in state $+1$ remains unchanged in an elementary time step. The probability of this event is 1 minus the above probabilities of changes:

$$\Pr\left\{N_A^{\uparrow}(t+\Delta t) = N_A^{\uparrow}(t)\right\} = 1 - \Pr\left\{N_A^{\uparrow}(t+\Delta t) = N_A^{\uparrow}(t) + 1\right\} - \Pr\left\{N_A^{\uparrow}(t+\Delta t) = N_A^{\uparrow}(t) - 1\right\}. \quad (8)$$

Analogous considerations can be conducted for clique B.

Given the states of the cliques at time t and the above transition probabilities, the expectations for the numbers of agents in state $+1$ at time $t+\Delta t$ may be written as

$$\begin{aligned} E\left(N_A^{\uparrow}(t+\Delta t)\right) = N_A^{\uparrow}(t) &+ \frac{1}{2}(1-c_A(t))\left(\frac{1}{2}h+\bar{h}[\bar{p}c_A(t)+p(1-c_B(t))]^q\right) \\ &- \frac{1}{2}c_A(t)\left(\frac{1}{2}h+\bar{h}[\bar{p}(1-c_A(t))+pc_B(t)]^q\right), \\ E\left(N_B^{\uparrow}(t+\Delta t)\right) = N_B^{\uparrow}(t) &+ \frac{1}{2}(1-c_B(t))\left(\frac{1}{2}h+\bar{h}[\bar{p}c_B(t)+p(1-c_A(t))]^q\right) \\ &- \frac{1}{2}c_B(t)\left(\frac{1}{2}h+\bar{h}[\bar{p}(1-c_B(t))+pc_A(t)]^q\right), \end{aligned} \tag{9}$$

where the abbreviations $\bar{p} = 1-p$ and $\bar{h} = 1-h$ have been introduced for the sake of readibility.

Under the very likely assumption that the random variables $c_{A,B} = \frac{N_{A,B}^{\uparrow}}{N}$ localize in the limit $N \to \infty$, after the division of both sides of the equations by N, we obtain

$$\begin{aligned} \frac{c_A(t+\Delta t)-c_A(t)}{\Delta t} &= (1-c_A(t))\left(\frac{1}{2}h+\bar{h}[\bar{p}c_A(t)+p(1-c_B(t))]^q\right) \\ &\quad -c_A(t)\left(\frac{1}{2}h+\bar{h}[\bar{p}(1-c_A(t))+pc_B(t)]^q\right), \\ \frac{c_B(t+\Delta t)-c_B(t)}{\Delta t} &= (1-c_B(t))\left(\frac{1}{2}h+\bar{h}[\bar{p}c_B(t)+p(1-c_A(t))]^q\right) \\ &\quad -c_B(t)\left(\frac{1}{2}h+\bar{h}[\bar{p}(1-c_B(t))+pc_A(t)]^q\right). \end{aligned} \tag{10}$$

In the limit $N \to \infty$, i.e., $\Delta t = \frac{1}{2N} \to 0$, we arrive at the dynamical system representing the annealed model:

$$\begin{aligned} \frac{\mathrm{d}x}{\mathrm{d}t} &= (1-x)\left(\frac{1}{2}h+\bar{h}[\bar{p}x+p(1-y)]^q\right) - x\left(\frac{1}{2}h+\bar{h}[\bar{p}(1-x)+py]^q\right), \\ \frac{\mathrm{d}y}{\mathrm{d}t} &= (1-y)\left(\frac{1}{2}h+\bar{h}[\bar{p}y+p(1-x)]^q\right) - y\left(\frac{1}{2}h+\bar{h}[\bar{p}(1-y)+px]^q\right), \end{aligned} \tag{11}$$

where x and y are the limiting values of concentrations c_A and c_B, respectively.

3. Results

We will assume that the number of agents in every clique in the quenched model is $N = 100$. Although the size of the system may seem very small, it was already shown in Refs. [21,22] that increasing the size does not qualitatively change the outcome of the simulations, but it takes substantially longer to finish them.

In our analysis, we considered influence groups of sizes ranging from 2 to 6, with the upper bound motivated by the conformity experiments by Asch [40]. Qualitatively, the results were independent of the actual value of q. Thus, we decided to present the results for $q = 4$, a value often used in the analysis of the q-voter model and its extensions.

If not stated otherwise, the results of the simulations were averaged over 1000 independent runs. In most cases, the asymtotic state was reached quickly, in less than 100 Monte Carlo steps. We used our own codes written in C++, Python and Matlab.

As for the initial condition, we used the total positive consensus, i.e., all agents in the state $+1$. As already pointed out in Ref. [21], this choice may be treated as a result of the following scenario. Two cliques with a natural tendency to disagree with each other first evolve independently. They get in touch by chance and establish some cross-links to the other group after they both reach consensus on a given issue.

When comparing the two models, quenched and annealed, we present the results with respect to the fraction of the existing cross-links, L, instead of p, using the relationship from Equation (1).

3.1. Direction Fields and Stationary Points

The set of Equations (11) is too cumbersome to solve analytically. However, we still can generate direction fields for the set to graphically trace out solution curves for various initial values [57]. Results for different independence levels h and two different probabilities of an inter-clique connection p are shown in Figure 3: the left column contains the plots for $p = 0.1$; the right one corresponds to $p = 0.2$. The values of h are equal to 0.0, 0.1, 0.2 and 0.5 (from top to bottom). Note that the case $h = 0$ is nothing but our original model with no independence, which was extensively studied in Ref. [22].

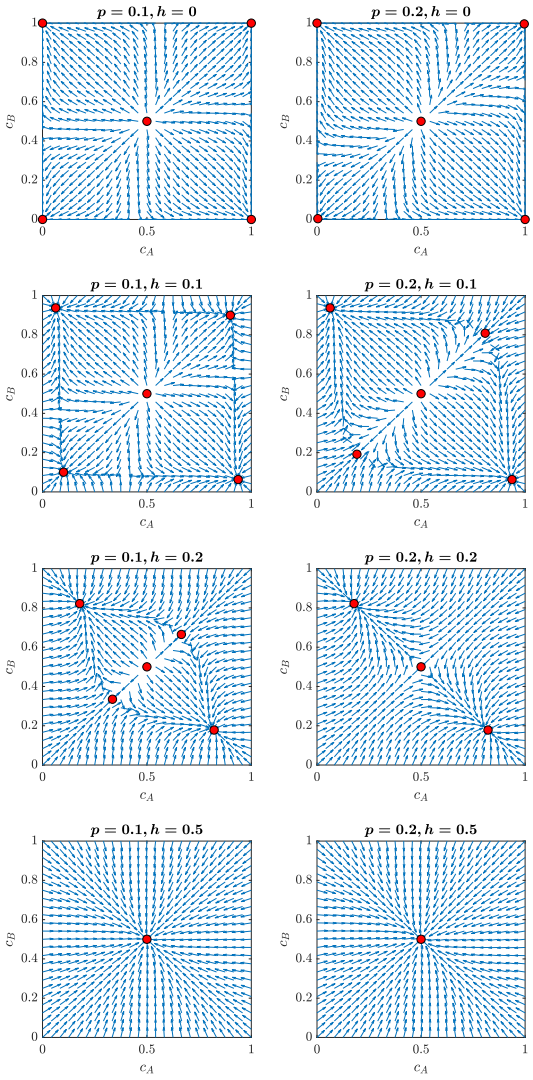

Figure 3. The annealed model: direction fields of the model described by Equation (11) with fixed points marked with circles for different values of independence h and two values of parameter p, 0.1 (**left** column) and 0.2 (**right** column).

From the flows in the state plane, it follows that for $p = 0.1$ and $h = 0$, there are five stationary points (already marked with dots in the plots). Two attractors, $P_1 = (0, 1)$ and $P_2 = (1, 0)$, correspond to a polarized state of the system, i.e., all agents in one clique are in state $+1$ and in the others are in state -1. There are two other symmetric attractors, C_1 and C_2, which are very close to the coordinates $(0, 0)$ and $(1, 1)$. Thus, the state of (almost)

complete consensus is possible in the system as well. The remaining point R is a repeller, because the system tends to evolve away from it.

To find the exact coordinates of the stationary points, we set x' and y' as equal to zero in Equation (11) and solve the resulting set of equations with respect to x and y,

$$\begin{aligned} 0 &= (1-x)\left(\frac{1}{2}h + \bar{h}[\bar{p}x + p(1-y)]^q\right) - x\left(\frac{1}{2}h + \bar{h}[\bar{p}(1-x) + py]^q\right), \\ 0 &= (1-y)\left(\frac{1}{2}h + \bar{h}[\bar{p}y + p(1-x)]^q\right) - y\left(\frac{1}{2}h + \bar{h}[\bar{p}(1-y) + px]^q\right). \end{aligned} \tag{12}$$

For $p = 0.1$ and $h = 0.0$, we obtain:

$$\begin{aligned} &P_1 = (0,1), \quad P_2 = (1,0), \\ &C_1 = (0.00015, 0.00015), \quad C_2 = (0.99985, 0.99985), \\ &R = (0.5, 0.5). \end{aligned} \tag{13}$$

Introducing a small level of independence ($h = 0.1$ and 0.2) into the model does not change the classification of the stationary points for $p = 0.1$. However, they are now shifted towards the center of the state plane, meaning that complete polarization and (almost) complete consensus have changed to partial ones. Although these states are still characterized by a majority of agents sharing the same opinion, due to the fluctuations induced by independence there is now always a minority with the opposite opinion. At a high independence level ($h = 0.5$), the point $R = (0.5, 0.5)$ becomes an attractor and the other stationary points disappear.

The situation for $p = 0.2$ is similar, but the effects induced by the independence h are stronger. This is why we explicitly see a state with only three fixed points at $h = 0.2$ (the same state for $p = 0.1$ would require $0.2 < h < 0.3$ and is not shown in Figure 3). We can see that, in this case, the consensus attractors C_1 and C_2 have already disappeared. The polarization ones are still there, but are closer to the center of the plane. The repeller $R = (0.5, 0.5)$ becomes hyperbolic. With further increases in h, the polarization attractors will disappear as well and point R will become an attractor (see case $h = 0.5$).

Compared to the model without independence [21,22], we observe an additional dynamical phase transition in the system—for high enough independence levels, it enters the disordered phase with the vanishing magnetization in every clique, as the asymptotic state.

3.2. Time Evolution of the System

The asymptotic dynamical system for the annealed model, given by Equation (11), was solved numerically. Results for different values of h, as a function of time and L, are shown in Figure 4 (right column). As was already concluded from the direction fields (Figure 3), in the absence of independence (top right plot in Figure 4), a consensus is observed in both cliques for a low number of cross-links. More connections between the cliques drive the system towards a polarized state. The picture is different for a low level of independence in the model (bottom right plot in Figure 4). We still observe a consensus if the cliques are poorly connected. However, polarization sets in at a much lower number of cross-links. Moreover, both the consensus and polarization are partial, because, due to independence, there is always a group of agents that do not go along with the majority. Increasing the independence level destroys the ordering in the system and the model ends up in an asymptotic state with no polarization (see Figure 5, right column). This last result is independent of the number of cross-links between the cliques.

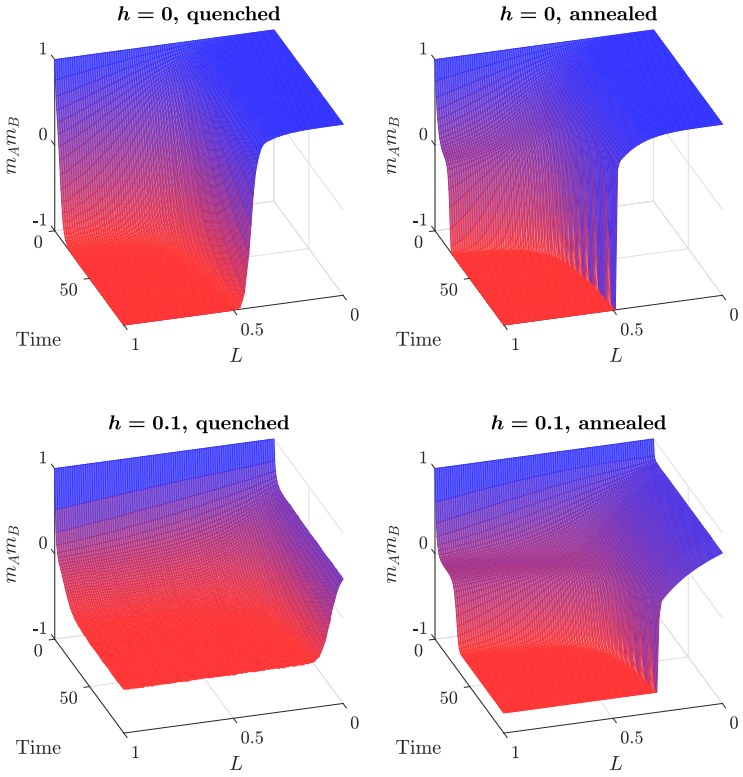

Figure 4. Comparison between the quenched (**left** column) and annealed (**right** column) models: product of magnetizations $m_A m_B$ as a function of time and L, for two different independence levels, $h = 0,\ 0.1$.

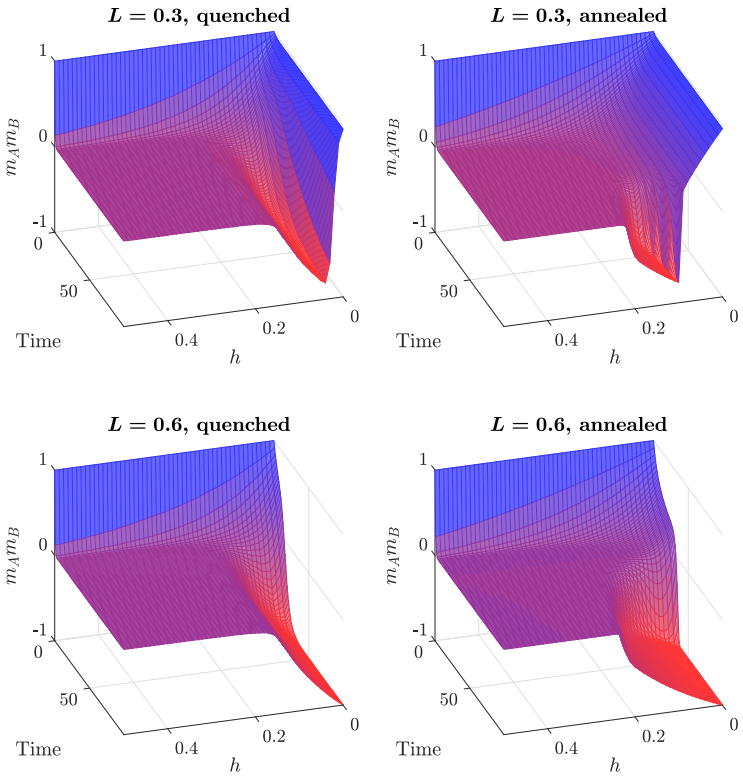

Figure 5. Comparison between the quenched (**left** column) and annealed (**right** column) models: product of magnetizations $m_A m_B$ as a function of time and h, for two different fractions of cross-links, $L = 0.3, 0.6$.

Monte Carlo simulations of the quenched version of the model produce a similar output (see Figures 4 and 5). However, the critical value of L for the dynamical consensus–polarization phase transition is smaller for the quenched model, in agreement with our previous findings for models without independence [21,22]. Moreover, in the quenched model, the inclusion of independence has a much greater impact (see Figure 4, bottom part).

3.3. Impact of Independence on the System

All results up to this point suggest that there are three effects resulting from the introduction of independence into the models: (1) final concentrations of agents sharing the same opinion are diminished, (2) the critical values of L at the consensus–polarization transition are smaller and (3) an additional dynamical phase transition from the polarized state to a disordered one occurs in the system.

To elaborate on those findings, let us have a look at Figure 4. The case $h = 0$ (no independence) corresponds to the original models from Refs. [21,22]. We see that, for values smaller than a critical value, L^*, both cliques end up reaching a consensus. In other words, in this regime, the intra-clique conformity wins with the inter-clique anti-conformity, and both communities are able to maintain their initial consensus, at least partially. Larger values of L are needed for the negative ties to take over and push the system into a polarized state.

The impact of independence is two-fold. First, the final magnetizations have been pushed away from the values ± 1 even in the case $L = 0$, i.e., the total consensus changed to a partial one. Since this corresponds to the weakening of the force exerted by conformity, one would expect that, in this case, fewer cross-links are needed between the cliques to polarize the system. Indeed, the critical value of L decreases with an increasing independence h.

It should be noted that, for each value of h, there is a difference in the critical values L^* between the quenched and annealed models. This is mainly a consequence of different system sizes—while Equation (11), defining the annealed model, was derived for an infinite system, we used only 200 agents in the simulations of the quenched one. It has been shown in Ref. [22] that the discrepancy between the models decreases with the increase in the size of the simulated system. We expect the models to converge for $N \to \infty$, despite the subtle changes in their dynamics.

To complete this picture, let us investigate how the product of magnetization changes with both fraction of cross-links L and independence h (Figure 6). At $L = 0$ (no connection between the cliques), independence continuously destroys the ordering in both communities. Finally, above a critical value h^*, the system enters the disordered phase with no magnetization in the cliques. For $L < L^*$ and small values of h, the system maintains the partial consensus, then we observe a transition to the polarized state. The magnetizations in the now-antagonistic cliques are diminishing with further increases of h. Finally, the system reaches the disordered phase. At $L > L^*$, the system is already polarized, even for $h = 0$. Increasing h introduces disorder into the cliques. Again, there is no ordering above the critical value of h.

As already discussed earlier in this section, there are some differences in absolute values between the annealed and quenched models, but the picture for the annealed case is qualitatively the same.

It is worth noting that the critical value of h for the polarization–disorder transition depends little on L (with a more noticeable effect in the annealed model). At the same time, the critical value of L for the consensus–polarization transition decreases with an increasing h, unless the value h is too high and disorder becomes the only possible state (see Figure 6).

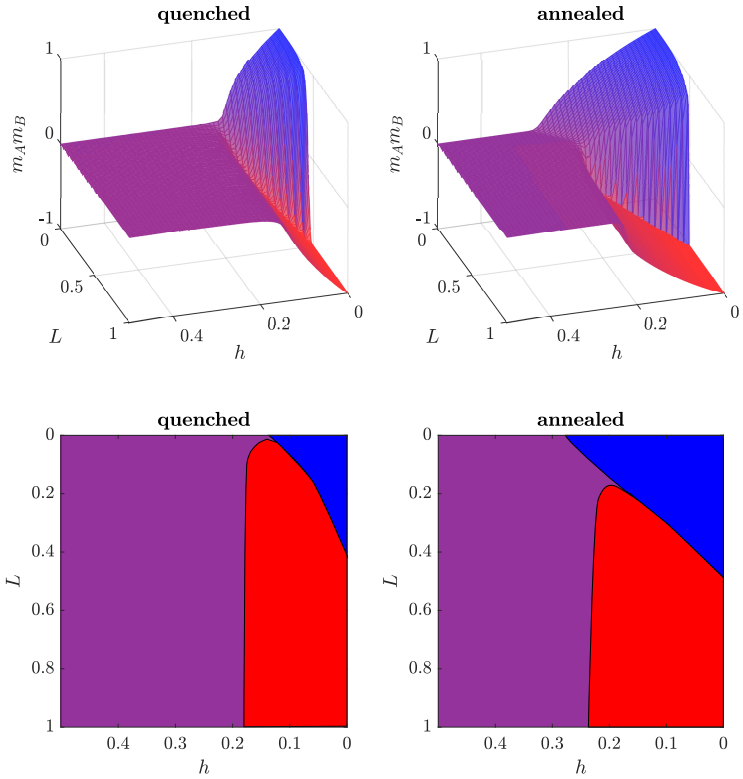

Figure 6. Comparison between the quenched (**left**) and annealed (**right**) models: final product of magnetizations $m_A m_B$ (**top**) and its projection on the (h, L) plane (**bottom**). The blue, red and purple colors correspond to consensus, polarization and disorder, respectively. In both models, we can observe that the critical value L^* decreases with an increase in h, while L has only a marginal impact on h^*.

4. Discussion

The most important message from our previous study was that the consensus between two antagonistic communities is only possible if they are loosely connected with each other and the initial state of the system belongs to the basin of attraction of the symmetric fixed-points of the model [21,22]. The more interactions there are between those communities, the less probable it is that the entire system will share the same opinion. Instead, anticonformity takes over and pushes the system towards polarization. Those results were unexpected in the sense that they, for instance, support the idea of the often-criticized filter bubbles in social media [5,13]. Since those bubbles separate users from information that disagrees with their viewpoints, they may help to weaken the problem with polarization. However, the models that we considered were very simple. For instance, they lacked some typical answers to social influence [29].

In order to make the models more realistic, in this work, we added independence as a response to social influence. From our results, it follows that this additional manifestation of social interactions impacts the system dynamics in at least two ways. Small independence levels help anticonformity to take over and polarize the society. More technically speaking, they lower the critical ratio of cross-links between cliques, which are needed to arrive at a polarized state. High independence levels destroy any ordering in the system. Consequently, the opinions of agents are perfectly mixed across the cliques, and neither consensus nor polarization are observed. Instead, a third phase–a disordered state–appears.

In sum, in the presented setting, low (but present) independence levels seem to enhance the polarization of the system. Thus, they counteract the effects of the filter bubbles, which, at least within our models, foster consensus across the cliques. At high levels, all manifestations of the interplay between conformity and anticonformity are suppressed by the noise induced due to independence.

It is worth mentioning that qualitatively similar results (but with a less detailed stability analysis) were obtained earlier within the majority model [23] and the Ising model [24] on a double-clique topology, with conformity as the only response to social influence. Although, in those models, the initial polarized state was found to become unstable with the increasing number of connections between the cliques (the consensus one in our case), the dynamics of those models turned out to be very similar to the behavior presented in this paper. Unique to our model is a more realistic response of agents to social influence. In fact, we took all types of responses into account, according to the diamond model by Nail et al. [28,29,53]. Hence, one may expect that what has been observed is more a general pattern of social behavior than an artifact of a particular choice of the modeling framework.

Author Contributions: Conceptualization, review and editing, T.W. and J.S.; implementation, analysis and visualisation, T.W.; original draft preparation and supervision, J.S. All authors have read and agreed to the published version of the manuscript.

Funding: T.W. was supported by the Ministry of Science and Higher Education, Poland within the "Diamond Grant" Program through grant no. DI2019 0008 49.

Institutional Review Board Statement: Not applicable.

Informed Consent Statement: Not applicable.

Data Availability Statement: Not applicable.

Conflicts of Interest: The authors declare no conflict of interest.

References

1. DiMaggio, P.; Evans, J.; Bryson, B. Have American's Social Attitudes Become More Polarized? *Am. J. Sociol.* **1996**, *102*, 690–755. [CrossRef]
2. Mäs, M.; Flache, A. Differentiation without Distancing. Explaining Bi-Polarization of Opinions without Negative Influence. *PLoS ONE* **2013**, *8*, e74516. [CrossRef] [PubMed]
3. Isenberg, D.J. Group polarization: A critical review and meta-analysis. *J. Personal. Soc. Psychol.* **1986**, *50*, 1141–1151. [CrossRef]
4. Sunstein, C.R. The Law of Group Polarization. *J. Political Philos.* **2002**, *10*, 175–195. [CrossRef]
5. Bail, C.A.; Argyle, L.P.; Brown, T.W.; Bumpus, J.P.; Chen, H.; Hunzaker, M.B.F.; Lee, J.; Mann, M.; Merhout, F.; Volfovsky, A. Exposure to opposing views on social media can increase political polarization. *Proc. Natl. Acad. Sci. USA* **2018**, *115*, 9216–9221. [CrossRef] [PubMed]
6. *The Global Risk Report 2017*; World Economic Forum: Geneva, Switzerland, 2017.
7. Mouw, T.; Sobel, M. Culture Wars and Opinion Polarization: The Case of Abortion. *Am. J. Sociol.* **2001**, *106*, 913–943. [CrossRef]
8. McCright, A.M.; Dunlap, R.E. The politization of climate change and polarization in the American public's views of global warming. *Sociol. Q.* **2011**, *52*, 2001–2010. [CrossRef]
9. Gruzd, A.; Roy, J. Investigating Political Polarization on Twitter: A Canadian Perspective. *Policy Internet* **2014**, *6*, 28–45. [CrossRef]
10. Adamic, L.A.; Glance, N. The political blogosphere and the 2004 US election: Divided they blog. In Proceedings of the 3rd International Workshop on Link Discovery (LinkKDD '05), Chicago, IL, USA, 21–25 August 2005; pp. 36–43.
11. Maoz, Z. Network Polarization, Network Interdependence, and International Conflict. *J. Peace Res.* **2006**, *43*, 1816–2002. [CrossRef]
12. Waugh, A.; Pei, L.; Fowler, J.H.; Mucha, P.J.; Porter, M.A. Party Polarization in Congress: A Network Science Approach. *arXiv* **2011**, arXiv:0907.3509.
13. Pariser, E. *The Filter Bubble. What the Internet Is Hiding from You?* Penguin Press: New York, NY, USA, 2011.
14. Axelrod, R. The Dissemination of Culture. A Model with Local Convergence and Global Polarization. *J. Confl. Resolut.* **1997**, *41*, 203–226. [CrossRef]
15. McPherson, M.; Smith-Lovin, L.; Cook, J.M. Birds of a Feather: Homophily in Social Networks. *Annu. Rev. Sociol.* **2001**, *27*, 415–444. [CrossRef]
16. Hengselmann, R.; Krause, U. Opinion dynamics and bounded confidence: Models, analysis and simulation. *J. Artif. Soc. Soc. Simul.* **2002**, *5*, 1–33.
17. Deffuant, G.; Neau, D.; Amblard, F.; Weisbuch, G. Mixing beliefs among interacting agents. *Adv. Complex Syst.* **2000**, *03*, 87–98. [CrossRef]

18. Macy, M.W.; Kitts, J.; Flache, A.; Benard, S. Polarization and Dynamic Networks. A Hopfield Model of Emergent Structure. In *Dynamic Social Network Modeling and Analysis: Workshop Summary and Papers*; Breiger, R., Carley, K., Pattison, P., Eds.; The National Academies Press: Washington, DC, USA, 2003; pp. 162–173.
19. Salzarulo, L. A Continuous Opinion Dynamics Model Based on the Principle of Meta-Contrast. *J. Artif. Soc. Soc. Simul.* **2006**, *9*, 13.
20. Traag, V.A.; Dooren, P.V.; Leenheer, P.D. Dynamical Models Explaining Social Balance and Evolution of Cooperation. *PLoS ONE* **2013**, *8*, e60063. [CrossRef] [PubMed]
21. Siedlecki, P.; Szwabiński, J.; Weron, T. The interplay between conformity and anticonformity and its polarizing effect on society. *J. Artif. Soc. Soc. Simul.* **2016**, *19*, 9. [CrossRef]
22. Krueger, T.; Szwabiński, J.; Weron, T. Conformity, anticonformity and polarization of opinions: Insights from a mathematical model of opinion dynamics. *Entropy* **2017**, *19*, 371. [CrossRef]
23. Lambiotte, R.; Ausloos, M.; Hołyst, J.A. Majority model on a network with communities. *Phys. Rev. E* **2007**, *75*, 030101. [CrossRef]
24. Suchecki, K.; Hołyst, J.A. Bistable-monostable transition in the Ising model on two connected complex networks. *Phys. Rev. E* **2009**, *80*, 031110. [CrossRef]
25. Martins, A.C.R. Continuous Opinions and Discrete Actions in Opinion Dynamics Problems. *Int. J. Mod. Phys. C* **2008**, *19*, 617–624. [CrossRef]
26. Martins, A.C.R.; Galam, S. Building up of individual inflexibility in opinion dynamics. *Phys. Rev. E* **2013**, *87*, 042807. [CrossRef] [PubMed]
27. Banisch, S.; Olbrich, E. Opinion polarization by learning from social feedback. *J. Math. Sociol.* **2019**, *43*, 76–103. [CrossRef]
28. Nail, P.R. Toward an integration of some models and theories of social response. *Psychol. Bull.* **1986**, *100*, 190–206. [CrossRef]
29. Nail, P.R.; MacDonald, G.; Levy, D.A. Proposal of a Four Dimensional Model of Social Response. *Psychol. Bull.* **2000**, *126*, 454–470. [CrossRef] [PubMed]
30. Nyczka, P.; Sznajd-Weron, K. Anticonformity or Independence?—Insights from Statistical Physics. *J. Stat. Phys.* **2013**, *151*, 174–202. [CrossRef]
31. Conover, M.; Ratkiewicz, J.; Francisco, M.; Gonçalves, B.; Flammini, A.; Menczer, F. Political Polarization on Twitter. In Proceedings of the Fifth International AAAI Conference on Weblogs and Social Media (ICWSM), Barcelona, Spain, 17–21 July 2011; pp. 89–96.
32. Newman, M.E.J. Modularity and community structure in networks. *Proc. Natl. Acad. Sci. USA* **2006**, *103*, 8577–8582. [CrossRef]
33. Zachary, W. An Information Flow Model for Conflict and Fission in Small Groups. *J. Anthropol. Res.* **1977**, *33*, 452–473. [CrossRef]
34. Sood, V.; Antal, T.; Redner, S. Voter models on heterogeneous networks. *Phys. Rev. E* **2008**, *77*, 041121. [CrossRef]
35. Watts, D.J.; Dodds, P.S. Influentials, Networks, and Public Opinion Formation. *J. Consum. Res.* **2007**, *34*, 441–458. [CrossRef]
36. Guerra, P.H.C.; Meira, M., Jr.; Cardie, C.; Kleinberg, R. A Measure of Polarization on Social Media Networks Based on Community Boundaries. In Proceedings of the Seventh International AAAI Conference on Web and Social Media, Cambridge, MA, USA, 8–11 July 2013; pp. 215–224.
37. Castellano, C.; Muñoz, M.A.; Pastor-Satorras, R. Nonlinear q-voter model. *Phys. Rev. E* **2009**, *80*, 041129. [CrossRef] [PubMed]
38. Myers, D.G. *Social Psychology*, 11th ed.; Freeman Press: New York, NY, USA, 2013.
39. Bond, R. Group Size and Conformity. *Group Process. Intergroup Relat.* **2005**, *8*, 331–354. [CrossRef]
40. Asch, S.E. Opinions and Social Pressure. *Sci. Am.* **1955**, *193*, 31–35. [CrossRef]
41. Nyczka, P.; Sznajd-Weron, K.; Cislo, J. Phase transitions in the q-voter model with two types of stochastic driving. *Phys. Rev. E* **2012**, *86*, 011105. [CrossRef] [PubMed]
42. Nyczka, P.; Byrka, K.; Nail, P.R.; Sznajd-Weron, K. Conformity in numbers—Does criticality in social responses exist? *PLoS ONE* **2018**, *13*, 1–18. [CrossRef] [PubMed]
43. Przybyła, P.; Sznajd-Weron, K.; Weron, R. Diffusion of innovation within an agent-based model: Spinsons, independence and advertising. *Adv. Complex Syst.* **2014**, *17*, 1450004. [CrossRef]
44. Sznajd-Weron, K.; Szwabiński, J.; Weron, R. Is the Person-Situation Debate Important for Agent-Based Modeling and Vice-Versa? *PLoS ONE* **2014**, *9*, e112203. [CrossRef]
45. Jędrzejewski, A.; Sznajd-Weron, K.; Szwabiński, J. Mapping the q-voter model: From a single chain to complex networks. *Phys. A* **2016**, *446*, 110–119. [CrossRef]
46. Jędrzejewski, A.; Sznajd-Weron, K. Person-Situation Debate Revisited: Phase Transitions with Quenched and Annealed Disorders. *Entropy* **2017**, *19*, 415. [CrossRef]
47. Jędrzejewski, A.; Marcjasz, G.; Nail, P.R.; Sznajd-Weron, K. Think then act or act then think? *PLoS ONE* **2018**, *13*, 1–19. [CrossRef]
48. Jędrzejewski, A.; Sznajd-Weron, K. Impact of memory on opinion dynamics. *Phys. A Stat. Mech. Its Appl.* **2018**, *505*, 306–315. [CrossRef]
49. Galam, S.; Moscovici, S. Towards a theory of collective phenomena: Consensus and attitude changes in groups. *Eur. J. Soc. Psychol.* **1991**, *21*, 49–74. [CrossRef]
50. Galam, S. Rational group decision making: A random field Ising model at T = 0. *Phys. A* **1997**, *238*, 66–80. [CrossRef]

51. Galam, S.; Jacobs, F. The role of inflexible minorities in the breaking of democratic opinion dynamics. *Phys. A* **2007**, *381*, 366–376. [CrossRef]
52. Mobilia, M. Does a Single Zealot Affect an Infinite Group of Voters? *Phys. Rev. Lett.* **2003**, *91*, 028701. [CrossRef]
53. Nail, P.R.; Domenico, S.I.; MacDonald, G. Proposal of a Double Diamond Model of Social Response. *Rev. Gen. Psychol.* **2013**, *17*, 1–19. [CrossRef]
54. Galam, S. Contrarian deterministic effects on opinion dynamics: "The hung elections scenario". *Phys. A* **2004**, *333*, 453–460. [CrossRef]
55. Sznajd-Weron, K.; Tabiszewski, M.; Timpanaro, A. Phase transition in the Sznajd model with independence. *Europhys. Lett.* **2011**, *96*, 48002. [CrossRef]
56. Liu, T.; Bundschuh, R. Quantification of the differences between quenched and annealed averaging for RNA secondary structures. *Phys. Rev. E* **2005**, *72*, 061905. [CrossRef]
57. Strogatz, S.H. *Nonlinear Dynamics and Chaos: With Applications to Physics, Biology, Chemistry, and Engineering*; Addison-Wesley: Reading, MA, USA, 1994.

Paper 3

Composition of the Influence Group in the q-Voter Model and Its Impact on the Dynamics of Opinions

Tomasz Weron, Piotr Nyczka, Janusz Szwabiński

entropy

MDPI

Article

Composition of the Influence Group in the q-Voter Model and Its Impact on the Dynamics of Opinions

Tomasz Weron, Piotr Nyczka and Janusz Szwabiński *

Department of Applied Mathematics, Wroclaw University of Science and Technology, 50-370 Wroclaw, Poland; tomasz.weron@pwr.edu.pl (T.W.); piotr.nyczka@pwr.edu.pl (P.N.)
* Correspondence: janusz.szwabinski@pwr.edu.pl

Abstract: Despite ample research devoted to the non-linear q-voter model and its extensions, little or no attention has been paid to the relationship between the composition of the influence group and the resulting dynamics of opinions. In this paper, we investigate two variants of the q-voter model with independence. Following the original q-voter model, in the first one, among the q members of the influence group, each given agent can be selected more than once. In the other variant, the repetitions of agents are explicitly forbidden. The models are analyzed by means of Monte Carlo simulations and via analytical approximations. The impact of repetitions on the dynamics of the model for different parameter ranges is discussed.

Keywords: opinion dynamics; q-voter model; agent-based modeling

Citation: Weron, T.; Nyczka, P.; Szwabiński, J. Composition of the Influence Group in the q-Voter Model and Its Impact on the Dynamics of Opinions. *Entropy* **2024**, *26*, 132. https://doi.org/10.3390/e26020132

Academic Editor: José F. F. Mendes

Received: 31 December 2023
Revised: 26 January 2024
Accepted: 29 January 2024
Published: 31 January 2024

1. Introduction

According to the Oxford Languages online dictionary, opinion is "a view or judgment formed about something, not necessarily based on fact or knowledge". In modern societies, due to the ongoing growth of communication technologies and social media platforms, people are constantly exposed to a steady flow of opinions about new technologies, products, or ideas [1]. By processing this flow and interacting with others, individuals may change their own opinions and beliefs [2]. Thus, opinions are an integral part of people's perception of reality. They shape social behavior and play a significant role in the evolution of societies.

Currently, agent-based models (ABMs) are one of the most popular and efficient tools in opinion dynamics and other social process studies. They can provide a detailed representation of reality, preserving the heterogeneity of individuals and an irregular structure of their mutual relations [3]. In social sciences, ABM is most often understood as a simulation of the behaviors of these individuals, called agents, and interactions between them. The aforementioned structure usually illustrates a network of friendships, contacts, or cooperation, within which agents' actions take place [4]. From a mathematical point of view, that structure can be represented by a graph, with vertices being the agents and edges—the connections between them [5].

In the case of complex problems such as the dynamics of opinions, simple deterministic models are often found to be insufficient [6]. They are complemented by ABMs, as the latter allow for bridging the gap between microscopic interactions of the agents and emergent phenomena at the macroscopic scale. For many years, ABMs have found use in various fields of social science. For example, in examining the diffusion of innovations, such as new products and market solutions [7–12], or in modeling the results of democratic elections and public debates [13–21].

Within the field of opinion dynamics, there exists a wide range of different ABMs [22]. However, if we narrow our focus to binary opinions, then the q-voter model will come out as one of the most successful ones [23]. Social conformity is the main driving force

in this model, and its dynamics are as follows. In each elementary event, we randomly choose a single agent and q of its neighbors (hence the name q-voter model) within the underlying graph structure. Then, if and only if all q neighbors, forming the so-called group of influence, present the same opinion, the agent conforms to it and changes its opinion accordingly.

Although the above requirement of full unanimity may seem too strict, it is strongly supported by the results of Asch's social experiment [24]. It clearly showed that conformity, i.e., adjusting to group behavior, plays an important role in our decision making and that its impact is severely reduced in the case of disagreement within a group. Consequently, unanimity is not the part of the q-voter model that causes our concern. The element that does is the composition of the group of influence. In the original formulation of the model the authors wrote: *"In order to simplify the numerical analysis, and allow for an arbitrary value of q in regular lattices, we consider here the possibility of repetition, i.e., a given neighbor can be selected more than once"* [22]. In the article they only briefly discuss outcomes when repetitions are prohibited, without much detail.

Since then, there has been a lot of research conducted on the q-voter model. Some authors followed the original assumption and studied the model with the possibility of repetitions [25–27]. Others took an opposite path and considered a variant without them [28–33], sometimes justifying it sociologically [34]. There are many papers that do not specify it at all [35–38]. To the best of our knowledge, there exists only one article that considers differences between these two variants in detail [39]. It does however mostly focus on the so-called threshold q-voter model, an extension that incorporates a threshold mechanism [40]. Still, it provides a valuable insight on the differences between the two aforementioned variants. We hope there is room for more.

Here, we consider two different compositions of the influence group, with or without repetitions. We examine their impact in the q-voter model with independence [28]. We do so by the means of both computer simulations and analytical approximation methods. As for the latter, the first method is a simple Mean-Field Approximation (MFA) [22]. We are aware that MFA is sufficient only for complete graphs or other dense networks. When a network is sparse, it fails. Despite its limitations, we incorporate it into this work, as it has never been used to describe a variant without repetitions, to the best of our knowledge. Nevertheless, more sophisticated recipes are also needed. Thus, the second method is the Pair Approximation (PA), which works reasonably well, even for sparse networks [29]. Unfortunately, a closed-form solution is possible to obtain only in the variant without repetitions. The repetitive version must be solved numerically [39]. In this paper, we propose yet another solution—a heuristic MFA. This method will provide closed-form solutions for both variants of the q-voter model. Moreover, these formulas will be much simpler than in the case of PA.

The rest of the paper is organized as follows. In Section 2, we provide details on the model, its variants and methods used to analyze them. Later, in Section 3 we present and discuss the results. Finally, the conclusions are drawn in Section 4.

2. Models and Methods

2.1. Simulation Model

Our starting point is the q-voter model with independence [28]. We consider a set of N agents, each of which is characterized by a binary variable—an opinion, positive or negative, on some given issue, $S_i = \pm 1$ for $i = 1, 2, \ldots, N$. We investigate the model through Monte Carlo simulations with a random sequential updating scheme. Within a single simulation, the time is measured in so-called Monte Carlo steps (MCS). One MCS consists of N elementary events, each divided into the following substeps of length $\Delta t = \frac{1}{N}$:

1. Select a target agent i randomly (uniformly from N nodes).
2. Draw a random number $r \sim U(0,1)$.
3. With probability p (that is if $r < p$), the agent acts independently, i.e., it changes its opinion to the opposite one with probability $f = \frac{1}{2}$, $S_i(t + \Delta t) \overset{f}{\leftarrow} -S_i(t)$.

4. With the complementary probability $1-p$ (if $r > p$), a group of influence is constructed:
   - (*repetition* variant) Randomly select q neighbors of agent i, $j_1, j_2, \ldots, j_q$, with possibility of repetition.
   - (*no repetition* variant) Randomly select q neighbors of agent i, $j_1, j_2, \ldots, j_q$, without the possibility of repetition.
5. If the group of influence is unanimous, $S_{j_1}(t) = S_{j_2}(t) = \cdots = S_{j_q}(t)$, the agent i conforms, i.e., $S_i(t+\Delta t) \leftarrow S_{j_1}(t)$. Otherwise, nothing happens.

As already mentioned above, we consider two variants of the model: the *repetition* and the *no–repetition* one (see Figure 1 for a schematic representation). We decided to examine their behavior and the differences between them on random regular graphs. Other choices for the underlying topology are, of course, possible, but this particular type of complex networks allows us to control the number of neighbors of each agent and to ensure that forming of the influence group will be always possible in the *no–repetition* variant. Thus, those networks seem to be the best choice to implement the group dynamics, as they allow the option to leave out the heterogeneity-induced effects and focus only on the ones related to the differences in the dynamics. It should be noted that the same choice was made in a similar context in Ref. [39].

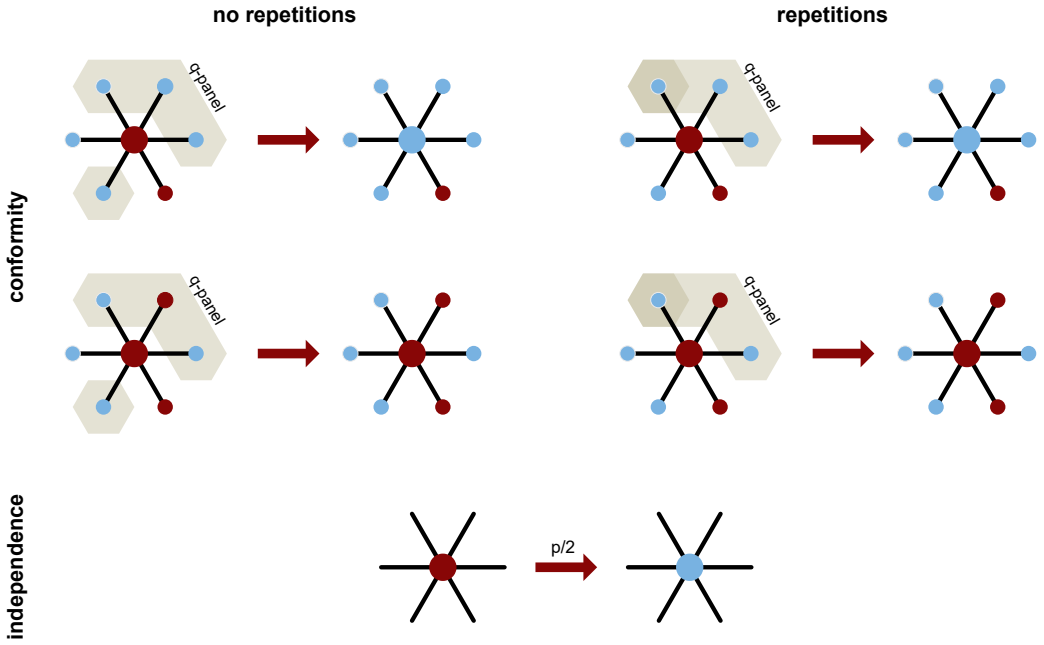

Figure 1. Depiction of the model dynamics in the *no repetition* (**left**) and the *repetition* (**right**) variants. The upper part corresponds to conformist behavior (probability $1-p$), while the bottom one corresponds to independence (probability p). The big circle portrays the target agent, smaller ones portray its neighbors. Light blue color represents a positive opinion ($S=+1$), dark red represents a negative one ($S=-1$), and beige marks a randomly chosen group of influence, with darker beige for repetitive choice. Degree $k=6$ and size of the influence group $q=4$ in all the above cases.

All methods presented in this work have also been tested on other networks, including square lattices, Watts-Strogatz graphs and scale-free networks. The results turned out to be qualitatively the same as for the random regular graphs.

In order to analyze stationary states, we define a macroscopic measure—the concentration of positive opinions ($S=+1$):

$$c^+ = \frac{N^+}{N} = \frac{1}{2N}\sum_{i=1}^{N}(S_i+1). \tag{1}$$

We will use it as our default measure throughout this paper. For simplicity, we will just call it "concentration" and omit the superscript $+$ ($c^+ \to c$).

To clarify, we perform simulations as follows. First, we generate a graph structure with a given degree k and assign agents their initial opinions $S(0)$, according to a specified initial concentration c_0, which can be understood as the probability of an agent having a positive opinion $S(0) = +1$. Then, we run the simulation until the system reaches its stable state and save final concentration. We repeat such simulation multiple times for a given set of parameters and average the results over these independent runs.

2.2. Mean-Field Approximation

Within the mean-field approximation we abstract away from the actual network of connections between the agents and assume that every agent may interact with anybody else [25]. In each elementary step, the number of agents in the state $S = 1$ may increase by 1, decrease by 1 or remain unchanged. The corresponding transition probabilities of the first two events in the repetition variant are qiven by

$$\begin{aligned} \Pr(c(t+\Delta t) \leftarrow c(t) + \Delta_N) &= (1-p)\alpha^+ + p\beta^+, \\ \Pr(c(t+\Delta t) \leftarrow c(t) - \Delta_N) &= (1-p)\alpha^- + p\beta^-, \end{aligned} \tag{2}$$

where

$$\begin{aligned} \alpha^+ &= (1-c)c^q, \;\; \alpha^- = c(1-c)^q, \\ \beta^+ &= \frac{1}{2}(1-c), \;\; \beta^- = \frac{1}{2}c. \end{aligned} \tag{3}$$

Assuming $N \to \infty$, the following dynamical equation may be derived from the above probabilities:

$$\frac{\partial c}{\partial t} = (1-p)\alpha + p\beta, \tag{4}$$

where

$$\begin{aligned} \alpha &= \alpha^+ - \alpha^-, \\ \beta &= \beta^+ - \beta^-. \end{aligned} \tag{5}$$

In the stationary state, we have $\frac{\partial c}{\partial t} = 0$. This leads to the following relationship between the probability of independence p and the stationary concentration c (hidden in α and β):

$$p = \frac{\alpha}{\alpha - \beta}. \tag{6}$$

The basic mean-field approximation does not distinguish between the variants of the model. However, we can modify it slightly to catch the characteristics of the *no-repetition* dynamics. We retain the assumption about the infinite size of the system ($N \to \infty$). Additionally, we introduce a finite degree (and equal for all the agents) k. Then, α^+ and α^- take the following forms:

$$\begin{aligned} \alpha^+ &= (1-c)\prod_{i=0}^{q-1} \max\left[\frac{k \times c - i}{k-i}, 0\right], \\ \alpha^- &= c\prod_{i=0}^{q-1} \max\left[\frac{k \times (1-c) - i}{k-i}, 0\right], \end{aligned} \tag{7}$$

while β^+ and β^- remain unchanged. The rest, including the condition for stationary states (Equation (6)), is the same as in the *repetition* variant. In the remaining part, we call this approach a network aware MFA (naMFA). It should be emphasized here that in the model with repetitions, naMFA reduces to MFA.

2.3. Pair Approximation

The pair approximation (PA) is a moment closure method in which the mean-field description of a model is supplemented by an approximate equation for the time evolution of the density of the active links, i.e., the edges in a network joining two agents in different states. PA is one of the possible ways to incorporate the structure of the underlying network into the description of the model. This approximation has been already used for the q-voter model with independence [29,39] and turned out to yield precise results for a wide variety of networks. However, regardless of all its advantages, it has a major flaw—it provides a closed-form solution only for the *no repetition* variant. For the *repetition* one, it seems impossible to obtain such a solution [39]. Therefore, we must rely on a numerical one. Although the latter can be very precise, it is not as satisfactory and informative as an analytical formula.

A detailed derivation of PA may be found in Refs. [29,39]. Here, we will only recall the most important results for the q-voter model on random regular graphs.

To recall, the degree distribution of a random regular graph is given by $P(k') = k\delta_{k,k'}$, where k is simply the degree of each node in the network. Following [39], the model reduces in this case to two closed rate equations for the density of active links $\rho(t)$ and the concentration $c(t)$ of agents in state $S = 1$:

$$\begin{aligned} \frac{d\rho}{dt} &= 2\sum_{i=\oplus,\ominus} P_i \langle (k-2l) F(l;k,q,p) \rangle_{\rho_i} \\ \frac{dc}{dt} &= -\sum_{i=\oplus,\ominus} S_i P_i \langle F(l;k,q,p) \rangle_{\rho_i} \end{aligned} \tag{8}$$

Here, $S_\oplus = 1$, $S_\ominus = -1$, $P_\oplus = c$, $P_\ominus = 1-c$, $\rho_\oplus = \rho/(2c)$, $\rho_\ominus = \rho/(2(1-c))$ and $\langle \dots \rangle_{\rho_i}$ is the average calculated over the binomial probability $\binom{k'}{l}\rho_i^l(1-\rho_i)^{k'-l}$. The probability that an agent with l active links flips its state is

$$F(l;k,q,p) = \frac{p}{2} + (1-p) f(l;k,q), \tag{9}$$

where

$$f(l;k,q) = \begin{cases} \binom{k-q}{l-q} / \binom{k}{l} & \text{no-repetition,} \\ \left(\frac{l}{k}\right)^q, & \text{repetition.} \end{cases} \tag{10}$$

Moreover, in the no-repetition variant it is understood that $f(l;k,q) = 0$ if $k < q$.

Due to some cancellations of the combinatorial numbers, the averages $\langle \dots \rangle_{\rho_i}$ in Equation (8) in the no-repetition variant lead to relatively simple expressions which are linear in k. In this case, the condition $dc/dt = 0$ yields the following relationship between the independence p and the stationary concentration c:

$$p^{-1} = 1 + \frac{2^{q-1}\left(\frac{k-1}{k-2}\right)^q}{q-1}. \tag{11}$$

In the model with repetitions, a closed-form expression does not exist, and one has to resort to numerical solutions. A difficulty in the numerical calculations relates to the fact that the binomial coefficients appearing in the rate equations take huge values for large k, while ρ^k is very small. To avoid this problem, Vieira et al. [39] made expansions in Equation (8) using the moments of the binomial distribution and the negative moments of the degree distribution.

In this work, we followed a slightly different approach. We took a log-transformed version of Equation (8) and solved it numerically for a given value of p (and other parameters of the model). The times taken were long enough to arrive at a stationary solution. The concentration at the last point along the time axis together with the corresponding p

was stored as the contribution to the $p(c)$ relationship, and the procedure was repeated for a different value of p. The logarithmic transformation [41] of Equation (8) solved the problem with both the huge values in the binomial coefficients and the small ones related to ρ^k. It worked well even with the standard Runge-Kutta methods of the second and fourth order [42].

2.4. Heuristic Mean-Field Approximation

To capture the characteristics of sparse networks, we may also look for a more sophisticated version of MFA. The one we propose here will be refered to as a heuristic MFA (hMFA) in the remaining part of the paper, since we are not (yet) able to derive all of its ingredients. However, it works quite well in all analyzed cases.

Let us first randomly pick a target and all its closest neighbors. This forms a local configuration. Then, we include P_{local} describing the probability of constructing an unanimous group of influence, for a given configuration:

$$\begin{aligned} \alpha^+ &= (1-c)\sum_{i=x}^{k}\binom{k}{i}c^i(1-c)^{k-i}P_{local}, \\ \alpha^- &= c\sum_{i=x}^{k}\binom{k}{i}(1-c)^i c^{k-i}P_{local}. \end{aligned} \tag{12}$$

In the above formulas, the first part describes initial stage of the process, i.e., probability of obtaining a certain configuration, while P_{local} stands for the probability of constructing an unanimous group of influence. Both P_{local} and x are dependent on the variant of the model. In the *no repetition* one they take the following form:

$$P_{local} = \prod_{j=0}^{q-1}\frac{i-j}{k-j}, \quad x = q. \tag{13}$$

Hence, Equation (12) becomes:

$$\begin{aligned} \alpha^+ &= (1-c)\sum_{i=q}^{k}\binom{k}{i}c^i(1-c)^{k-i}\prod_{j=0}^{q-1}\frac{i-j}{k-j}, \\ \alpha^- &= c\sum_{i=q}^{k}\binom{k}{i}(1-c)^i c^{k-i}\prod_{j=0}^{q-1}\frac{i-j}{k-j}. \end{aligned} \tag{14}$$

In the *repetition* variant, P_{local} and x are:

$$P_{local} = \left(\frac{i}{k}\right)^q, \quad x = 1, \tag{15}$$

and Equation (12) becomes

$$\begin{aligned} \alpha^+ &= (1-c)\sum_{i=1}^{k}\binom{k}{i}c^i(1-c)^{k-i}\left(\frac{i}{k}\right)^q, \\ \alpha^- &= c\sum_{i=1}^{k}\binom{k}{i}(1-c)^i c^{k-i}c\left(\frac{i}{k}\right)^q. \end{aligned} \tag{16}$$

Now, we can use these α^+ and α^- to compute stationary states, analogously to the ordinary MFA (Equation (6)). Unfortunately, this approach turned out to perform poorly in the case of sparse networks. Thus, it provides only little advantage over the ordinary MFA

so far. To change that, we will append some corrections. First, let us introduce a corrected formula for stationary states (see Equation (6)):

$$p' = \frac{\alpha}{\alpha - h\beta}, \tag{17}$$

where h is a positive value, related to the impact of a sparse network on the model's dynamics. We assume h of the form

$$h = 1 + q/k + 2p(q/k)^2 + 32(qk)^{-2}. \tag{18}$$

The first element is just 1 and corresponds to the ordinary MFA without any corrections (Equation (6)). The second term , q/k, is there to catch the characteristics of a sparse network. It describes the probability of destroying unanimity within the q-panel by a single neighbor (see Figure 2 for a graphical explanation).

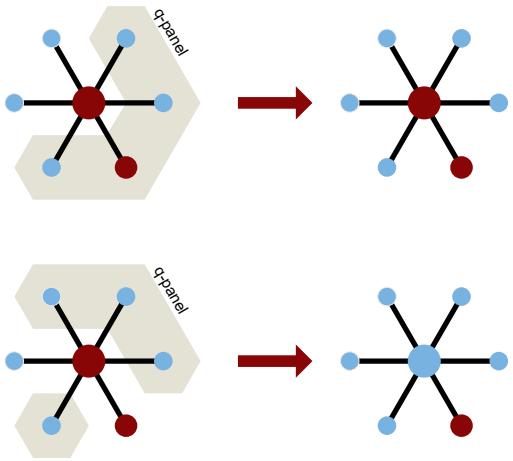

Figure 2. Depiction of two possible configurations. The big circle portrays the target agent, the smaller ones portray its neighbors. Light blue color represents a positive opinion ($S = +1$), dark red represents a negative one ($S = -1$). Beige color marks a chosen group of influence. Degree $k = 6$ and size of the influence group $q = 4$ in both cases. The first (top) group of influence is not unanimous and provides no change, while the second one (bottom) is unanimous and leads to change in target's opinion. The difference is all due to the single neighbor with negative opinion (dark red), being in or outside the group of influence. Probability of containing this neighbor inside the q-panel is equal to q/k.

Adding the q/k correction has already significantly improved the results yielded by our method. However, the agreement with the ABM simulations was still much worse than that of PA. Thus, we decided to add two other terms based on the calibration of the method to the simulation data. The first of them, $2p(q/k)^2$, improves the accuracy of the method in all cases except the low values of k. And finally, the $32(qk)^{-2}$ term provides the needed correction for low values of k.

Interestingly, the $2p(q/k)^2$ term was proposed after calibrating the model with the simulation data in the case $k = 50$, $q = 5$. The last correction was added after the analysis of the $k = 5$ and $q = 4$ case. However, the Formula (18) works reasonably well for all parameter sets we have tested in the preparation phase of this paper. As it will be shown in Section 3.2, the method works only slightly worse than PA, especially in the variant with repetitions, but allows for easier and quicker generation of the results.

2.5. Comparison of Methods

In order to compare accuracy of different approximation methods, we introduce the following measure:

$$\Delta = \ln\left[\frac{1}{< p_s >}\sum_{i}^{n}|p_s(c_i) - p_t(c_i)| : c_i \geq 0.6\right], \tag{19}$$

where p_s is the simulated value, p_t is the value from one of our theoretical models and 0.6 is a cutoff threshold for the simulated values of c to remove the finite size effects near the critical value of p (see Section 3.1 for explanation). The outcome is normalized by the factor $\frac{1}{<p_s>}$, to make comparison between various values of q possible. The logarithm function is there to display differences using the same scale in different charts.

3. Results

3.1. Simulations

We run most of the simulations on random regular graphs of size $N = 1000$, with various degrees k. The size of the networks may seem too small at first glance. However, we also checked the simulations on larger networks, and the results were practically the same, except for a small region close to the phase transition (i.e., for $c(t)$ close to 0.5, see Figure 3 for an explanation). In larger systems, the order-disorder phase transition is well defined. In smaller ones, we observe a slower decay of the ordered phase due to the finite size effects [43]. Since a detailed analysis of the phase transition is out of the scope of this paper, we decided to keep the size of the system rather small to reduce computational efforts in the simulations. To ensure that the system reaches its stable state, we set the time horizon $T = 1000$ MCS in each simulation. For each set of the parameters, we perform 100 independent simulations and then average the final concentration, $c(T)$, over these runs.

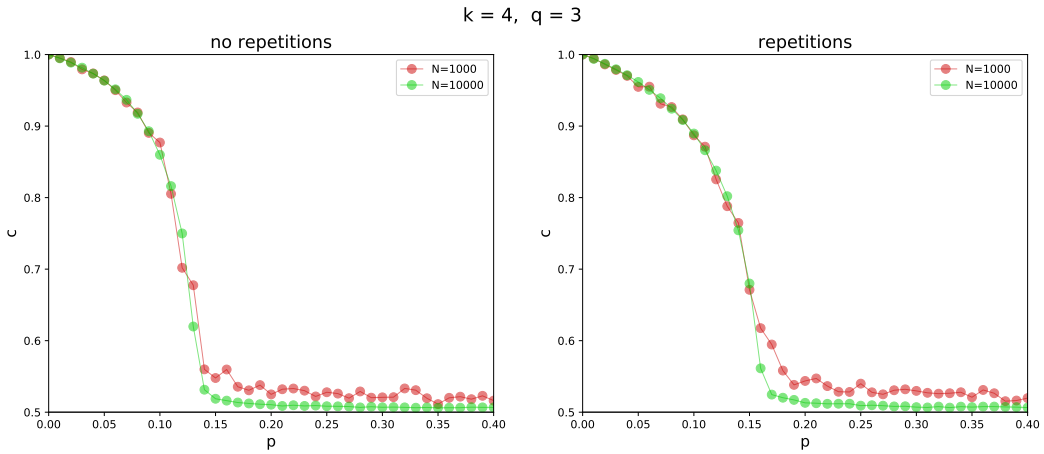

Figure 3. Comparison between the *no repetition* (left) and *repetition* (right) variants in the simulation model (see Section 2.1). Concentration c as a function of independence probability p is plotted for two different system sizes. Every circle corresponds to the state of the system after 1000 MCS, for a random regular graph with degree $k = 4$, averaged over 100 independent runs. Initial concentration $c_0 = 1$ in all simulations. The size of the group of influence is $q = 3$. Note the longer decay of the ordered phase, characterized by $c(t) > 0.5$, in the case of the smaller system.

The actual comparison between *no repetition* and *repetition* variants is shown in Figure 4. Although at first glance both variants behave similarly, there are some major differences. First of all, in the *no repetition* variant, a group of influence cannot be greater than the degree of a target ($q \leq k$). It is not an issue in the *repetition* one, as we can choose a single neighbor multiple times, when constructing the group of influence. In the *no repetition* variant with $q = k$, the system becomes disordered ($c \approx 0.5$) whenever independence is

present ($p > 0$). This is not the case in the *repetition* one. In addition to that, the models behave differently for other values of q as well. For larger influence groups, the system in the *no repetition* variant becomes disordered for much smaller probabilities of independence p than in the *repetition* one. The closer the value of q to k, the greater the difference. It is an expected, yet important, outcome. The greater the degree k in respect to q, the lower the probability of choosing a single neighbor multiple times in the *repetition* variant and thus, the less visible the differences between the variants.

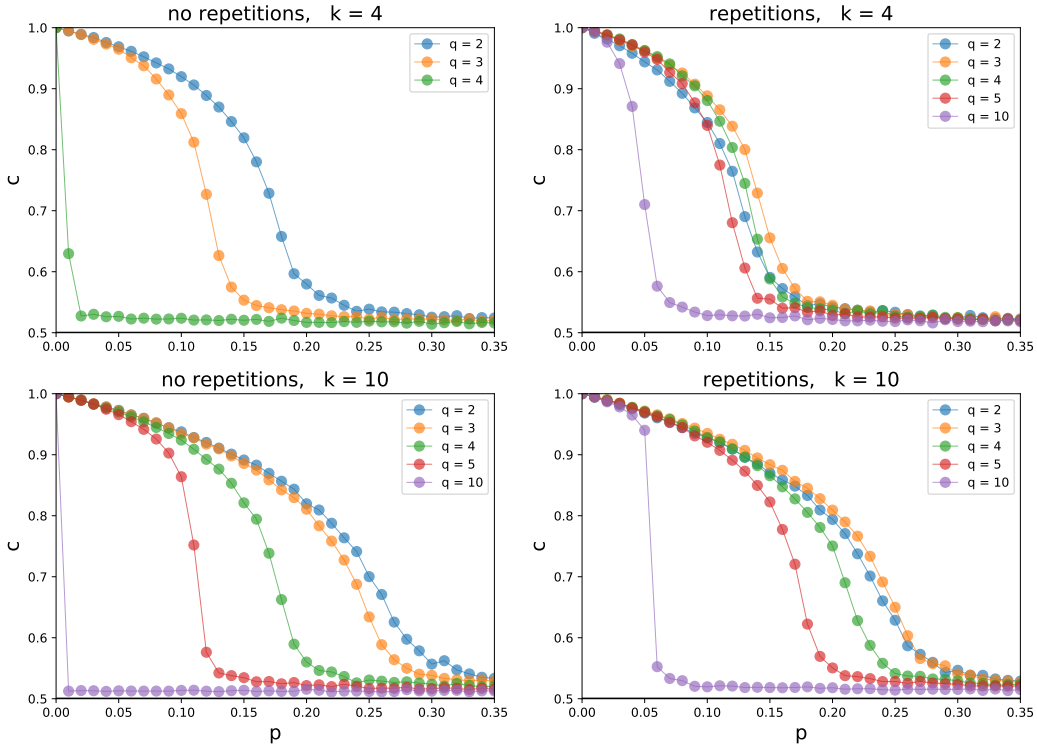

Figure 4. Comparison between the *no repetition* (left) and *repetition* (right) variants in the simulation model (see Section 2.1). Concentration c as a function of independence probability p is plotted for different sizes q of the group of influence. Every circle corresponds to the state of the system after 1000 MCS, for a random regular graph of size $N = 1000$, with degree $k = 4$ (**top**) and $k = 10$ (**bottom**), averaged over 100 independent runs. Initial concentration $c_0 = 1$ in all simulations. Please note that in the *repetition* variant, q can be greater than k.

3.2. Approximation Methods

The ABMs constitute state-of-the-art tools to simulate complex systems and emergent phenomena, including opinion dynamics on networks. However, understanding and analyzing the ABMs is very challenging. The behavior of those models often depends on many parameters. Even in the case of the simple q-voter model, we have to deal with the size of the system N, the independence p, the degree k (which fortunately is the same for all nodes in a random regular graph) and the size q of the group of influence. Exploring the parameter space and discovering the impact of different parameter sets on the time evolution of the model can be very time-consuming and usually requires a high-performance computing infrastructure. In many cases, running the model with all possible combinations of parameters is infeasible. On the other hand, varying only one chosen parameter at time may lead to overlooking some interesting patterns in the behavior of the system. This is actually why one is still interested in some analytical approximations of an agent-based system. Although some microscopic details of the dynamics may be ignored, those approximations generate results much faster than computer simulations of ABMs.

As mentioned before, we are going to compare four approximation methods, i.e., MFA, naMFA, hMFA and PA, with the results of our simulations. We are not only interested in the overall agreement with ABMs, but also in the ease of producing the results. Based on the findings for the q-voter model so far, we expect that the closer the network is to a complete graph, the more accurate the methods should be. Let us check how well they perform in less obvious cases.

First, a dense network (with the degree $k = 50$) was considered (Figure 5). Although it is still far from a complete graph (for which we would have $k = 999$), it is dense enough for almost all approximation methods to perform well and nearly identically. The only one falling behind is the ordinary mean-field approximation in the *no repetition* variant. The MFA does not utilize the information about the density of the network and assumes the possibility of repetitions when constructing a group of influence. Still, differences between the variants of the model remain small for such a large value of k, as mentioned in the Section 2.1.

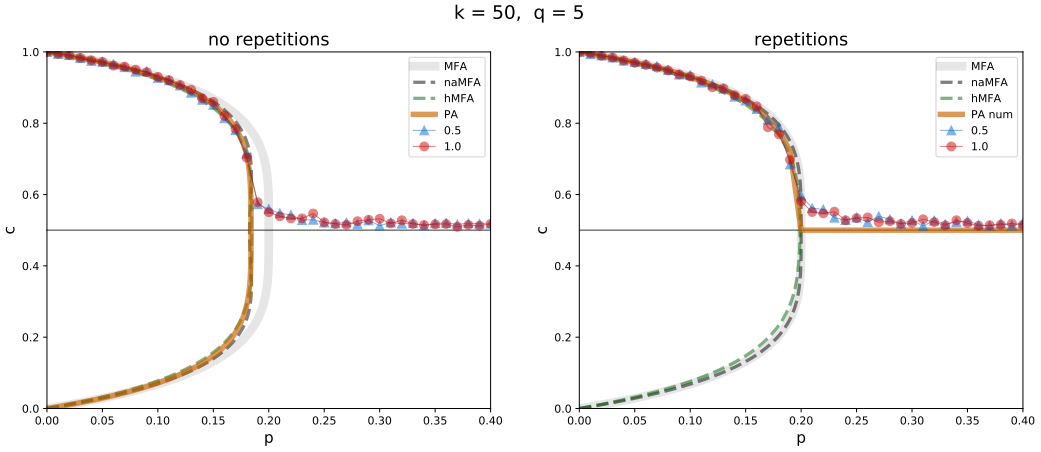

Figure 5. Comparison between the simulation results and the approximation methods in the *no repetition* (**left**) and *repetition* (**right**) variants of the model, for a random regular graph of size $N = 1000$, with the degree $k = 50$ and the size of a group of influence $q = 5$. The solid, light gray line indicates ordinary MFA, the dashed dark gray one indicates naMFA, the dashed green one indicates hMFA, and the solid orange one indicates PA. Simulation results for the initial concentration $c_0 = 0.5$ (blue triangles) and 1 (red circles) are shown. In the *repetition* variant, PA is obtained numerically.

Next, a sparser network (degree $k = 10$) was examined (Figure 6). Here, the differences between the methods and variants become visible. As mentioned earlier, the system in the *no repetition* variant disorders sooner, i.e., for lower values of p, than in the *repetition* one. This becomes even more apparent as we increase q from 4 to 5. As expected, the ordinary MFA performs poorly in the *repetition* variant and terribly in the *no repetition* one. The network-aware MFA works slightly better in the *no repetition* variant, but only for $q = 4$. For values of q approaching k it fails as well. Note that the naMFA method in the *repetition* version is equivalent to ordinary MFA. The pair approximation performs best in all cases studied. However, the heuristic MFA is not far behind. Moreover, it has a significant advantage over the PA—it uses a closed-form formula in both variants of the model.

Last but not least, a very sparse network ($k = 5$) was analyzed (Figure 7). Here, inaccuracies of the methods are magnified. Both ordinary MFA and naMFA perform terribly, regardless of the variant of the model or the value of q. The PA is still the most accurate method, although the hMFA is again not that far behind. Especially in the *repetition* variant, for which the closed form of the PA cannot be obtained. Since in this case one must rely on a numerical solution of the PA, the hMFA may be an attractive alternative.

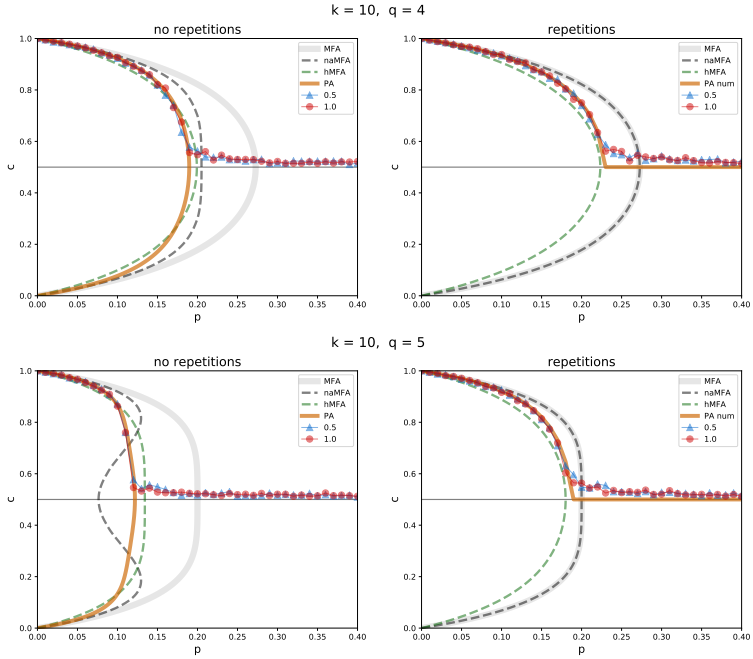

Figure 6. Comparison between the simulation results and the approximation methods in the *no repetition* (**left**) and *repetition* (**right**) variants, for a random regular graph of size $N = 1000$, with the degree $k = 10$ and the sizes of the group of influence $q = 4$ (**top**), and 5 (**bottom**). The solid, light gray line indicates ordinary MFA, the dashed dark gray one indicates naMFA, the dashed green one indicates hMFA, and the solid orange one indicates PA. Simulation results for the initial concentration $c_0 = 0.5$ (blue triangles) and 1 (red circles) are shown. In the *repetition* variant, PA is obtained numerically.

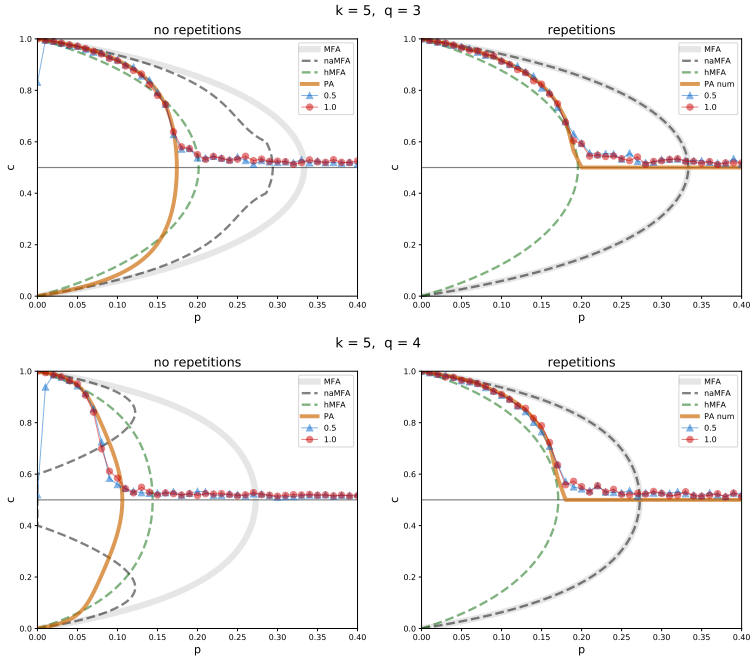

Figure 7. Comparison between the simulation results and the approximation methods in the *no repetition* (**left**) and *repetition* (**right**) variants, for a random regular graph of size $N = 1000$, with the degree $k = 5$ and the sizes of the group of influence $q = 3$ (**top**), and 4 (**bottom**). The solid, light gray line indicates ordinary MFA, the dashed dark gray one indicates naMFA, the dashed green one indicates hMFA, and the solid orange one indicates PA. Simulation results for the initial concentration $c_0 = 0.5$ (blue triangles) and 1 (red circles) are shown. In the *repetition* variant, PA is obtained numerically.

The summary of the differences between various approximation methods is presented in Figure 8. The methods are presented from top to bottom in the order of growing accuracy: MFA, naMFA, hMFA and PA. Note that the differences are displayed in a logarithmic scale. The first row corresponds to the ordinary MFA. As already mentioned, it performs satisfactorily only for large values of k and fails miserably in all other cases. The second row presents the network aware MFA, a slight modification of MFA with an attempt to capture some aspects of the underlying network. In the *no repetition* variant it performs slightly better. The third row shows the heuristic MFA (hMFA). Overall it yields better accuracy than the former methods, especially in the *repetition* variant. The last row is the PA—the most accurate method, yet it is still not perfect (see $k = q = 3$ and $k = q = 4$ in the *no repetition* variant). Moreover, in the *repetition* variant, its performance becomes worse when q is large (see $q = 20$). It is not a numerical artifact, but a property of the PA itself.

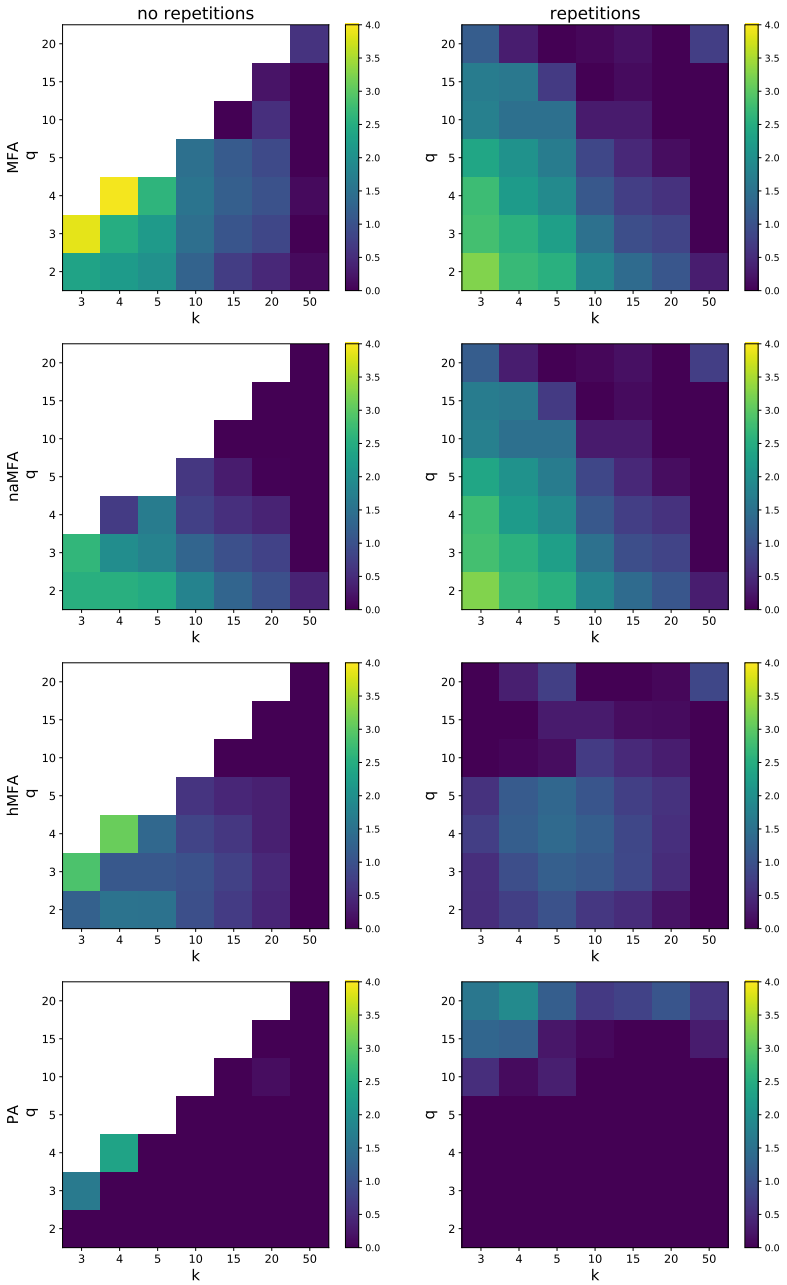

Figure 8. Difference Δ (Equation (19)) between the simulation results and the ordinary MFA (first row), the naMFA (second row), the hMFA (third row), and the PA (fourth row), in the *no repetition* (**left**) and *repetition* (**right**) variants.

4. Discussion and Conclusions

This paper consists of two parts. First, we studied the differences between the *repetition* and *no repetition* variants of the q-voter model. We found out that differences between them occur and become significant for sparse networks. Thus, one cannot simply use these variants interchangeably without any information.

Secondly, we examined two known approximation methods: the mean-field approximation and the pair approximation, and proposed two additional ones: the network-aware MFA and the heuristic MFA. We compared all these methods in terms of accuracy with the results of agent-based simulations. Two findings stand out as the most significant in our opinion. First, the PA remains the most accurate method overall. Unfortunately, it provides a closed form solution only in the *no repetition* variant. In the *repetition* one we must rely on numerical methods. Second, the hMFA is quite accurate as well. Moreover, it yields formulas much simpler than PA, and thus allows for an analytical solution in both variants of the model. As such, it is an alternative worth considering.

Author Contributions: Conceptualization, T.W. and J.S.; implementation, analysis and visualisation, T.W., P.N. and J.S.; original draft preparation, T.W. and P.N.; supervision, review and editing, T.W. and J.S. All authors have read and agreed to the published version of the manuscript.

Funding: T.W. was supported by the Ministry of Science and Higher Education, Poland within the "Diamond Grant" Program through grant no. DI2019 0008 49.

Data Availability Statement: The data presented in this study are available on request from the corresponding author.

Conflicts of Interest: The authors declare no conflict of interest. The founders had no role in the design of the study; in the collection, analyses, or interpretation of data; in the writing of the manuscript; or in the decision to publish the results.

References

1. Wu, F.; Huberman, B.A. Novelty and collective attention. *Proc. Natl. Acad. Sci. USA* **2007**, *104*, 17599–17601. [CrossRef]
2. Gigerenzer, G.; Todd, P.M. *Simple Heuristics That Make Us Smart*; Oxford University Press: New York, NY, USA, 1999.
3. Krueger, T.; Szwabiński, J.; Weron, T. Conformity, anticonformity and polarization of opinions: Insights from a mathematical model of opinion dynamics. *Entropy* **2017**, *19*, 371. [CrossRef]
4. Macy, M.W.; Willer, R. From factors to actors: Computational sociology and agent-based modeling. *Annu. Rev. Sociol.* **2002**, *28*, 143–166. [CrossRef]
5. Newman, M. *Networks: An Introduction*; Oxford University Press: New York, NY, USA, 2010.
6. Rahmandad, H.; Sterman, J. Heterogeneity and network structure in the dynamics of diffusion: Comparing agent-based and differential equation models. *Manag. Sci.* **2008**, *54*, 998–1014. [CrossRef]
7. Kiesling, E.; Günther, M.; Stummer, C.; Wakolbinger, L. Agent-based simulation of innovation diffusion: A review. *Cent. Eur. J. Oper. Res.* **2012**, *20*, 183–230. [CrossRef]
8. Kowalska-Pyzalska, A.; Maciejowska, K.; Suszczyński, K.; Sznajd-Weron, K.; Weron, R. Turning green: Agent-based modeling of the adoption of dynamic electricity tariffs. *Energy Policy* **2014**, *72*, 164–174. [CrossRef]
9. Jensen, T.; Holtz, G.; Chappin, E. Agent-based assessment framework for behavior-changing feedback devices: Spreading of devices and heating behavior. *Technol. Forecast. Soc. Change* **2015**, *98*, 105–119. [CrossRef]
10. Byrka, K.; Jędrzejewski, A.; Sznajd-Weron, K.; Weron, R. Difficulty is critical: The importance of social factors in modeling diffusion of green products and practices. *Renew. Sustain. Energy Rev.* **2016**, *62*, 723–735. [CrossRef]
11. Weron, T.; Kowalska-Pyzalska, A.; Weron, R. The role of educational trainings in the diffusion of smart metering platforms: An agent-based modeling approach. *Physica A* **2018**, *505*, 591–600. [CrossRef]
12. Van Der Kam, M.; Peters, A.; Van Sark, W.; Alkemade, F. Agent-based modelling of charging behaviour of electric vehicle drivers. *J. Artif. Soc. Soc. Simul.* **2019**, *22*, 7. [CrossRef]
13. Galam, S. Minority opinion spreading in random geometry. *Eur. Phys. J. B* **2002**, *25*, 403–406. [CrossRef]
14. Galam, S. Contrarian deterministic effects on opinion dynamics: "The hung elections scenario". *Physica A* **2004**, *333*, 453–460. [CrossRef]
15. Galam, S.; Jacobs, F. The role of inflexible minorities in the breaking of democratic opinion dynamics. *Physica A* **2007**, *381*, 366–376. [CrossRef]
16. Chen, P.; Redner, S. Majority rule dynamics in finite dimensions. *Phys. Rev. E* **2005**, *71*, 036101. [CrossRef]
17. Sznajd-Weron, K.; Sznajd, J. Who is left, who is right? *Phys. A Stat. Mech. Its Appl.* **2005**, *351*, 593–604. : 10.1016/j.physa.2004.12.038 [CrossRef]

18. Vilela, A.L.; Wang, C.; Nelson, K.P.; Stanley, H.E. Majority-vote model for financial markets. *Phys. A Stat. Mech. Its Appl.* **2019**, *515*, 762–770. [CrossRef]
19. Lima, J.R.S.; Lima, F.W.S.; Alves, T.F.A.; Alves, G.A.; Macedo-Filho, A. Diffusive majority-vote model. *Phys. Rev. E* **2022**, *105*, 034105. [CrossRef]
20. Hawthorne, F.; Harunari, P.E.; de Oliveira, M.J.; Fiore, C.E. Nonequilibrium Thermodynamics of the Majority Vote Model. *Entropy* **2023**, *25*, 1230. [CrossRef]
21. Gołębiowska, M.; Sznajd-Weron, K. The Evolution of Political Views Within the Model with Two Binary Opinions. In Proceedings of the Computational Science—ICCS 2021, Krakow, Poland, 16–18 June 2021; Paszynski, M., Kranzlmüller, D., Krzhizhanovskaya, V.V., Dongarra, J.J., Sloot, P.M., Eds.; Springer International Publishing: Cham, Switzerland, 2021; pp. 302–308.
22. Castellano, C.; Fortunato, S.; Loreto, V. Statistical physics of social dynamics. *Rev. Mod. Phys.* **2009**, *81*, 591–646. [CrossRef]
23. Castellano, C.; Muñoz, M.A.; Pastor-Satorras, R. Nonlinear q-voter model. *Phys. Rev. E* **2009**, *80*, 041129. [CrossRef]
24. Asch, S.E. Studies of independence and conformity: I. A minority of one against a unanimous majority. *Psychol. Monogr. Gen. Appl.* **1956**, *70*, 1–70. [CrossRef]
25. Moretti, P.; Liu, S.; Castellano, C.; Pastor-Satorras, R. Mean-field analysis of the q-voter model on networks. *J. Stat. Phys.* **2013**, *151*, 113–130. [CrossRef]
26. Mobilia, M. Nonlinear q-voter model with inflexible zealots. *Phys. Rev. E* **2015**, *92*, 012803. [CrossRef] [PubMed]
27. Vieira, A.R.; Anteneodo, C. Threshold q-voter model. *Phys. Rev. E* **2018**, *97*, 052106. [CrossRef] [PubMed]
28. Nyczka, P.; Sznajd-Weron, K. Anticonformity or Independence?—Insights from Statistical Physics. *J. Stat. Phys.* **2013**, *151*, 174–202. [CrossRef]
29. Jędrzejewski, A. Pair approximation for the q-voter model with independence on complex networks. *Phys. Rev. E* **2017**, *95*, 012307. [CrossRef] [PubMed]
30. Abramiuk, A.; Sznajd-Weron, K. Generalized Independence in the q-Voter Model: How Do Parameters Influence the Phase Transition? *Entropy* **2020**, *22*, 120. [CrossRef] [PubMed]
31. Chmiel, A.; Sienkiewicz, J.; Fronczak, A.; Fronczak, P. A Veritable Zoology of Successive Phase Transitions in the Asymmetric q-Voter Model on Multiplex Networks. *Entropy* **2020**, *22*, 1018. [CrossRef]
32. Gradowski, T.; Krawiecki, A. Pair approximation for the q-voter model with independence on multiplex networks. *Phys. Rev. E* **2020**, *102*, 022314. [CrossRef]
33. Abramiuk-Szurlej, A.; Lipiecki, A.; Pawłowski, J.; Sznajd-Weron, K. Discontinuous phase transitions in the q-voter model with generalized anticonformity on random graphs. *Sci. Rep.* **2021**, *11*, 17719. [CrossRef]
34. Jędrzejewski, A.; Sznajd-Weron, K.; Szwabiński, J. Mapping the q-voter model: From a single chain to complex networks. *Physica A* **2016**, *446*, 110–119. [CrossRef]
35. Sznajd-Weron, K.; Szwabiński, J.; Weron, R.; Weron, T. Rewiring the network. What helps an innovation to diffuse? *J. Stat. Mech.* **2014**, *2014*, P03007. [CrossRef]
36. Sznajd-Weron, K.; Szwabiński, J.; Weron, R. Is the Person-Situation Debate Important for Agent-Based Modeling and Vice-Versa? *PLoS ONE* **2014**, *9*, e112203. [CrossRef] [PubMed]
37. Javarone, M.A.; Squartini, T. Conformism-driven phases of opinion formation on heterogeneous networks: The q-voter model case. *J. Stat. Mech. Theory Exp.* **2015**, *2015*, P10002. [CrossRef]
38. Muslim, R.; Nqz, R.A.; Khalif, M.A. Mass Media and Its Impact on Opinion Dynamics of the Nonlinear q-Voter Model. *Physica A* **2024**, *633*, 129358. [CrossRef]
39. Vieira, A.R.; Peralta, A.F.; Toral, R.; Miguel, M.S.; Anteneodo, C. Pair approximation for the noisy threshold q-voter model. *Phys. Rev. E* **2020**, *101*, 052131. [CrossRef]
40. Granovetter, M. Threshold models of collective behavior. *Am. J. Sociol.* **1978**, *83*, 1420–1443. [CrossRef]
41. Tang, Y. Applying a transformation-based method to extract optical traveling waves from the Kundu-Mukherjee-Naskar equation. *Results Phys.* **2023**, *53*, 106943. [CrossRef]
42. Butcher, J.C. On the attainable order of Runge-Kutta methods. *Math. Comp.* **1965**, *19*, 408–417. [CrossRef]
43. Toral, R.; Tessone, C.J. Finite Size Effects in the Dynamics of Opinion Formation. *Commun. Comput. Phys.* **2007**, *2*, 177–195.

Paper 4

Multi-layer diffusion model of photovoltaic installations

Tomasz Weron

Multi-layer diffusion model of photovoltaic installations

Tomasz Weron

Department of Applied Mathematics, Faculty of Pure and Applied Mathematics, Wrocław University of Science and Technology, Wrocław, Poland

Abstract

Nowadays, harmful effects of climate change are becoming increasingly apparent. A vital issue that must be addressed is the generation of energy from non-renewable and often polluting sources. For this reason, the development of renewable energy sources is of great importance. Unfortunately, too rapid spread of renewables can disrupt stability of the power system and lead to energy blackouts. One should not simply support it, without ensuring sustainability and understanding of the diffusion process. In this research, we propose a new agent-based model of diffusion of photovoltaic panels. It is an extension of the q-voter model that utilizes multi-layer network structure. The novelty is studying both opinion dynamics and diffusion of innovation simultaneously, on a multidimensional structure. The model is analyzed with Monte Carlo simulations and mean-field approximation. The impact of parameters and specifications on the basic properties of the model is discussed. Firstly, we show that for a certain range of parameters, innovation always succeeds, regardless of the initial conditions. Secondly, that the mean-field approximation gives qualitatively the same results as computer simulations, even though it does not utilize knowledge of the network structure.

Keywords: agent-based modeling, complex networks, computational statistics, diffusion of innovation, dynamical system, opinion dynamics, mathematical modeling, renewable energy

1. Introduction

Nowadays, we are experiencing effects of climate change and environmental pollution more and more often. What might have once seemed insignificant, such as glaciers melting thousands of kilometers away, now begins to affect us directly. While the gigantic fires that devastated countries like Australia, Canada or Greece have spared the one of the author's origin, Poland, we experience another environmental disaster – air pollution. In Poland, low-quality heating installations in single-family households or multi-family tenements are among the main causes of its formation [1]. Generally speaking, the problem is the generation of energy from non-renewable and often polluting sources. High emissions of pollutants directly

Email address: tomasz.weron@pwr.edu.pl (Tomasz Weron)

threaten our lives and, in the already coming future, lead to dangerous climate change [2], of which global warming is probably the most widely discussed. It not only affects entire ecosystems and the comfort of life, but according to some studies may lead to aggravation and spread of many dangerous diseases as well [3].

That is why the development of renewable energy sources (renewables, RES) is so important. Across the European Union in 2023, about 45% of electricity generation came from RES [4]. Poland, although it saw a rapid expansion of renewables, still falls behind with around 26% [5]. In Europe, wind is the main source of renewable energy [6]. Unfortunately, wind farms require huge investments and vast free space, far from residential buildings. An alternative devoid of these limitations, and rapidly gaining popularity in Poland over the past few years, are photovoltaic panels (PVs), see Fig. 1 for exact numbers. Those can be installed on a roof of a single-family house without adversely affecting the quality of life, while the cost of such a project is achievable already for a middle-income family [7]. However, it is not only important to provide this opportunity and encourage it through subsidy programs or public campaigns, but to ensure sustainability as well. Excessive support of RES diffusion can lead to a significant increase in the variability of demand for conventional generation on a 24-hour basis, and in extreme cases can even cause loss of stability of the power system. Examples are countries/regions with a large operation of the sun during a year, such as Australia [8] or California [9], but also Poland's neighbor – Germany [10]. Apart from that, there is another threat, more closely related to the common folk. Present transmission system grids in Poland and other countries are not prepared for such a rapid PVs expansion. If unrestricted, it may lead to grid overload and blackouts. In fact, this is an already emerging risk [11].

The aim of this research is to better understand how various factors impact the diffusion of PVs. Diffusion is understood here as the process of spreading a new product through a population [12]. Diffusion of innovation has been modeled for years. It began in a very simplified manner. A classic example is the Bass diffusion model – a fully deterministic one, consisting of a single differential equation [13]. However, for a problem as complex as the diffusion of PV installations, aggregated models are just not enough [14]. They are unable to describe clustering of individuals, a phenomenon observed in real life [15]. The aforementioned Bass diffusion of innovation model can dramatically change its behavior, when rewritten to an agent-based model (ABM) and tested on a network structure [16]. In social sciences, an agent-based model is usually understood as a simulation of certain interactions between so-called agents (representing individuals, households, companies, etc.), and taking place within a certain structure, symbolizing a network of acquaintances, contacts or cooperation [17]. Mathematically, we would call such a structure a graph, with vertices being the agents, and edges – the connections between them [18]. ABMs allow for a much more accurate representation of reality, including heterogeneity of individuals and the interactions between them [18]. As such, ABMs are currently one of the most powerful tools in studying opinion dynamics and diffusion of innovation [19]. Although they have been used for years to model the diffusion of new energy solutions [20, 21, 22, 23, 24], their applications in modeling the diffusion of PVs remain few [25, 26, 27, 28].

Although much more advanced than simple deterministic models, ABMs are still merely

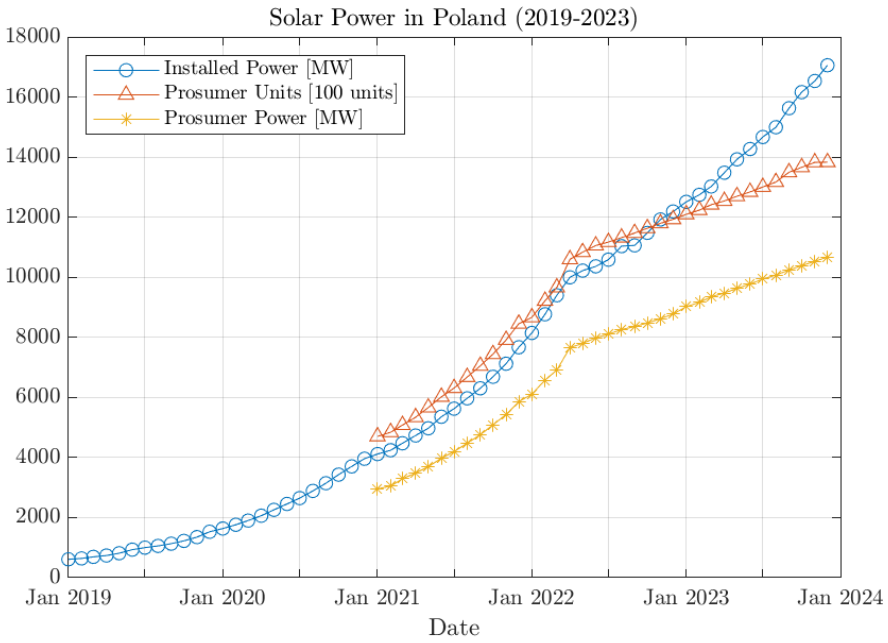

Figure 1: Data on solar installations in Poland in years 2019–2023, according to ARE (Polish energy market agency). More detailed data is being collected from 2021 onward, most likely due to the growing interest in the prosumer market. Data freely available at www.are.waw.pl.

a hypothetical approximation of reality. With that in mind, one should adjust them to a problem at hand as accurately as possible, instead of constructing a one-size-fits-all model. A huge role here is played by the underlying structure. For example, when modeling a spread of gossip in a high school class, a simple network of class acquaintances would be sufficient. However, to properly represent the flow of information and exchange of opinions in the modern world, a much more complex structure is needed. This is where multi-layer networks come in. They are applied in many fields of science [29], for they can provide multi-level representation of real world dependencies [30]. For instance, an individual (agent) may learn about recent sport results either from friends at work (one layer), or through social media (another layer).

Sociologists have long pointed out that structures of social interaction should not be reduced to single-layer networks [30]. However, multi-layer structures have only been studied intensively since the last decade [31]. Recently, they have been used in modeling the diffusion of innovation [32, 33]. Nevertheless, this is still a relatively fresh concept. One issue that arises with multi-layer networks is generalization of models' rules that where originally implemented on single-layer structures. For instance, one may assume that social influence is only effective if it comes from all the layers (AND rule). However, it can also be assumed that the influence is effective even if it comes from a single layer only (OR rule) [34]. In this research, we follow the approach from [35] and study both variants.

Monte Carlo (MC) computer simulations are the main research method for ABMs. However, in some limited cases, as for networks being complete or random graphs with a low

clustering coefficient, analytical methods such as mean-field (MFA) or pair approximation (PA) can be used [36, 37, 38]. Unfortunately, real world networks are characterized by a high clustering coefficient [18], so often the analytical results obtained this way differ quantitatively from ones given by Monte Carlo simulations [37]. The need to sweep a multidimensional space of input parameters and perform multiple independent repetitions to obtain good statistical parameters makes Monte Carlo simulations very time-consuming. For this reason, we utilize both computer simulations and analytical methods in this research.

A popular agent-based model that already has found its use in studying diffusion of eco-innovation is the q-voter model [20, 23, 39]. In this model, conformity is the basic form of social response. Agents are characterized by a single binary variable denoting their opinion and placed in nodes of some underlying graph structure. Their opinions change upon impact with so-called groups of influence, i.e. q of the agent's neighbors chosen randomly, but only if a given group presents an unanimous opinion. A well-established extension to the q-voter model is the addition of independence – a probability that an agent acts and changes opinion independently of the group of influence [40]. The q-voter model has been already examined on multi-layer networks, but to the best of our knowledge only ones consisting of two identical layers [35, 41].

In this paper, we introduce a new model based on the aforementioned q-voter model with independence. Our goal is to capture both opinion dynamics and diffusion of innovation jointly. Hence, we introduce (compared to the original q-voter model) a second agent's attribute, in addition to the opinion – an adoption state. Similarly to the opinion, it is a binary one. Positive value means that an agent possesses a PV installation, negative – it does not. An agent (in this case a household) can acquire knowledge of PVs from two sources. Either it sees panels on the roofs of neighboring households, or communicates with friends/colleagues. To model this twofold dynamic, we utilize a two-layer network as the underlying topology. The first layer of the network depicts the spacial location of an agent, similarly to [42, 43]. From a mathematical point of view it is just a square lattice (SL) with Moore's neighborhood [44]. At this level, each agent possesses only knowledge of the adoption states of the closest neighborhood, and these adoption states shape agent's opinion, according to the q-voter rule. The agent cannot share opinion or be subject to the opinions of the neighborhood. This is the visual observation part. A single-family house owner sees only PV panels, or lack thereof, on the roofs of neighboring houses, and does not exchange information or opinions with neighbors. The second layer of the network corresponds to structure of contacts and relationships of agents. For this reason, here we use two-dimensional Watts-Strogatz graph (WS2D) [45]. It possesses some characteristics of real world social networks [18, 46] and, in a specific case (when randomness equals 0), reduces to a square lattice. At this level, a connection between two agents implies their familiarity, through which they can exchange opinions, but do not observe their adoption states. In this case, social influence is also described by the q-voter model. Lastly, it is an agent's opinion solely that impacts its adoption state. An agent with a positive opinion can install photovoltaic panels with probability a_1, one with a negative one can resign with probability a_2. The reason for this research is to thoroughly examine this mathematical model, to understand how its parameters shape the outcome.

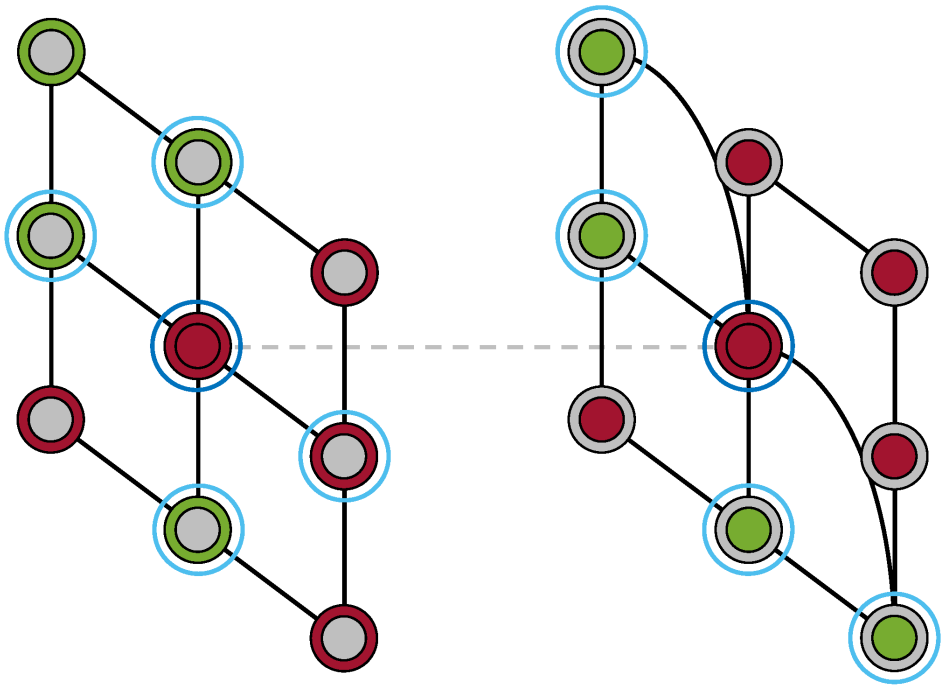

Figure 2: Graphical representation of the model. The network consists of 2 layers: Square Lattice (SL, left side), on which adoption states A_i are visible and two-dimensional Watts-Strogatz (WS2D, right side) with opinions S_i. Adoption states A_i are represented by outer circles (green – $A_i = +1$, red – $A_i = -1$), while opinions – by inner circles. Grey areas correspond to adoption states or opinions unknown to the target agent (marked with a dark blue circle). Groups of influence (of size $q = 4$, marked with light blue circles) are constructed independently on each layer. In the given example, such a choice would be sufficient to change target's opinion ($S_{target} \to +1$) in the OR variant, but not in the AND variant, as unanimity is only achieved in one of the two groups of influence.

The rest of this article is organized as follows. In the next section, we provide a more detailed description of the model and the methods used. Then, in Section 3, we examine the two variants, AND and OR rules, which were explained above. Both by means of computer simulations, numerical and analytical methods. Finally, in Section 4, we wrap up. Additionally, in Appendix, we consider various initial conditions.

2. Model and Methods

2.1. Simulation Model

We consider a set of N agents, each of which is characterized by 2 binary variables: adoption $A_i = \pm 1$ (adopted or not adopted), and opinion $S_i = \pm 1$ (positive or negative), for $i = 1, 2, \ldots, N$. Agents are located on a two-layer network (Fig. 2). The first layer of the network depicts the spacial location of an agent and is represented by a square lattice (SL) with Moore's neighborhood, meaning that each agent possesses 8 neighbors surrounding it (except for agents in corners and along edges, which have 3 and 5 neighbors, respectively) [44]. At this level, an agent sees only the adoption states of its neighbors. The second layer

corresponds to the structure of social ties of agents, which is described by a two-dimensional Watts-Strogatz graph [45]. Here, an agent sees only the opinions of its neighbors. Each layer is a connected simple graph [47], as described in Definition 1.

Definition 1. *Let $G = [G_{X,i,j}]$ denote an adjacency matrix for the two-layer network, with each layer X, $X \in \{1, 2\}$, being a connected simple graph, i.e. an unweighted, undirected graph containing no graph loops or multiple edges [47]. Then, for $i, j = 1, 2, \ldots, N$:*

- $\forall_X \forall_i \forall_j G_{X,i,j} = 1 \iff$ *edge between i and j exists on layer X,*
- $\forall_X \forall_i \forall_j G_{X,i,j} = 0 \iff$ *edge between i and j does not exist on layer X,*
- $\forall_X \forall_i \forall_j G_{X,i,j} = G_{X,j,i}$,
- $\forall_X \forall_i G_{X,i,i} = 0$.

We investigate the model through Monte Carlo simulations with a random sequential updating scheme. Within a single simulation, the time is measured in so-called Monte Carlo sweeps (MCS) [48]. One MCS consists of N elementary events, each of length $\Delta t = \frac{1}{N}$. In each elementary event, an agent i is chosen at random (uniformly from all N). Then, with probability p, agent i acts independently and changes its opinion S_i randomly. With complementary probability $1 - p$, the agent is susceptible to social influence (based on the q-voter model [39]), combined from both layers of the network with respect to the variant, AND or OR. Lastly, if agent i has positive opinion $S_i = +1$, but negative adoption state $A_i = -1$, it changes the latter to positive, $A_i \to +1$, with probability a_1. Otherwise, if it possesses negative opinion $S_i = -1$, but positive adoption state $A_i = +1$, it looses the latter, i.e. $A_i \to -1$, with probability a_2. Simulation details are shown in Algorithm 1, and the graphical representation of the model in Fig. 2. In Algorithm 1:

- $\mathcal{U}[0, 1]$ stands for a continuous uniform distribution, while $\mathcal{U}\{X\}$ – for a discrete one, where each element from set X is chosen with equal probability.
- G is an adjacency matrix for the two-layer network, as per Definition 1,
- p, a_1, and a_2 denote probabilities of independence, adopting (getting positive adoption state) and unadopting, respectively. As probabilities, p, a_1, $a_2 \in [0, 1]$. In this research, we only consider $a_1 \in (0, 1]$ and:

$$a_2 = h \times a_1, \tag{1}$$

  where $h \in (0, 1)$.

- q stands for the size (the number of neighbors) of the group of influence. In here, we consider $q \in \mathbb{N}$, $q \geq 2$.

Algorithm 1: Simulation dynamics

```
for t := 1 to T do
    for k := 1 to N do
        i := i ~ U{1, ..., N}
        r := r ~ U[0, 1]
        if r < p then
            r := r ~ U[0, 1]
            if r < 1/2 then
                S_i := -S_i
        else
            for l := 1 to q do
                j_{1,l} := j_1 ~ U{j_1 : G_{1,i,j_1} = 1}
                j_{2,l} := j_2 ~ U{j_2 : G_{2,i,j_2} = 1}
            end
            Q_1 := (1/q) sum_l^q A_{j_{1,l}}
            Q_2 := (1/q) sum_l^q S_{j_{2,l}}
            if Variant = AND then
                if Q_1 + Q_2 = -2S_i then
                    S_i := -S_i
            else if Variant = OR then
                if (Q_1 = -S_i and Q_2 ≠ S_i) or (Q_1 ≠ S_i and Q_2 = -S_i) then
                    S_i := -S_i
            end
        end
        r := r ~ U[0, 1]
        if S_i = 1 and A_i = -1 and r < a_1 then
            A_i = 1
        else if S_i = -1 and A_i = 1 and r < a_2 then
            A_i = -1
        end
    end
end
```

To clarify, we do the following. At the beginning of each independent simulation (trajectory), we set the initial conditions. In simulations, we always start from a fully unadopted, negative state, i.e., $\forall_i\ A_i(0) = -1,\ S_i(0) = -1$. Then, we perform Monte Carlo sweeps until a determined time horizon T is reached (T is the number of MCS). We repeat independent simulations multiple times with the same set of parameter values for a better statistical accuracy. We also run separate simulations for different sets of parameter values.

To examine the model on a macroscopic scale, we use two measures: concentration (fraction) of positive adoption states and concentration of positive opinions.

Definition 2. *Let N be the number of agents, $A_i \pm 1$ the adoption state and $S_i = \pm 1$ the*

opinion of agent i, for $i = 1, 2, \ldots, N$. Then, the concentrations of positive adoption states c_A and opinions c_S are given by:

$$c_A = \frac{1}{N}\sum_{i=1}^{N}(2A_i - 1), \quad c_S = \frac{1}{N}\sum_{i=1}^{N}(2S_i - 1). \tag{2}$$

By definition $c_A \in [0, 1]$ and $c_S \in [0, 1]$. For the sake of simplicity, we refer to them as just concentrations of adoption states (or adopted) and opinions, respectively.

2.2. Mean-Field Approximation

Here, we utilize the mean-field approximation (MFA) [40] to derive a set of equations describing the dynamical system.

Theorem 1. *Let c_A and c_S denote the concentrations of positive adoption states and positive opinions respectively (as per Definition 2). Under the assumption that each layer of the network is a complete graph of size $N \to \infty$, the dynamics of the system is described in the AND variant by:*

$$\frac{dc_A}{dt} = c_S(1 - c_A)a_1 - (1 - c_S)c_A h a_1, \tag{3}$$

$$\frac{dc_S}{dt} = (1 - c_S)\left(\frac{1}{2}p + (1 - p)c_S^q c_A^q\right) - c_S\left(\frac{1}{2}p + (1 - p)(1 - c_S)^q(1 - c_A)^q\right), \tag{4}$$

and in the OR variant by:

$$\begin{aligned}\frac{dc_A}{dt} &= c_S(1 - c_A)a_1 - (1 - c_S)c_A h a_1,\\ \frac{dc_S}{dt} &= (1 - c_S)\Big\{\frac{1}{2}p + (1 - p)\left(c_S^q(1 - c_A^q - (1 - c_A)^q)\right.\\ &\quad \left. + c_A^q(1 - c_S^q - (1 - c_S)^q) + c_S^q c_A^q\right)\Big\}\\ &\quad - c_S\Big\{\frac{1}{2}p + (1 - p)\left((1 - c_S)^q(1 - c_A^q - (1 - c_A)^q)\right.\\ &\quad \left. + (1 - c_A)^q(1 - c_S^q - (1 - c_S)^q) + (1 - c_S)^q(1 - c_A)^q\right)\Big\}.\end{aligned} \tag{5}$$

Proof. Under the assumption that each layer of the network is a complete graph of size $N \to \infty$, we can write down probability γ_A^+ that a number of agents with positive adoption states will increase by 1 and probability γ_A^- that it will decrease by 1:

$$\gamma_A^+ = c_S(1 - c_A)a_1, \tag{6}$$

$$\gamma_A^- = (1 - c_S)c_A a_2. \tag{7}$$

Then, we derive the differential equation, analogously to [19, 49]:

$$\frac{\mathrm{d}c_A}{\mathrm{d}t} = \gamma_A^+ - \gamma_A^-, \tag{8}$$

which gives us Eq. (3), after replacing a_2 with ha_1 (Eq. (1)). Eq. (3) is common for both AND and OR variants of the model. Similarly, we can write down probabilities γ_S^+ and γ_S^- that a number of agents with positive opinion will increase or decrease by 1 respectively. These are:

$$\gamma_{S,AND}^+ = (1-c_S)\left(\frac{1}{2}p + (1-p)c_S^q c_A^q\right), \tag{9}$$

$$\gamma_{S,AND}^- = c_S\left(\frac{1}{2}p + (1-p)(1-c_S)^q(1-c_A)^q\right), \tag{10}$$

in the AND variant, and:

$$\gamma_{S,OR}^+ = (1-c_S)\left\{\frac{1}{2}p + (1-p)\left(c_S^q\sum_{i=1}^{q-1}\binom{q}{i}c_A^i(1-c_A)^{q-i} + c_A^q\sum_{i=1}^{q-1}\binom{q}{i}c_S^i(1-c_S)^{q-i} + c_S^q c_A^q\right)\right\}, \tag{11}$$

$$\gamma_{S,OR}^- = c_S\left\{\frac{1}{2}p + (1-p)\left((1-c_S)^q\sum_{i=1}^{q-1}\binom{q}{i}(1-c_A)^i c_A^{q-i} + (1-c_A)^q\sum_{i=1}^{q-1}\binom{q}{i}(1-c_S)^i c_S^{q-i} + (1-c_S)^q(1-c_A)^q\right)\right\}, \tag{12}$$

in the OR variant. Using the binomial formula, we can replace sums in $\gamma_{S,OR}^+$ and $\gamma_{S,OR}^-$ with:

$$\sum_{i=1}^{q-1}\binom{q}{i}c_X^i(1-c_X)^{q-i} = \sum_{i=1}^{q-1}\binom{q}{i}(1-c_X)^i c_X^{q-i} = 1-(1-c_X)^q - c_X^q, \quad X = A, S. \tag{13}$$

Then:

$$\frac{\mathrm{d}c_A}{\mathrm{d}t} = \gamma_{S,AND}^+ - \gamma_{S,AND}^- \tag{14}$$

gives us Eq. (4), and

$$\frac{\mathrm{d}c_A}{\mathrm{d}t} = \gamma_{S,OR}^+ - \gamma_{S,OR}^- \tag{15}$$

gives Eq. (5). □

Due to the power of q in Eqs. (4)-(5), time trajectories of the system given by Eqs. (3)-(5) cannot be determined analytically. Hence, one must resort to numerical methods, which we show in Section 3. However, stationary states can be found analytically and there existence can be proven.

Theorem 2. *Let c_A and c_S denote the concentrations of positive adoption states and positive opinions respectively (as per Definition 2). Under the assumption that each layer of the network is a complete graph of size $N \to \infty$, for any $q \in \mathbb{N}$, $q \geq 2$, $p \in [0,1]$, $h \in (0,1)$ and*

$a_1 \in (0, 1]$, there always exists at least one stationary state (c'_A, c'_S), and all stationary states (c'_A, c'_S) must satisfy:

$$c_A = \frac{c_S}{c_S + h - c_S h}, \tag{16}$$

$$p = \frac{f_2(c_S)}{f_2(c_S) + f_3(c_S)}, \tag{17}$$

in the AND variant, and:

$$c_A = \frac{c_S}{c_S + h - c_S h},$$

$$p = \frac{f_5(c_S)}{f_5(c_S) + f_3(c_S)}, \tag{18}$$

in the OR variant. Here:

$$\begin{aligned}
f_2(c_S) &= c_S(1 - c_S)\left(c_S^{2q-1} - h^q(1 - c_S)^{2q-1}\right), \\
f_3(c_S) &= \left(c_S - \frac{1}{2}\right)(c_S + h - c_S h)^q, \\
f_5(c_S) &= c_S(1 - c_S)\Big\{\left(c_S^{q-1} - (1 - c_S)^{q-1}\right)(c_S + h - c_S h)^q \\
&\quad + c_S^{q-1}(1 - c_S)^{q-1}(1 + h^q)(2c_S - 1) \\
&\quad + c_S^{q-1} - c_S^{2q-1} + h^q(1 - c_S)^{2q-1} - h^q(1 - c_S)^{q-1}\Big\}.
\end{aligned}$$

Proof. A stationary state (c'_A, c'_S) must satisfy:

$$\frac{\mathrm{d}c_A}{\mathrm{d}t} = 0, \quad \frac{\mathrm{d}c_S}{\mathrm{d}t} = 0. \tag{19}$$

First, let us consider Eq. (3), common for both AND and OR variants of the model:

$$0 = c_S(1 - c_A)a_1 - (1 - c_S)c_A h a_1. \tag{20}$$

Since $a_1 > 0$, we can rewrite it as:

$$c_S = c_A(c_S + h - c_S h). \tag{21}$$

Because $c_S \in [0, 1]$ and $h \in (0, 1)$, $(c_S + h - c_S h) > 0$ always, and hence:

$$c_A = \frac{c_S}{c_S + h - c_S h} = \frac{c_S}{(1 - h)c_S + h} = f_1(c_S). \tag{22}$$

Note, that function $f_1(c_S)$ is a rational one of degree 1. Therefore, for any $c_S \in [0, 1]$, there always exists exactly one $c_A \in [0, 1]$ that satisfies Eq. (22).

Now, let us consider Eq. (4) from the AND variant:

$$0 = (1 - c_S)\left(\frac{1}{2}p + (1-p)c_S^q c_A^q\right) - c_S\left(\frac{1}{2}p + (1-p)(1-c_S)^q(1-c_A)^q\right). \tag{23}$$

By expanding the brackets and putting all the terms containing p on one side, we arrive at:

$$p\left(c_S^q c_A^q - c_S^{q+1}c_A^q - c_S(1-c_S)^q(1-c_A)^q + c_S - \frac{1}{2}\right) = \\ c_S^q c_A^q - c_S^{q+1}c_A^q - c_S(1-c_S)^q(1-c_A)^q. \tag{24}$$

Next, by replacing c_A with $f_1(c_S)$ and multiplying all the terms by $(c_S + h - c_S h)^q$, we get:

$$p\left\{c_S(1-c_S)\left(c_S^{2q-1} - h^q(1-c_S)^{2q-1}\right) + \left(c_S - \frac{1}{2}\right)(c_S + h - c_S h)^q\right\} = \\ c_S(1-c_S)\left(c_S^{2q-1} - h^q(1-c_S)^{2q-1}\right). \tag{25}$$

Then, denoting:

$$f_2(c_S) = c_S(1-c_S)\left(c_S^{2q-1} - h^q(1-c_S)^{2q-1}\right), \tag{26}$$

$$f_3(c_S) = \left(c_S - \frac{1}{2}\right)(c_S + h - c_S h)^q, \tag{27}$$

we obtain:

$$p\left(f_2(c_S) + f_3(c_S)\right) = f_2(c_S). \tag{28}$$

If $f_2(c_S) + f_3(c_S) = 0$, then $f_2(c_S) = 0$, and hence $f_3(c_S) = 0$ as well. Function $f_3(c_S) = 0$ only if $c_S = \frac{1}{2}$, as $(c_S + h - c_S h) > 0$. For $c_S \in \left[\frac{1}{2}, 1\right)$, function $f_2(c_S)$:

$$f_2(c_S) = \underbrace{c_S(1-c_S)}_{>0}\underbrace{\left(c_S^{2q-1} - h^q(1-c_S)^{2q-1}\right)}_{>0} > 0, \tag{29}$$

because for $c_S \in \left[\frac{1}{2}, 1\right)$, $c_S \geq 1 - c_S$, and $h \in (0,1)$. Hence, there is no c_S for which $f_2(c_S) = f_3(c_S) = 0$, and therefore no c_S for which $f_2(c_S) + f_3(c_S) = 0$ that satisfies Eq. (28). As further we consider only $f_2(c_S) + f_3(c_S) \neq 0$, we can write:

$$p = \frac{f_2(c_S)}{f_2(c_S) + f_3(c_S)} = f_4(c_S). \tag{30}$$

From Eqs. (26)-(30), we can notice that:

$$\begin{aligned} &\text{for } \; c_S = 1 : f_2(c_S) = 0,\ f_3(c_S) > 0 \implies f_4(c_S) = 0 \\ &\text{for } \; c_S = \frac{1}{2} : f_2(c_S) > 0,\ f_3(c_S) = 0 \implies f_4(c_S) = 1, \\ &\text{for } \; c_S \in \left(\frac{1}{2}, 1\right) : f_2(c_S) > 0,\ f_3(c_S) > 0 \implies f_4(c_S) \in (0,1). \end{aligned} \tag{31}$$

When $c_S \in \left[\frac{1}{2}, 1\right]$, $f_4(c_S)$ is a rational function with positive denominator, and hence continuous within that interval. As it is continuous in $\left[\frac{1}{2}, 1\right]$, $f_4(1) = 0$ and $f_4\left(\frac{1}{2}\right) = 1$, it achieves any value of between 0 and 1. Hence, for any $p \in [0, 1]$ there always exists at least one $c_S \in [0, 1]$ that satisfies Eq. (30). Therefore, in the AND variant, there always exists at least one stationary state.

Similarly in the OR variant, we have:

$$\begin{aligned} 0 = (1 - c_S)\Big\{ & \frac{1}{2}p + (1-p)\left(c_S^q\left(1 - c_A^q - (1-c_A)^q\right)\right. \\ & \left. + c_A^q\left(1 - c_S^q - (1-c_S)^q\right) + c_S^q c_A^q\right)\Big\} \\ & - c_S\Big\{\frac{1}{2}p + (1-p)\left((1-c_S)^q\left(1 - c_A^q - (1-c_A)^q\right)\right. \\ & \left. + (1-c_A)^q\left(1 - c_S^q - (1-c_S)^q\right) + (1-c_S)^q(1-c_A)^q\right)\Big\}, \end{aligned} \tag{32}$$

from Eq. (5). Analogously to the AND variant, by expanding the brackets, putting all the terms containing p on one side, then, by replacing c_A with $f_1(c_S)$ and multiplying all the terms by $(c_S + h - c_S h)^q$, we get:

$$p\left(f_5(c_S) + f_3(c_S)\right) = f_5(c_S), \tag{33}$$

where

$$\begin{aligned} f_3(c_S) = & \left(c_S - \frac{1}{2}\right)(c_S + h - c_S h)^q, \\ f_5(c_S) = & c_S(1-c_S)\Big\{\left(c_S^{q-1} - (1-c_S)^{q-1}\right)(c_S + h - c_S h)^q \\ & + c_S^{q-1}(1-c_S)^{q-1}(1+h^q)(2c_S - 1) \\ & + c_S^{q-1} - c_S^{2q-1} + h^q(1-c_S)^{2q-1} - h^q(1-c_S)^{q-1}\Big\}. \end{aligned} \tag{34}$$

Again, if $f_5(c_S) + f_3(c_S) = 0$, then $f_5(c_S) = 0$, and hence $f_3(c_S) = 0$ as well. Function $f_3(c_S) = 0$ only if $c_S = \frac{1}{2}$. For $c_S \in \left[\frac{1}{2}, 1\right)$, function $f_5(c_S)$:

$$\begin{aligned} f_5(c_S) = & \underbrace{c_S(1-c_S)}_{>0}\Big\{\underbrace{\left(c_S^{q-1} - (1-c_S)^{q-1}\right)}_{\geq 0}\underbrace{(c_S + h - c_S h)^q}_{>0} \\ & + \underbrace{c_S^{q-1}(1-c_S)^{q-1}(1+h^q)(2c_S - 1)}_{\geq 0} \\ & + \underbrace{c_S^{q-1} - c_S^{2q-1} + h^q(1-c_S)^{2q-1} - h^q(1-c_S)^{q-1}}_{>0, \text{ by Lemma 1}}\Big\} > 0, \end{aligned} \tag{35}$$

because for $c_S \in \left[\frac{1}{2}, 1\right)$, $c_S \geq 1 - c_S$, and $h \in (0, 1)$. Lemma 1 is presented below this proof. Hence, there is no c_S for which $f_5(c_S) = f_3(c_S) = 0$, and therefore no c_S for which

$f_5(c_S) + f_3(c_S) = 0$ that satisfies Eq. (33). As further we consider only $f_5(c_S) + f_3(c_S) \neq 0$, we can write:

$$p = \frac{f_5(c_S)}{f_5(c_S) + f_3(c_S)} = f_6(c_S). \tag{36}$$

From Eqs. (33)-(36), we can notice that:

$$\begin{aligned}
&\text{for } \; c_S = 1 : f_5(c_S) = 0, \; f_3(c_S) > 0 \implies f_6(c_S) = 0 \\
&\text{for } \; c_S = \frac{1}{2} : f_5(c_S) > 0, \; f_3(c_S) = 0 \implies f_6(c_S) = 1, \\
&\text{for } \; c_S \in \left(\frac{1}{2}, 1\right) : f_5(c_S) > 0, \; f_3(c_S) > 0 \implies f_6(c_S) \in (0, 1).
\end{aligned} \tag{37}$$

When $c_S \in \left[\frac{1}{2}, 1\right]$, $f_6(c_S)$ is a rational function with positive denominator, and hence continuous within that interval. As it is continuous in $\left[\frac{1}{2}, 1\right]$, $f_6(1) = 0$ and $f_6\left(\frac{1}{2}\right) = 1$, it achieves any value of between 0 and 1. Hence, for any $p \in [0, 1]$ there always exists at least one $c_S \in [0, 1]$ that satisfies Eq. (36). Therefore, in the OR variant, there always exists at least one stationary state. □

Lemma 1. *Let $c_S \in \left[\frac{1}{2}, 1\right)$, $h \in (0, 1)$ and $q \in \mathbb{N}$, $q \geq 2$. Then:*

$$c_S^{q-1} - c_S^{2q-1} + h^q(1 - c_S)^{2q-1} - h^q(1 - c_S)^{q-1} > 0. \tag{38}$$

Proof. First, we show that for $c_S \in \left[\frac{1}{2}, 1\right)$:

$$\begin{aligned}
c_S^{2q-2} - (1 - c_S)^{2q-2} &\geq c_S^{2q-1} - (1 - c_S)^{2q-1} \\
c_S^{2q-2} - c_S^{2q-1} &\geq (1 - c_S)^{2q-2} - (1 - c_S)^{2q-1} \\
c_S^{2q-2}(1 - S) &\geq (1 - c_S)^{2q-2}(1 - (1 - c_S)) \\
c_S^{2q-3} &\geq (1 - c_S)^{2q-3}
\end{aligned} \tag{39}$$

is true, because $c_S \geq 1 - c_S$ and $2q - 3 \geq 1$. Then:

$$\begin{aligned}
&c_S^{q-1} - c_S^{2q-1} + h^q(1 - c_S)^{2q-1} - h^q(1 - c_S)^{q-1} = \\
&c_S^{q-1} - c_S^{2q-1} - h^q \underbrace{\left((1 - c_S)^{q-1} - (1 - c_S)^{2q-1}\right)}_{>0} \overset{h<1}{>} \\
&c_S^{q-1} - c_S^{2q-1} - \left((1 - c_S)^{q-1} - (1 - c_S)^{2q-1}\right) = \\
&c_S^{q-1} - (1 - c_S)^{q-1} - \left(c_S^{2q-1} - (1 - c_S)^{2q-1}\right) \overset{\text{Eq. 39}}{\geq} \\
&c_S^{q-1} - (1 - c_S)^{q-1} - \left(c_S^{2q-2} - (1 - c_S)^{2q-2}\right) = \\
&c_S^{q-1} - (1 - c_S)^{q-1} - \left(c_S^{q-1} - (1 - c_S)^{q-1}\right)\left(c_S^{q-1} + (1 - c_S)^{q-1}\right) = \\
&\underbrace{\left(c_S^{q-1} - (1 - c_S)^{q-1}\right)}_{\geq 0}\underbrace{\left(1 - c_S^{q-1} - (1 - c_S)^{q-1}\right)}_{\geq 0} \geq 0.
\end{aligned} \tag{40}$$

□

3. Results

3.1. Simulation Details

First, we examine our model with Monte Carlo computer simulations. In order to measure the outcomes at a macroscopic level, we use concentrations, i.e. fractions, of positive adoption states c_A and positive opinions c_S, see Definition 2. In all the simulations, we study a system of size $N = 2500$ (number of agents, which may be interpreted as a borough in a city). As mentioned in the Introduction, the first layer of the two-layer network is always a Square Lattice with Moore's neighborhood [44], and no periodic boundary conditions, which means that almost every agent has exactly 8 neighbors (except those on the edges of the lattice). We denote it as SL($N = 2500$, $m = 1$), where $m = 1$ indicates the range of a neighborhood on a square grid. The second layer is always a two-dimensional Watts-Strogatz graph [45], with Moore's neighborhood before rewiring and rewiring probability $\beta = 0.2$, and again, without periodic boundary conditions. We wanted a layer that possesses characteristics of a real world social network, but still bears a resemblance to the other layer. We denote it as WS2D($N = 2500$, $m = 1$, $\beta = 0.2$). We study the behavior of the system with respect to the parameters p, a_1 and a_2. Although the size of the group of influence q is a parameter as well, here we keep it constant, as its impact in the q-voter model with independence is well studied [40]. We choose $q = 4$ motivated by real life experiments [50]. This will help us to reduce computational efforts slightly. In all the simulations, we start from a fully unadopted, negative state, i.e., $c_A(0) = 0$, $c_S(0) = 0$. Lastly, for illustrative purposes, the time horizon T for each simulation is limited to 5000 Monte Carlo steps (MCS), and the number of time trajectories to 10.

3.2. Simulation Model

Let us begin with Fig. 3. It shows evolution of the system, for both variants (AND and OR), and a range of values of p, a_1 and a_2, where $a_2 = 0.5a_1$ in all cases. We can observe that several final outcomes are possible. When p is low, we retain an unadopted state ($c_A(T) \approx 0$, $c_S(T) \approx 0$). None of the agents have a positive opinion or adoption state, except for a few rebels. Then, there is a critical value of p, above which the system becomes adopted ($c_A(T) \approx 1$, $c_S(T) \approx 1$). If the value of p is high, independence surpasses conformity and we end up with a disordered system ($c_A(T) \approx 0.5$, $c_S(T) \approx 0.5$). There is a visible difference between the two variants: AND and OR. In the first, much lower values of p are required to enter adopted or disordered state than in the latter. Finally, the value of a_1 itself has no impact on the final state (except for $a_1 = 0$, which is not shown here), only on the time needed to reach it, with the higher value speeding up the process.

What affects the final state, however, is the relationship between a_1 and a_2, namely the coefficient h (Eq. (1)). Let us move to Fig. 4. There, a_2 is twice as small relative to a_1 as before, $a_2 = 0.25a_1$. With this decrease in a_2 much lower values of p are needed, in both variants, for the system to become adopted. This itself is a rather trivial conclusion, as now the probability of loosing adoption is four times smaller that the one of adopting. There is, however, a secondary effect to it, due to the fact how the first layer of the network impacts opinions in our model. Positive adoption states support positive opinions (and vice versa).

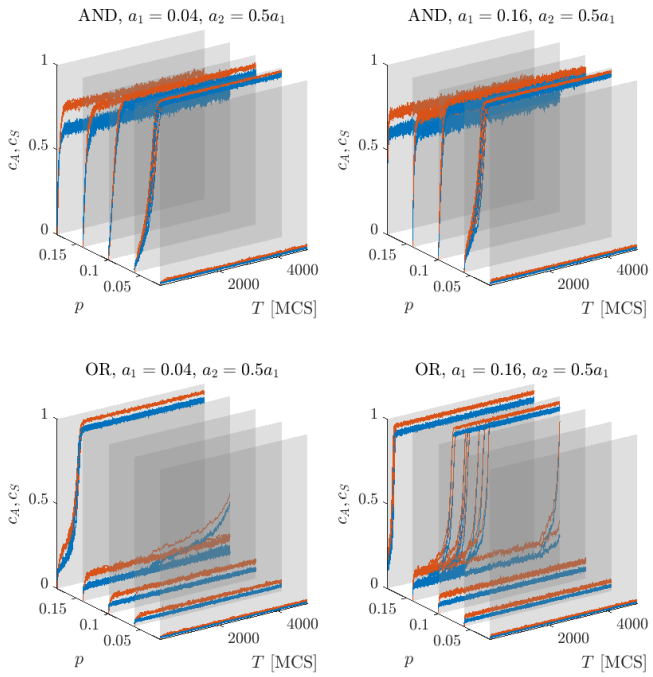

Figure 3: 10 simulated time trajectories of c_A (red) and c_S (blue) for different values of p: the AND variant (top), the OR variant (bottom). Values of a_1: $a_1 = 0.04$ (left), $a_1 = 0.16$ (right). First layer – SL(N,1), second layer – WS2D(N,1,0.2), size $N = 2500$ and $a_2 = 0.5a_1$ in all cases.

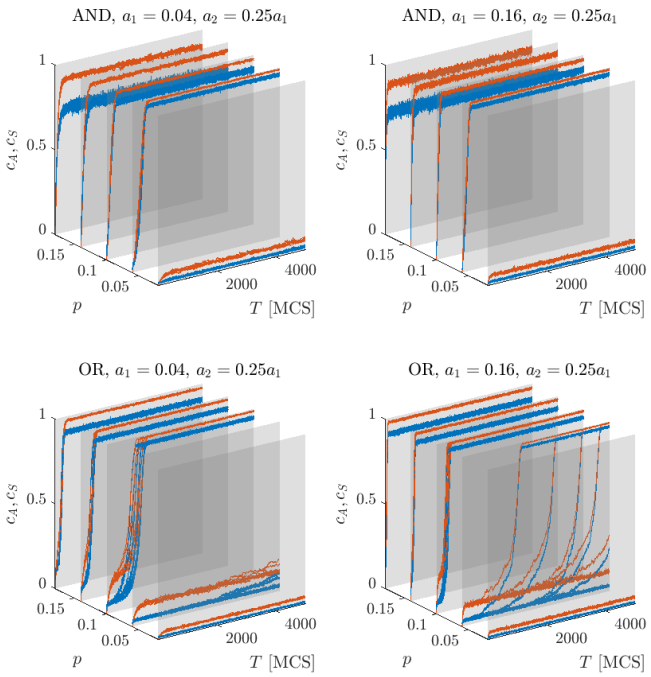

Figure 4: 10 simulated time trajectories of c_A (red) and c_S (blue) for different values of p: the AND variant (top), the OR variant (bottom). Values of a_1: $a_1 = 0.04$ (left), $a_1 = 0.16$ (right). First layer – SL(N,1), second layer – WS2D(N,1,0.2), size $N = 2500$ and $a_2 = 0.25a_1$ in all cases.

For this reason, the adopted state is not only easier to reach, but also more difficult to disorder.

We decided not to examine a symmetrical case $a_1 = a_2$, i.e. $h = 1$, because there is no adopted state there. From $c_A(0) = 0$, $c_S(0) = 0$, the system can only evolve into total disorder or remain unadopted.

3.3. Mean-Field Approximation

Monte Carlo computer simulations are the first choice when it comes to agent-based models. Unfortunately, as mentioned in the Introduction, they can be very time-consuming. For this reason, we derive a set of equations describing dynamics of the system (Eqs. (3)-(5)), under the assumption that each layer of the network is a complete graph of size $N \to \infty$. Thanks to this approach, we can examine a wide range of parameter values, which we could not achieve with Monte Carlo simulations in any reasonable amount of time.

Before discussing the analytical results themselves, we compare them with the simulations. For this, see Fig. 5, where we combine the latter and numerically obtained time trajectories from Eqs. (3)-(5). As shown there, mean-field gives fairly good approximation, except for the bottom row (OR variant, $p = 0.2$). This is due to the fact, that in the MFA critical values of p required for the system to adopt are slightly higher, as presented in the next two Figures (Figs. 6 and 7).

Mean-field time trajectories, and hence times to reach a stationary state, are obtained numerically from Eqs. (3)-(5). Analytically, we are only able to compute stationary states (Eqs. (16)-(18)). We compare the two in Fig. 6, for $a_2 = 0.5a_1$. Numerically computed stationary states perfectly match analytical ones. Segments not covered by the numerical results are due to the fact that the analytical solution shows all the possible stationary states, while the numerical one only those achievable from given initial conditions ($c_A(0) = 0$, $c_S(0) = 0$). Clearly visible here are the three possible groups of stationary states: unadopted ($c_A(T) \approx 0$, $c_S(T) \approx 0$), adopted ($c_A(T) \approx 1$, $c_S(T) \approx 1$) and disordered ($c_A(T) \approx 0.5$, $c_S(T) \approx 0.5$), although a transition between the latter two in the OR variant is very smooth. As already mentioned, the value of a_1 ($a_1 \in (0, 1]$) itself has no impact on a stationary state. Therefore, we set it arbitrarily to 0.5 (only left side of Fig. 6). On the right, times to reach a stationary state with respect to a_1 and p are presented. These drop dramatically with an increase of a_1, but only for very low values of a_1. After that, the change is unnoticeable. There are significant „ridges" for the values of p corresponding to transitions between groups of stationary states (left side). There are two such ridges in the AND variant, but only one in the OR variant, as transition between adopted and disordered is very smooth there. These increases in times are logical, as the system needs more time to „decide" which path to take, and consistent with our knowledge on phase transitions.

When we decrease a_2 to $0.25a_1$ (see Fig. 7), transitions between adopted and disordered states become less apparent in both variants of the model. Moreover, values of p needed for adoption decrease, while those needed for disorder increase, which is consistent with the simulations results.

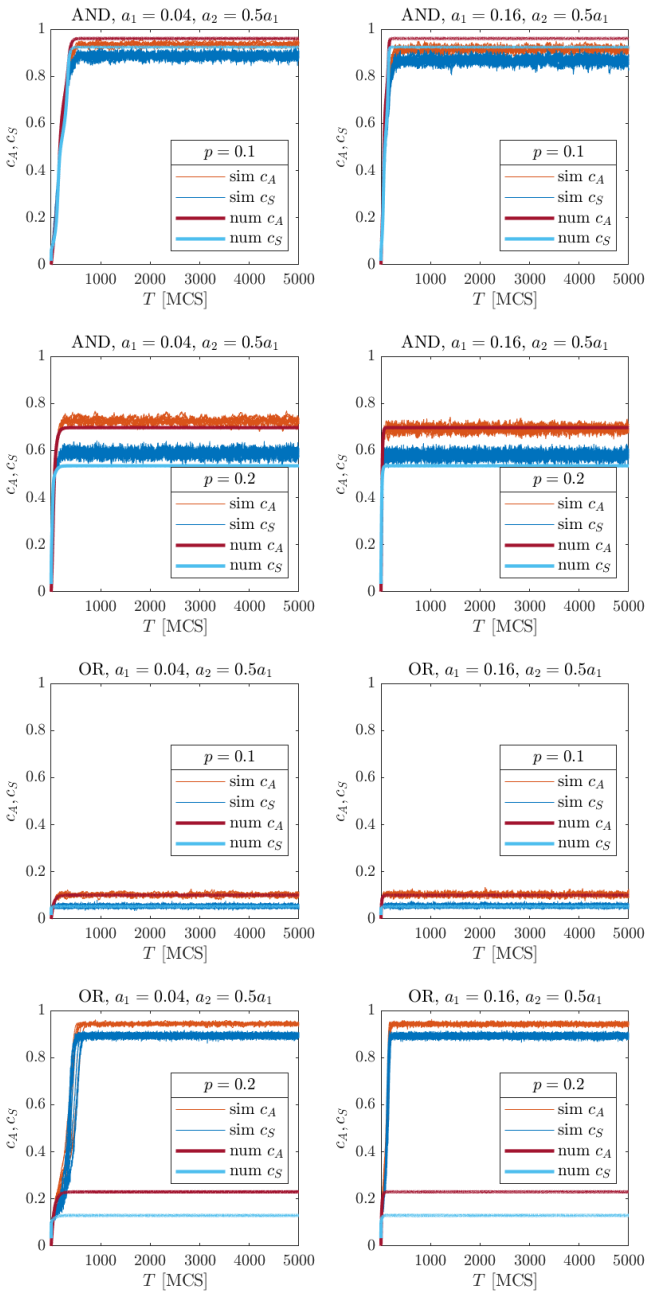

Figure 5: 10 simulated time trajectories of c_A and c_S versus numerically obtained time trajectory (from Eqs. (3)-(5)), for different values of p and a_1. the AND variant (top 4) and the OR variant (bottom 4). First layer – SL(N,1), second layer – WS2D(N,1,0.2), size $N = 2500$ and $a_2 = 0.5a_1$ in all cases.

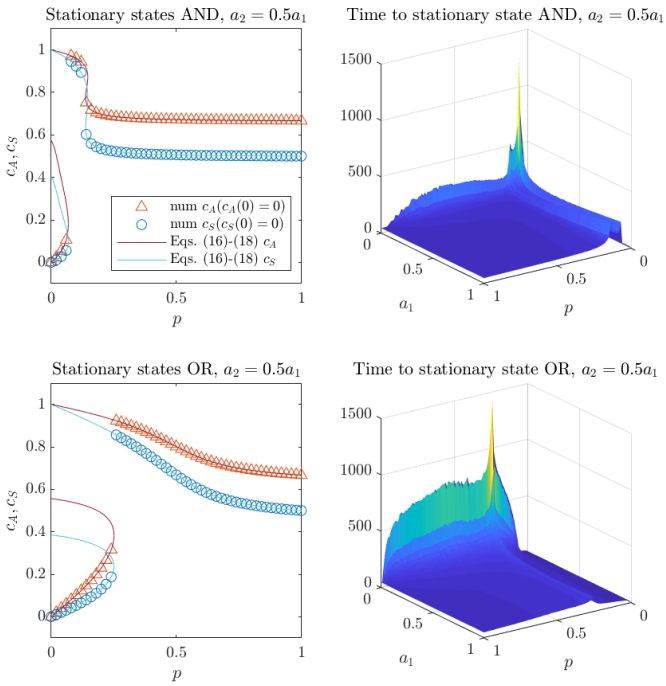

Figure 6: Stationary states (left) and time to reach a stationary state (right) for the AND variant (top) and the OR (bottom). Left side compares numerical results (from Eqs. (3)-(5); markers) vs analytical (from Eqs. (16)-(18); continuous lines). Numerical results cover only a portion of analytical ones, as they present stationary states from a single pair of initial conditions ($c_A(0) = 0, c_S(0) = 0$) only, while the latter show all the possible stationary states. Right side shows time to reach a stationary state obtained with numerical methods. Adoption probabilities $a_1 = 0.5$ (left side only) and $a_2 = 0.5a_1$.

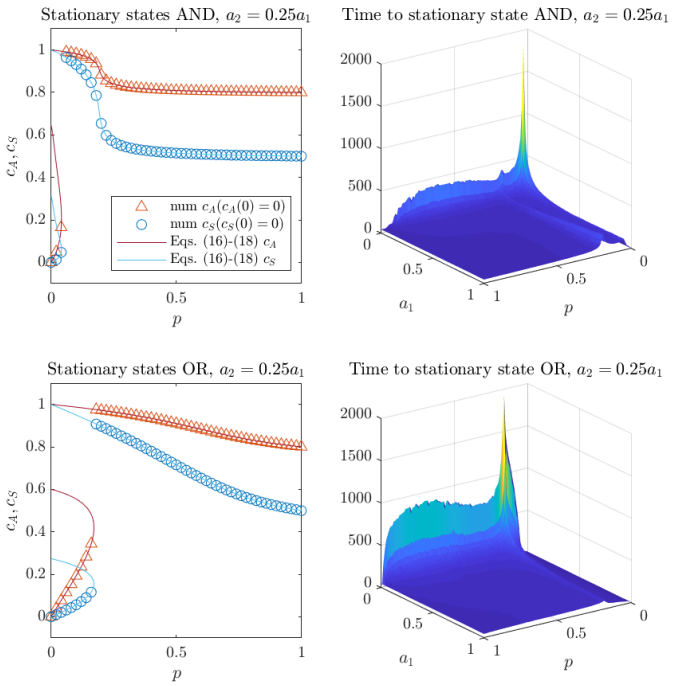

Figure 7: Stationary states (left) and time to reach a stationary state (right) for the AND variant (top) and the OR (bottom). Left side compares numerical results (from Eqs. (3)-(5); markers) vs analytical (from Eqs. (16)-(18); continuous lines). Numerical results cover only a portion of analytical ones, as they present stationary states from a single pair of initial conditions ($c_A(0) = 0, c_S(0) = 0$) only, while the latter show all the possible stationary states. Right side shows time to reach a stationary state obtained with numerical methods. Adoption probabilities $a_1 = 0.5$ (left side only) and $a_2 = 0.25a_1$.

4. Conclusions

In this research, we proposed a new agent-based model that describes both opinion formation and diffusion of photovoltaic panels. Although, it is based on the well-known model of binary opinion dynamics, the q-voter model, we extended it by adding a second agent attribute (adoption state) and rewrote it to a two-layer network structure. To generalize the model from a single-layer, we considered two variants. First, when the q-voter's social influence is required on both layers of the network to impact one's opinion (the AND variant). Second, where influence from just one layer is sufficient (the OR variant). We investigated the model, the effect of parameters on stationary states and times to reach them, using both Monte Carlo computer simulations and Mean-Field Approximation. For the approximation's results, we used analytical methods wherever it was possible, and numerical ones otherwise.

Let us begin with our main goal, which was to build a diffusion of innovation model that does not reduce the dynamics to a one-dimensional mechanism, as classical models do [13], but combines the adoption process with opinion formation. Consequently, diffusion of innovation and opinion dynamics are dependent on each other, with parameters only impacting one of these directly, influencing the other as well.

More specifically, within the model there exist three possible final states: unadopted system, adopted and finally, disordered one. The system transitions from the first, through the second, to the third, as the probability of independence p increases. Broadly speaking, independence is initially essential for the adoption process to take off. However, as the diffusion accelerates, independence hinders innovation and ultimately prevents full adoption. Except for $a_1 = 0$, the probability of adoption has no impact on the stationary states, only on times to reach them. What impacts stationary states, however, is the relation between a_1 and probability of loosing adoption a_2. As a_2 becomes less and less of a_1, critical values of p required to reach the adopted state decrease, while those required for the disordered one increase. Basically, the greater the difference between people's willingness to install solar panels versus their willingness to get rid of them, the better for the innovation. This difference not only amplifies independence in the initial phase of adoption, but dilutes it in the final phase as well.

Regarding the studied variants, there is a significant difference between the two, AND and OR. In the AND variant, other states are achieved more easily than in the OR variant, i.e. lower values of p are sufficient, but the transitions between these states are more pronounced. This is because, in the AND variant the initial negative consensus is more easily disrupted than in the OR variant, but so is the later positive consensus.

Finally, it should be noted that MFA approximates the simulation results fairly well. Although, in the simulation version the network consists of Square Lattice and two-dimensional Watts-Strogatz graph, structures pretty far from complete graph. Still, there are visible differences. Critical values of p to reach various states differ slightly, but the general picture remains.

Appendix

In the basic research, only $c_A(0) = 0$, $c_S(0) = 0$ initial state was considered. However, one could investigate others as well. Here, we examine, what happens if initially a small fraction of agents possess positive opinions and adoption states, $A(0) = +1$, $S(0) = +1$. These agents could be chosen randomly or determined by some centrality measure. We compare time trajectories for the basic case (no such agents), with a number of such agents chosen randomly and the same number determined by highest degree on the second layer (degree centrality).

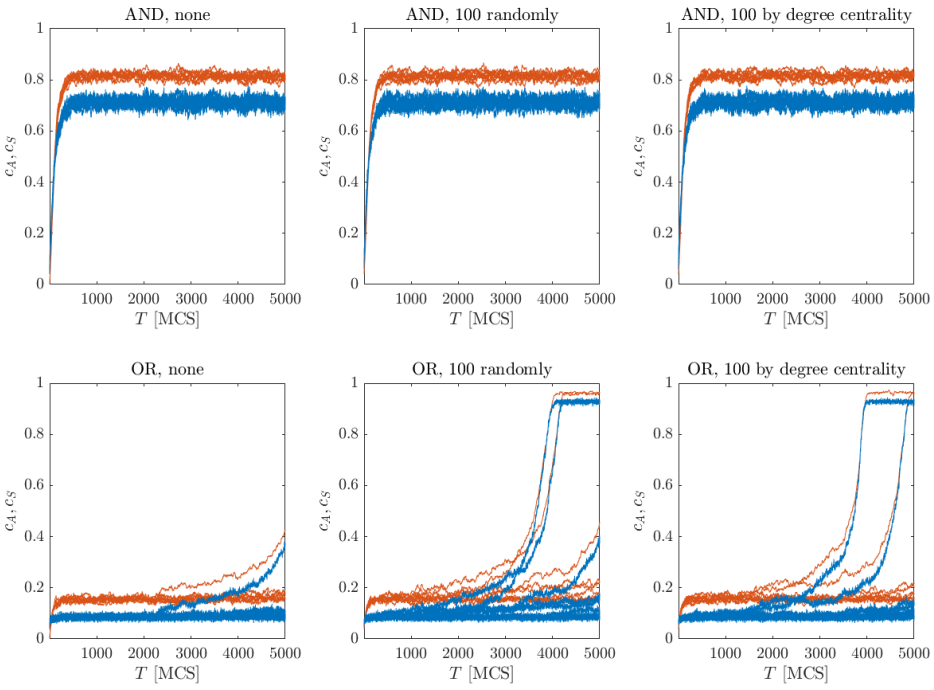

Figure 8: 10 simulated time trajectories of c_A (red) and c_S (blue) for $c_A(0) = 0$, $c_S(0) = 0$ (left), 100 agents with $A(0) = +1$, $S(0) = +1$ chosen randomly (middle) and 100 agents with $A(0) = +1$, $S(0) = +1$ determined by highest degree on the second layer (number of neighbors, right). The AND variant (top) and the OR variant (bottom). First layer – SL(N,1), second layer – WS2D(N,1,0.2), size $N = 2500$ and $a_2 = 0.5a_1$ in all cases.

Results are shown in Fig. 8. In AND variant there are no visible changes, as such agents easily loose either their positive opinion or adoption state when their numbers are low. Then, with the AND rule in play, they have negligible impact on the whole system. In the OR variant however, there are significant differences. Existence of such agents visibly decreases the time needed for the system to reach the adopted state. Method of their choice bears a lesser impact. This is due to the fact, that the second layer is described by the two-dimensional Watts-Strogatz graph, WS2D($N = 2500$, $m = 1$, $\beta = 0.2$). Distribution of degrees of such a random graph corresponds to the binomial (for small networks, $N = 10^2$)

or the Poisson distribution (for larger networks, $N \geq 10^3$) [51]. Therefore, the network lacks agents with degrees greatly exceeding the average, who could bear an impact.

Acknowledgements

T. W. was supported by the Ministry of Science and Higher Education, Poland, within the "Diamond Grant" Program through grant no. DI2019 0008 49.

References

[1] W. Bank, Air Quality Management in Poland, World Bank, 2019.
[2] F. Geels, B. Sovacool, T. Schwanen, S. Sorrell, Sociotechnical transitions for deep decarbonization, Science 357 (6357) (2017) 1242–1244.
[3] C. Mora, T. McKenzie, I. M. Gaw, J. M. Dean, H. von Hammerstein, T. A. Knudson, R. O. Setter, C. Z. Smith, K. M. Webster, J. A. Patz, et al., Over half of known human pathogenic diseases can be aggravated by climate change, Nature climate change 12 (9) (2022) 869–875.
[4] Eurostat, Renewables take the lead in power generation in 2023, https://ec.europa.eu/eurostat/web/products-eurostat-news/w/ddn-20240627-1 (2024).
[5] A. Ptak, Poland produced record 26% of electricity from renewables in 2023, https://notesfrompoland.com/2024/01/03/poland-produced-record-26-of-electricity-from-renewables-in-2023/ (2024).
[6] Eurostat, Electricity from renewable sources up to 41
[7] B. Derski, Ile kosztuje instalacja fotowoltaiczna dofinansowana z programu „mój prąd"?, https://wysokienapiecie.pl/24972-ile-kosztuje-instalacja-fotowoltaiczna-dofinansowana-z-programu-moj-prad/ (2019).
[8] M. Maticka, The SWIS DUCK – value pricing analysis of commercial scale photovoltaic generation in the South West Interconnected System, Electricity Journal 32 (6) (2019) 57–65.
[9] K. Maize, Duck hunting at the California Independent System Operator, Power 161 (3) (2017).
[10] S. Goodarzi, H. Perera, D. Bunn, The impact of renewable energy forecast errors on imbalance volumes and electricity spot prices, Energy Policy 134 (2019) 110827.
[11] R. Reibsch, P. Blechinger, J. Kowal, The importance of battery storage systems in reducing grid issues in sector-coupled and renewable low-voltage grids, Journal of Energy Storage 72 (2023) 108726.
[12] E. M. Rogers, Diffusion of Innovations, 5th Edition, Simon and Schuster, 2003.
[13] F. M. Bass, A new product growth for model consumer durables, Management science 15 (5) (1969) 215–227.
[14] H. Rahmandad, J. Sterman, Heterogeneity and network structure in the dynamics of diffusion: Comparing agent-based and differential equation models, Management Science 54 (5) (2008) 998–1014.
[15] K. Wolske, K. Gillingham, P. Schultz, Peer influence on household energy behaviours, Nature Energy 5 (01 2020). doi:10.1038/s41560-019-0541-9.
[16] W. Rand, R. Rust, Agent-based modeling in marketing: Guidelines for rigor, International Journal of Research in Marketing 28 (2011) 181–193.
[17] M. W. Macy, R. Willer, From factors to actors: Computational sociology and agent-based modeling., Annual Review of Sociology 28 (2002) 143–166.
URL http://www.jstor.org/stable/3069238
[18] M. Newman, Networks: An Introduction, Oxford University Press, 2010.
[19] T. Krueger, J. Szwabiński, T. Weron, Conformity, anticonformity and polarization of opinions: insights from a mathematical model of opinion dynamics, Entropy 19 (2017) 371.
[20] A. Kowalska-Pyzalska, K. Maciejowska, K. Suszczyński, K. Sznajd-Weron, R. Weron, Turning green: Agent-based modeling of the adoption of dynamic electricity tariffs, Energy Policy 72 (2014) 164–174.

[21] T. Jensen, G. Holtz, E. Chappin, Agent-based assessment framework for behavior-changing feedback devices: Spreading of devices and heating behavior, Technological Forecasting & Social Change 98 (2015) 105–119.
[22] K. Byrka, A. Jędrzejewski, K. Sznajd-Weron, R. Weron, Difficulty is critical: The importance of social factors in modeling diffusion of green products and practices, Renewable & Sustainable Energy Reviews 62 (2016) 723–735.
[23] T. Weron, A. Kowalska-Pyzalska, R. Weron, The role of educational trainings in the diffusion of smart metering platforms: An agent-based modeling approach, Physica A 505 (2018) 591–600.
[24] M. Van Der Kam, A. Peters, W. Van Sark, F. Alkemade, Agent-based modelling of charging behaviour of electric vehicle drivers, JASSS 22 (4) (2019) 7.
[25] J. Palmer, G. Sorda, R. Madlener, Modeling the diffusion of residential photovoltaic systems in Italy: An agent-based simulation, Technological Forecasting & Social Change 99 (2015) 106–131.
[26] A. Mittal, C. Krejci, M. Dorneich, D. Fickes, An agent-based approach to modeling zero energy communities, Solar Energy 191 (2019) 193–204.
[27] C. Caprioli, M. Bottero, E. De Angelis, Supporting policy design for the diffusion of cleaner technologies: A spatial empirical agent-based model, ISPRS International Journal of GEO-information 9 (10) (2020) 581.
[28] N. Zhang, Y. Lu, J. Chen, B.-G. Hwang, An agent-based diffusion model for residential photovoltaic deployment in singapore: Perspective of consumers' behaviour, Journal of Cleaner Production 367 (2022) 132793.
[29] A. Aleta, Y. Moreno, Multilayer networks in a nutshell, Annual Review of Condensed Matter Physics 10 (2019) 45–62.
[30] G. Bianconi, Multilayer Networks: Structure and Function, Oxford University Press, 2018.
[31] M. Kivelä, A. Arenas, M. Barthelemy, J. Gleeson, Y. Moreno, M. Porter, Multilayer networks, Journal of Complex Networks 2 (3) (2014) 203–271.
[32] H. Xiong, D. Payne, S. Kinsella, Identifying mechanisms underlying peer effects on multiplex networks, JASSS 21 (4) (2018) 6.
[33] W. Li, L. Tian, H. Liu, Q. Su, Heterogeneous adoption of eco-innovation considering commuting mobility patterns, Journal of Cleaner Production (2019) 119499.
[34] K.-M. Lee, C. Brummitt, K.-I. Goh, Threshold cascades with response heterogeneity in multiplex networks, Physical Review E 90 (6) (2014) 062816.
[35] A. Chmiel, K. Sznajd-Weron, Phase transitions in the q-voter model with noise on a duplex clique, Physical Review E 92 (5) (2015) 052812. doi:10.1103/PhysRevE.92.052812.
[36] J. Gleeson, Binary-state dynamics on complex networks: Pair approximation and beyond, Physical Review X 3 (2) (2013) 021004. doi:10.1103/PhysRevX.3.021004.
[37] A. Jędrzejewski, Pair approximation for the q -voter model with independence on complex networks, Physical Review E 95 (2017) 012307. doi:10.1103/PhysRevE.95.012307.
[38] T. Weron, P. Nyczka, J. Szwabiński, Composition of the influence group in the q-voter model and its impact on the dynamics of opinions, Entropy 26 (2) (2024) 132.
[39] C. Castellano, M. A. Muñoz, R. Pastor-Satorras, Nonlinear q-voter model, Physical Review E 80 (2009) 041129. doi:10.1103/PhysRevE.80.041129.
[40] P. Nyczka, K. Sznajd-Weron, J. Cislo, Phase transitions in the q-voter model with two types of stochastic driving., Physical Review E 86 (2012) 011105. doi:10.1103/PhysRevE.86.011105.
[41] T. Gradowski, A. Krawiecki, Pair approximation for the q-voter model with independence on multiplex networks, Physical Review E 102 (2020) 022314. doi:10.1103/PhysRevE.102.022314.
[42] T. Schelling, Dynamic models of segregation, Journal of Mathematical Sociology 1 (2) (1971) 143–186.
[43] A. Kowalska-Styczeń, K. Malarz, K. Paradowski, Model of knowledge transfer within an organisation, JASSS 21 (2) (2018) 3.
[44] E. F. Moore, Machine models of self-reproduction, in: Proceedings of symposia in applied mathematics, American Mathematical Society New York, 1962, pp. 17–33.
[45] A. Batool, Z. Danku, G. Pál, F. Kun, Temporal evolution of failure avalanches of the fiber bundle

model on complex networks, Chaos: An Interdisciplinary Journal of Nonlinear Science 32 (6) (2022).
[46] S. Wasserman, K. Faust, Social Network Analysis: Methods and Applications., Cambridge University Press, 1994.
[47] A. Gibbons, Algorithmic graph theory, Cambridge university press, 1985.
[48] M. E. Newman, G. T. Barkema, Monte Carlo methods in statistical physics, Clarendon Press, 1999.
[49] T. Weron, J. Szwabiński, Opinion evolution in divided community, Entropy 24 (2) (2022) 185.
[50] S. E. Asch, Opinions and social pressure., Scientific American 193 (1955) 31–35.
[51] A.-L. Barabási, M. Pósfai, Network Science, Cambridge University Press, 2016.